



**HAL**  
open science

# Analyse et optimisation d'une nouvelle architecture de réseau optique futuriste

Amira Kamli

► **To cite this version:**

Amira Kamli. Analyse et optimisation d'une nouvelle architecture de réseau optique futuriste. Réseaux et télécommunications [cs.NI]. Institut Polytechnique de Paris, 2019. Français. NNT : 2019IPPAS001 . tel-02469703

**HAL Id: tel-02469703**

**<https://theses.hal.science/tel-02469703>**

Submitted on 6 Feb 2020

**HAL** is a multi-disciplinary open access archive for the deposit and dissemination of scientific research documents, whether they are published or not. The documents may come from teaching and research institutions in France or abroad, or from public or private research centers.

L'archive ouverte pluridisciplinaire **HAL**, est destinée au dépôt et à la diffusion de documents scientifiques de niveau recherche, publiés ou non, émanant des établissements d'enseignement et de recherche français ou étrangers, des laboratoires publics ou privés.



INSTITUT  
POLYTECHNIQUE  
DE PARIS

NNT : 2019IPPAS001

Thèse de doctorat



# Analysis and Optimization of a new futuristic optical network architecture

Thèse de doctorat de l'Institut Polytechnique de Paris  
préparée à Télécom SudParis

École doctorale n°626 Institut Polytechnique de Paris (IP Paris)  
Spécialité de doctorat : Réseaux, Information et Communications

Thèse présentée et soutenue à Télécom SudParis , le 13/11/2019, par

**AMIRA KAMLI**

Composition du Jury :

Catherine Lepers Professeur, Télécom SudParis (SAMOVAR)	Président
Guy Pujolle Professeur, Professeur - Paris 6 University (LIP6)	Rapporteur
Thomas Begin Maître de Conférences, Université Claude Bernard Lyon 1 (LIP lab)	Rapporteur
Dominique Chiaroni Ingénieur Recherche et Développement, Nokia Bell Labs	Examineur
Stefano Secci Professeur, Conservatoire national des arts et métiers (Cnam)	Examineur
Tadeusz Czachórski Professeur, Institut d'informatique Théorique et Appliquée, Académie Polonaise des Sciences	Examineur
Tülin Atmaca Professeur, Télécom SudParis (SAMOVAR)	Directrice de thèse

*"Success is getting through defiance, adversity and difficulties, feeling hopeless and defeated but never giving up until you achieve your goal"*

***Rodrigo De Saro***

# Résumé

**Titre :** Analyse et Optimisation d'une nouvelle architecture de réseau optique futuriste.

**Mots clés :** Réseaux optiques, N-GREEN, Trafic sporadique, Optimisation, Modulation de fréquence.

**Résumé :** La demande en débit dans les réseaux augmente en raison de la croissance continue de trafic mondial et l'émergence de nouveaux services avec des exigences de plus en plus élevées. Dans ce contexte, la capacité du réseau devrait être augmentée tout en prenant en compte la consommation énergétique, son coût de construction et de maintenance. La combinaison des réseaux optiques avec un traitement orienté paquet pourrait répondre avantageusement à ces exigences. Cependant, à cause de l'absence de mémoire tout optique pratique, la commutation de paquets est le plus souvent exécutée électriquement rendant l'architecture plus chère et moins performante.

De ce fait, dans le cadre du projet ANR/N-GREEN, une nouvelle architecture de commutateur/routeur qui apporte des solutions à ces contraintes a été proposée par une équipe de recherche à Nokia Bell Labs. L'architecture a été conçue pour répondre aux exigences strictes de 5G telle qu'un délai de bout en bout de moins de  $250 \mu s$ , mais aussi pour répondre à l'augmentation du trafic prévue spécialement dans la partie métropolitaine de réseau (MAN).

Dans le cadre de cette thèse, nous nous sommes intéressés à l'analyse et l'amélioration des performances de cette nouvelle architecture de noeud quand elle est utilisée dans la partie métro de réseau. En effet, considérons cette partie, un réseau en anneau à commutation de slot optique OSS (Optical Slot Switching) combinant la flexibilité, la mise à l'échelle de la technique de commutation de slot avec les avantages de la topologie en anneau promettaient une bonne solution pour les réseaux MAN du futur. Cette nouvelle architecture offre des fonctions intelligentes, avec un coût moins élevé en optimisant le type/nombre des composants utilisés. Tous ces avantages le rendent un bon candidat pouvant remplacer les architectures optoélectroniques existantes telles que Ethernet ou d'autres architectures prometteuses proposées dans la littérature telle que POADM (Packet

Optical Add Drop Multiplexing) ou TWIN (Time-domain Wavelength Interleaved Network). L'élément fondamental du réseau est le WSADM (Wavelength Slotted Add Drop Multiplexer) qui est implémenté à l'intérieur des noeuds des réseaux. Ceci permet de garantir la transparence optique et donc une commutation plus rapide et une réduction de consommation énergétique. Dans cette thèse, nous avons analysé les performances en matière de délais d'accès et d'efficacité d'utilisation des ressources d'un réseau en anneau composé d'un certain nombre de noeuds N-GREEN. Les résultats préliminaires indiquent une latence élevée, une faible efficacité d'utilisation des ressources et une dégradation des performances sous certaines conditions telle que des modèles des trafics complexes. Afin d'adapter l'architecture aux différents types de trafics, nous avons utilisé quelques méthodes d'optimisation telle que Nelder Mead Simplex calculant ainsi les valeurs optimales des timers (temps d'attente moyen d'un paquet avant d'être inséré dans l'anneau optique). Trois différents modèles de trafics ont été considérés dans cette étude : outre que le modèle de base Poisson, on a considéré deux modèles basés sur des traces de trafic réel déduit à partir de traces de CAIDA.

En ayant recours aux régulateurs mono boucles, nous avons essayé par la suite de trouver un moyen afin d'auto-adapter les réseaux aux changements constants des trafics. Comme on parle d'une adaptation constante de la stratégie dans des conditions bruyantes, nous avons proposé un modèle de trafic très variable.

Ce modèle est composé d'un certain nombre de sources mixés formant ainsi un nouveau générateur caractérisé par sa variabilité. En observant l'effet de changement de fréquence de l'un des coefficients qui réagissent sur la stratégie de transmission des paquets sur les performances momentanées du réseau; nous déduisons une relation entre ces deux paramètres.

# Abstract

**Title :** Analysis and Optimization of a new futuristic optical network architecture.

**Keywords :** Optical network, N-GREEN, bursty traffic, optimization, Frequency modulation.

## Abstract :

The demand for network throughput is increasing due to the continued growth of global traffic and the emergence of new services with ever-higher requirements. In this context, the capacity of the network should be increased while taking into account the energy consumption, its cost of construction and maintenance. The combination of optical networks with packet-oriented processing could meet these requirements. However, because of the lack of all practical optical memory ; packet switching is most often performed electrically resulting in the architecture expensiveness and least efficiency.

A team study at Nokia Bell Labs has thus, suggested a fresh switch/router architecture as part of the ANR/N-GREEN project providing solutions to these constraints. The architecture was initially designed to satisfy the stringent 5G demands such as a 250  $\mu s$  end-to-end delay for some applications. It also responds to the traffic forecast particularly in the MAN (Metropolitan Area Network) part of the network. Therefore, this architecture could be introduced not only in the access/core part of the MAN but also in the core as well as in the Xhaul consider the 5G technology.

In this dissertation, we were interested in evaluating and improving the effectiveness of this fresh node architecture when used in the MAN. Indeed, considering this segment, an Optical Slot Switching (OSS) ring network would promise a great alternative for future MAN networks. With this combination, the ring topology guarantees a fast restoration in the case of failure and the OSS approach offers the flexibility and scaling of good multiplexing.

In this thesis, we assessed NGREEN's performance in terms of mean access delay and resource effectiveness. We used some methods of optimization such as Nelder Mead Simplex to dynamically calculate the optimal timer values (average waiting time for a packet to be inserted into the optical ring) thus, allowing the architecture to be adapted to different types of traffic. In this study, three distinct traffic models were suggested and applied : two models based on the traces of real traffic which were deduced from CAIDA [1], and the third most well-known Poisson model.

Inspired by the concept of loop controllers, we later attempted to find a way in order to allow the network to adapt itself to steady traffic modifications. As we were talking about a self adaptation of the network in noisy circumstances ; we have suggested a very variable traffic model, much more variable than CAIDA trace one. Observing the impact of the evolving frequency of one of the coefficients governing the network's transmission strategy on its current results allowed us to find a frequency range where the immediate reliance between the stimulus and the immediate response indicated the self-adaptation schema of the strategy.

The performance assessment of this architecture, taking into consideration various traffic models, demonstrates that the network answers the requirements of customers in terms of packet loss rates (PLR) and latency thanks to the suggested techniques and the implementation of optimization.

## *Acknowledgments*

First of all, I would like to thank the members of my PhD thesis examination committee for the honor they gave me by accepting to judge my work. Special gratitude to both Prof. Guy Pijolle and Prof. Thomas Begin for the time they have taken to revise my thesis, in details and for providing me with some constructive comments.

I would like to express my sincere thanks to my supervisor Prof. Tulin Atmaca for kindly accepting me as her PhD student, for her guidance and assistance and for her availability and encouragement during the various stages of my research work. I would like to thank her from the bottom of my heart specifically for her understanding and kindness.

I am particularly grateful for the guidance, availability and meaningful understanding of Dr. Artur Ratay. I was lucky to have been able to work many hours with him. I am so grateful for the time he spent working with me. He taught me a lot of concepts and helped me solve a lot of issues and questions. I felt closer to the solution after every conversation with him. Thank you for your valuable help, for your support and kindness.

I would like to thank Dr. Wiem Samoud, a postdoctoral researcher with whom I have shared the same office and worked for almost one year. She was a very kind co-worker and she taught me many interesting and important concepts in optical networks.

My deepest gratitude goes to Mr. Dominique Chiaroni; our project manager who has guided the project well, who have been always there to answer all our questions and encourage us. At the same time, I would also like to thank all our partners in N-GREEN project : Prof. Annie and Philippe Gravey, Dominique Barth, Jean Michel Fourneau, Catherine Lepers, Mounia Lourdiane and all students and PhD students with whom, we did some very effective meetings, discussed and validated our results and future work plans.

Last but not least, I want to thank all Telecom SudParis professors specially Mr. Djamel Zeghlache and my colleagues for their kindness and help. Specific thanks goes to Omar Houidi and Hadjer Touati, my companions.

Finally, I am indebted to my mother Rawdha for her infinite love, patience, and effort to guarantee the best circumstances for my education. I dedicate this thesis to my father's soul; to the soul of Mohamed. I am particularly grateful for the infinite encouragement

and unconditional support of my sisters and brothers. I would also like to express my gratitude to Souad, Donia, Asma and all my friends.

# Table of Contents

<b>Résumé</b>	<b>ii</b>
<b>Abstract</b>	<b>iii</b>
<b>Acknowledgements</b>	<b>iv</b>
<b>List of Figures</b>	<b>ix</b>
<b>List of Tables</b>	<b>xii</b>
<b>Acronyms</b>	<b>xiii</b>
<b>1 General Introduction</b>	<b>1</b>
1.1 Problem Formulation . . . . .	2
1.2 Dissertation outline . . . . .	3
1.3 Framework . . . . .	4
<b>2 State of the art</b>	<b>5</b>
2.1 Description of optical networks . . . . .	6
2.1.1 Optical networks Overview . . . . .	8
2.1.1.1 Telecommunication networks structure . . . . .	8
2.2 Traffic evolution in terms of volume and distribution . . . . .	10
2.3 Optical Switching Technologies . . . . .	12
2.3.1 Concurrent technologies . . . . .	19
2.3.1.1 Opaque Packet Networks . . . . .	20
2.3.1.2 Optical Packet Switched Networks . . . . .	21
2.4 Conclusion . . . . .	30
<b>3 N-GREEN Architecture</b>	<b>31</b>
3.1 Introduction . . . . .	31
3.2 N-GREEN concept . . . . .	32



3.2.1	N-GREEN Functional and Physical Description . . . . .	32
3.2.2	Overview of N-GREEN specificities . . . . .	34
3.2.2.1	Insertion processes . . . . .	34
3.2.2.2	Reception and extraction process . . . . .	36
3.3	N-GREEN network scenarios . . . . .	37
3.4	N-GREEN Optical Packet Switched Ring . . . . .	39
3.4.1	Studied Network Architecture . . . . .	39
3.4.2	Scenarios . . . . .	39
3.5	Conclusion . . . . .	41
<b>4</b>	<b>Adaptation of the N-GREEN Architecture for a Bursty Traffic</b> . . . . .	<b>42</b>
4.1	Intoduction . . . . .	42
4.2	Performance improvement of N-GREEN network . . . . .	45
4.2.1	WDM Slot Sharing . . . . .	45
4.2.2	Time Slot Sharing (Ssh-time) . . . . .	47
4.3	Adaptation of N-GREEN to bursty traffic . . . . .	49
4.3.1	Optimization Methods . . . . .	51
4.3.2	Traffic models . . . . .	52
4.3.3	Packet management . . . . .	55
4.3.3.1	Adaptation of $t_{\max}$ . . . . .	56
4.3.3.1.1	Parameters of the optimization method . . . . .	56
4.3.4	Performance achieved in terms of latency . . . . .	59
4.3.4.1	$t_{\max}$ as a function of local conditions . . . . .	59
4.3.4.2	$t_{\max}$ as a function of global conditions . . . . .	61
4.3.4.3	Discussion . . . . .	62
4.4	Concluding remarks and future works . . . . .	64
<b>5</b>	<b>Analysis of a frequency response of a telecommunication network for its self-adaptation</b> . . . . .	<b>65</b>
5.1	Introduction . . . . .	65
5.2	Background and Related Work . . . . .	66
5.2.1	PID (Proportional Integral Derivative) controllers . . . . .	66
5.2.2	Key Concepts . . . . .	67
5.2.2.1	Frequency-domain adaptation . . . . .	67
5.2.2.2	Bode Diagram . . . . .	68
5.3	Steps of Auto Adaptation of the Network . . . . .	69
5.3.1	Traffic Models . . . . .	69
5.3.2	Responses to stimuli . . . . .	72
5.3.2.1	Step response . . . . .	72
5.3.2.2	Frequency response . . . . .	74
5.3.2.3	Optimization . . . . .	77
5.4	Conclusion . . . . .	80

---

<b>6</b>	<b>General conclusions and perspectives</b>	<b>81</b>
<b>A</b>	<b>Synthèse en Français</b>	<b>84</b>
	<b>Bibliography</b>	<b>88</b>

## List of figures

2.1	Telecommunication network architecture : core, metro and access networks.	9
2.2	Forecasted global fixed and mobile traffic growth (from CISCO-VNI [2]).	11
2.3	Forecasted growth rates of the different network segments (from CISCO-VNI [2]).	12
2.4	Optical Packet Switching.	14
2.5	Optical Burst Switching (OBS).	15
2.6	Optical Add/Drop Multiplexer (OADM) (according to [3]).	15
2.7	ROADM Reconfigurable Optical Add-Drop Multiplexer.	16
2.8	Optical Cross-Connect (OXC) (according to [3]).	17
2.9	Wavelength Selective Switch (WSS).	17
2.10	Layer model displaying N-GREEN competitor applicants.	19
2.11	Node architecture of OTN.	20
2.12	RINGO Optical network.	22
2.13	Structure of the first version of RINGO node (from [4]).	22
2.14	Schematic representation of DBORN architecture and node (according to [5]).	24
2.15	Optical asynchronous protocol CSMA/CA.	24
2.16	Metro Network based on Packet-OADM Ring Model (according to [6]).	26
2.17	Packet Optical Add Drop Multiplexer Node Architecture.	27
2.18	Illustration of TWIN principle.	28
3.1	Main sub-blocks of the global node functional structure.	33
3.2	Physical N-GREEN node architecture.	35
3.3	A symbolic presentation of a N-GREEN node connected to a 10Gbps Ethernet. There is set of fixed lasers, an optical gate, an amplifier and a receiver.	36
3.4	Optical ring topology.	39
4.1	Packets insertion as WDM slot-wavelength method.	46
4.2	Mean Access delay for different scenarios in N-GREEN network while considering B&S mode [7]	46
4.3	Packets insertion as Ssh-time method.	47
4.4	Mean Access delay and container filling within unicast mode (Note that Ssh-20 and Ssh-40 stands respectively for 20, 40 $\mu s$ timer based mechanism with sharing	48

4.5	Mean Access delay and container filling within B&S mode (Note that Ssh-10, Ssh-20 and Ssh-30 stands respectively for 10,20 and 30 $\mu s$ timer based mechanism with sharing . . . . .	48
4.6	Real and Poisson traffic variations of one traffic flow. . . . .	50
4.7	Difference between overdimensioning with smoothie traffic and burtsy one. . . . .	51
4.8	Normalized histograms of the traffic models raw and balanced. Addresses represented by their two MSB. . . . .	53
4.9	An example state of input buffers and of the ring (displayed as a bar for brevity). Colours show the number of bytes of packets destined to a given node; a number in the WDM slot depicts the emitter node. Network interfaces symbolize a node that can read a WDM slot; then delete it and later insert new contents into the just–emptied WDM slot. In the visualised state, $N_9$ produced a burst of WDM slots containing packets to $N_6$ , $N_7$ and $N_8$ causing a packet loss in the input buffer of $N_5$ . . . . .	54
4.10	Timer expiration $t_{\max}$ against sizes of buffers' input considering the variants const, local and global against $S_i$ . . . . .	60
4.11	Latency after optimizations (a) $O_{\text{load}}$ and (b) $O_{\text{univ}}$ , against $L$ using the variants const, local and global. Latency values out of scale are caused by packet loss. . . . .	60
4.12	Timer expiration $t_{\max}$ against sizes of input buffers considering the variant $O_{\text{univ}}$ . It shows the variant global against $S_{\text{mean}}$ and $S_{\text{max}}$ . For the variant global, only a mean value of an underlying PDF is shown. Columns depict traffic models exp, balanced and raw. . . . .	61
4.13	Dependency between $L$ and $S_{\text{mean}}$ for different traffic models using the variants (a) local and (b) global. . . . .	62
5.1	Normalized histograms (or discrete probability distributions) of the CAIDA traces (a) A and (b) B against a source and and a target node found by dividing the two MSB of anonymized IP addresses into 10 equal fragments. (c) A cumulative chart flow showing the probabilities of acceptance of packets in three sources, $m_n = 0.95$ . Assuming that each of the sources has a mean rate of 1; the upper edge of the colored area shows the effective packet rate. . . . .	70
5.2	Intensity taken from three different CAIDA traces . . . . .	71
5.3	A cumulative flow chart showing the probabilities of acceptance of packets in three sources, $m_n = 10$ . Assuming that each of the sources has a mean rate of 1; the upper edge of the colored area shows the effective packet rate without normalisation . . . . .	71
5.4	Step response : optimal $a_{\text{mean}}$ is multiplied by a square waveform of levels 0, 2 and a given frequency. Vertical dashed lines show respectively the beginning and the end of the higher value of $a_{\text{mean}}$ . . . . .	73
5.5	Bode diagrams of an N-GREEN ring against different $L$ and traffic models, $A = 1$ . As the stimulus and the response are in different units, we normalized the magnifications by comparing them at high frequencies and assuming 0 dB at low frequencies. . . . .	75

---

5.6	$S_{\text{mean}}$ against different $L$ and $a_{\text{mean}}$ , both table during an entire simulation : lines for $a_{\text{opt}}^{\text{mean}}$ , triangles for $a_{\text{mean}} = \{0, 2a_{\text{opt}}^{\text{mean}}\}$ ; due to the limited effect of $a_{\text{mean}}$ on $\hat{S}_{\text{mean}}$ , the actual distance of triangles to the line is exaggerated by a multiplier of 5 for a better visibility. Phase values interpreted as in Bode diagrams. . . . .	76
5.7	Adaptation of $a_{\text{mean}}$ during different optimization processes, the central frequency is always 354 Hz. . . . .	78
5.8	Quality for different loads and the traffic model MIXED, without and with different types of strategy oscillation. See that an extended simulation time $2T_s$ is important for larger $L$ . . . . .	78

# List of Tables

2.1	Fiber optic advantages compared to other media. . . . .	7
2.2	Optical Packet Ring Architectures. . . . .	29
4.1	List of symbols used in section 4.3. . . . .	52

# Acronyms

<b>CoS</b>	Classes of Services
<b>DBORN</b>	Dual Bus Optical Ring Network
<b>EDFA</b>	Erbium Doped Fiber Amplifier
<b>EP</b>	Electronic Packet
<b>FDL</b>	Fiber Delay Lines
<b>FTTX</b>	Fiber To The X
<b>MAN</b>	Metropolitan Area Network
<b>N-GREEN</b>	New Generation Of Routers For Energy Efficiency
<b>OADM</b>	Optical Add/Drop Multiplexers
<b>OBS</b>	Optical Burst Switching
<b>OCS</b>	Optical Circuit Switching
<b>OEO</b>	Optical Electrical Optical
<b>OPS</b>	Optical Packet Switching
<b>OP</b>	Optical Packet
<b>OTN</b>	Optical Transport Network
<b>OXC</b>	Optical Cross Connect
<b>PDU</b>	Packet Data Unit
<b>PID</b>	Proportional Integral Derivative
<b>PLR</b>	Packet Loss Rate
<b>POADM</b>	Packet Optical Add/Drop Multiplexing
<b>PON</b>	Passive Optical Network

<b>QoS</b>	Quality of Service
<b>RINGO</b>	Ring Optical Network
<b>RITA</b>	Research and Innovative Technology Administration
<b>SDU</b>	Service Data Unit
<b>SOA</b>	Semiconductor Optical Amplifier
<b>TDM</b>	Time Division Multiplexing
<b>TWIN</b>	Time Domain Wavelength Interleaved Networking
<b>WAN</b>	Wide Area Network
<b>WDM</b>	Wavelength Division Multiplexing
<b>WSADM</b>	Wavelength Slotted Add Drop Multiplexing



# Chapter 1

## General Introduction

Driven by the interconnectivity between the cloud, data centers, content delivery and 5G mobile communications; telecommunication networks will experience a **strict volume traffic growth**. In addition to this grow in quantity, the evolution of traffic is witnessing a shift in patterns. This is mostly due to the introduction of new services such as a new format requiring a higher bit rate per video channel from SDTV to HDTV and then to UHD TV etc. Another important factor is the increasing video usage particularly with mobile terminals connected either to a fixed access network using WiFi interfaces or to a mobile access network (4G and soon 5G standard). Adding to this, we need to consider the deployment of the Machine to Machine (M2M) traffic taking into account the introduction of the Internet of Things (IoT).

The second significant challenge is that today's network power consumption goes hand in hand with the increase in traffic. In fact, it has been acknowledged that optical systems are more energy-efficient than electrical systems when used to transport information. Nevertheless, due to the lack of mature optical buffers, packet switching and routing can not presently be carried out in the optical domain. All-optical packets must be converted to the electrical domain at the level of routers to be processed ; then re-converted to optical signals for further transmission. Re-amplifying, reshaping and re-timing (3R) functions are done electronically. The required Optical-Electrical-Optical (OEO) conversions make the switching process one of the areas with the fastest-growing energy consumption [8].

To deal with this new trend, network operators must design a new network architecture, taking the previously mentioned two main challenges into consideration and fulfilling the following features :

- **Scalability** : The capability to expand the network capacity in terms of bandwidth and node number without affecting both the already deployed architecture and the used protocol stack.
- **Multi-service** : The architecture's capacity to support distinct packet classes with distinct services and to guarantee the particular Packet Loss Rate (PLR) , latency, jitter, packetization interval and bandwidth .. etc needed by each packet.
- **Switching granularity** : In contrast to a rigid circuit-level switching, the nature of optical network traffic needs various levels of granularity to share the bandwidth and boost the throughput.
- **Optical transparency** : As mentioned earlier, lowering the OEO conversions also leads to cost reduction. It is therefore compulsory to remove unnecessary bottlenecks in the processing of electronics in the new optical network.
- **Network management and Simplicity** : Extensive control and management facilities must be available in optical network in order to operate the network. Mostly dynamic end to end service provisioning for emerging applications is required.
- **Availability and reliability** : Optical networks must be able to surpass failures such as one or more nodes or links break up. Protection mechanisms must be available in order to provide the necessary reliability for carrier grade transport network.

A set of features has to be provided by operators while taking into consideration both capital and operational expenses (CAPEX and OPEX) given that the general evolution of the business models leads to a steady decrease of the operator's revenue per transported bit.

In this context, reducing the number of unnecessary optical to electronic conversions is a goal that the research community has identified as primary key for an energy-efficient network. This has been considered as challenging for a long time and still under study until to date. Moreover, it would be great to combine the reduction of OEO with the multiplexing granularity provided by packet/slot switching. To address the above requirements within the next generation of optical network, we need to find a way for "all optical packet switching" [9]. There are many experimental projects studied and proposed for that purpose [10]; a few of them are presented in the chapter State of the art (Chapter 2). The syntheses of these works gave birth to N-GREEN network.

## 1.1 Problem Formulation

The research in this thesis focuses on the performance analysis and enhancement of one of the most sophisticated designs of futuristic optical network architectures. The

modern architecture falls within the framework of the N-GREEN project. N-GREEN is a project carried out in France between 2016-2019. This project introduces Wavelength Slotted-ADM (WSADM) technology in a WDM time slotted architecture [11]. A primary study was conducted during the project considering a unidirectional ring. Issues such as network modeling and simulation, performance evaluations for unidirectional ring and dimensioning were addressed [7, 12].

Our purpose at the beginning of this study was to extend the work carried out on N-GREEN. The essential goal is to enhance the effectiveness of the resource's use considering other network segments as well as other applications. We then attempted to adapt the architecture to other circumstances. In the latter, we consider other traffic models starting with a more real model extracted from CAIDA traces to a personalized one.

Encouraged by the previous findings, we later scrutinized a more complicated model in which the traffic model was specifically suggested for this research. Indeed, the first contribution determines the optimal parameters of the network based on the designer's input values. However, these parameters should be changed whenever network circumstances alter such as traffic shifts...etc. This issue is addressed in the second part of this thesis.

## 1.2 Dissertation outline

A general overview of the thesis structure is as follows :

- In chapter 2 of this manuscript, we present an overview of optical networks : their structure, their difficulties, and the advantages and disadvantages of optical transmission while concentrating on optical switching methods and optical transmission technologies in MANs. It proposes the main forgoing, used or promised technologies to date while highlighting the primary components that have contributed to the evolution of optical networks.
- Chapter 3 is entirely devoted to defining N-GREEN's architecture. The chapter starts with a functional and physical description of the N-GREEN node architecture's fundamental features. Then we list the set of cases where it is possible to use the new architecture. The chapter is closed by identifying the scheme under investigation with reference to the considered scenarios.
- Chapter 4 explores N-GREEN's performance once used in the MAN. The considered network is a unidirectional slotted ring on which several models of traffic were

considered. This section suggests some sophisticated packet management scheme aimed to improving and adapting the architecture to distinct circumstances and situations. The chapter begins with defining the performance criteria and the simulation's conditions and setup. The rest of the section is divided into two primary parts : The findings achieved when implementing techniques to enhance architectural efficiency are discussed in the first section. As for the second part, we show the measures we have taken into account to adapt the architecture to the bursty traffic.

- In chapter 5, we extend our inquiry by considering a more complicated traffic model together with a more independent packet management scheme. Indeed, within this chapter, we display the measures taken to identify the specific traffic patterns. The results will be discussed while assisting the optimization process.
- Finally, the last chapter 6 concludes the dissertation with a summary of the main topics covered in this thesis followed by some perspectives for subsequent scientists' researches.

### 1.3 Framework

As part of the program of the doctoral school of STIC, Science of Technologies of Information and Communication of Paris, the work of this thesis took place within Télécom SudParis which belongs to the IP Paris tech university under the direction of Professor Mrs **Tulin Atmaca**.

The majority of this study is performed as part of the ANR/N-GREEN project suggested by Nokia Bell Labs, an international telecommunications company. Throughout the past three years of thesis studies, I had the opportunity to make two short-term stays at the Polish Academy of Science in Poland and the Istanbul Technical University during which I had the opportunity to exchange and discuss ideas and knowledge with high-caliber professors.

This thesis is mainly financed by a national scholarship issued by the Ministry of Higher Education and Scientific Research of Tunisia and it is basically set on academic merit.

## Chapter 2

### State of the art

This chapter provides a global overview of current optical switching and transport technologies. It emphasizes the most mature components and techniques with reference to the architecture of N-GREEN. It roughly summarizes the optical network history and shows researches results that served as the basis for N-GREEN network proposal.

This chapter is organized as follows :

In [2.1](#), we present an overview of the domain of optical network while highlighting this technology strengths and limitations and the particular requirements for each part of the network.

A traffic growth prediction study is provided in [2.2](#), thus identifying the portion of the network with the most expected traffic development. The choice of the metro part on which the majority of the work was done is therefore justified.

In [2.3](#), optical WDM networks are classified according to switching granularity and the expected advantages of optical packet/slot switching that is highlighted in comparison to other switching techniques. The main forgoing used or promised technologies aiming to guarantee fast optical switches are exposed. The purpose is to explain how studies arrived to propose N-GREEN network.

Finally, conclusions are given in [2.4](#) .

## 2.1 Description of optical networks

Optical technology is now the most promising or even the only studies' outcome able to meet the expected traffic requirements for the next 5-10 years to come[13]. As support for data transmission, optical fibers provide enormous ability, reliable transmission routes and flexibility. An optical network is merely a network of communication in which information is transferred as pulses of light over fiber optical lines. It allows the transmission of high-bit information signals over lengthy distances. This capacity has been enhanced by the discovery of Erbium Doped Fiber Amplifier (EDFA)'s outstanding amplifiers performances. Such a discovery allowed the penetration of WDM (Wavelength Division Multiplexing) technology in the Wide Area Network (WAN) and Metropolitan Area Network (MAN). While its dominance established during the 1990s; it continues until today. All these features and evolution had made optical communication benefits from countless advantages over copper wire. The optical fiber, as it is known, has a very low propagation loss while the transmission bandwidth is extremely large, enabling a high speed, broad bandwidth and long distance transmission.

Table 2.1 shows a few of the most significant advantages of optical networks relative to other media.

Large optical bandwidth	Fiber offer nearly 1.6 Tbps, copper achieves 100 Mbps wherever coaxial can carry up to 1Gbps.
Lower Errors	Bit Error Rate A very low rate of transmission errors ( $10^{-15}$ for optical fiber compared to $10^{-3}$ for a copper cable and $10^{-8}$ for a coaxial one).
Attractive cost per foot	Cost per foot for fiber is now approximately \$0.20 compared with \$0.13 for copper(category 5+).
Performances	<ul style="list-style-type: none"> <li>— Light as a transmission medium provides the ability for the use of optical fiber in dangerous environments. Fiber is less susceptible to temperature fluctuations and fires than copper and can be submerged in water.</li> <li>— Immune from to electromagnetic interference (EMI), radio-frequency interference (RFI), crosstalk, impedance problems... without extra cost shielding on copper <math>\Rightarrow</math> This permits to reach these interesting values in bit error rate <a href="#">2.1</a>.</li> </ul>
Distances	Greater distance with fewer repeaters. Now it can achieve 30 to 200 miles without repeaters compared to less than 30 miles once using copper and radio
Capable of carrying analog and digital	Fiber optic is both digital and frequency multiplexed, increasing its capacity.
Security	Optical fiber is difficult to tap since it does not radiate signals, thus it provides a higher degree of security than possible with copper wire.

TABLE 2.1: Fiber optic advantages compared to other media.

Despite the fact that optical technology remains unsurpassed for reliable transportation of bits over lengthy distances, they have certain restrictions preventing us to benefit from its overall capacity :

- The price of installing optical fiber is quite high, much higher than the cost of the fiber itself. For example, for the deployment of FTTx; the cost of fiber is only 6% while the cost of civil works is the major share according to [14]. In addition, it requires costly precision splicing and measuring equipment. The Department of Transportation Research and Innovative Technology Administration (RITA) in the United States provides fiber optic cable assembly expenses for multiple projects [15] in response to the fiber deployment request everywhere.
- Copper wires can carry information as well as power. A last-mile switch or a terminal (e.g. a phone) just need to be connected to the end of the network where the power

comes from the central distribution. This is not the case with fiber optic wires that only carry information. Indeed, an Optical Network Terminal (ONT) must be linked not only to the optical fiber carrying the information but also to the power source or outlet.

- **The absence of optical memory** is the greatest barrier preventing service suppliers from taking advantage of the complete fiber capacity. Although most wired traffic is transferred via optical fibers, particularly in core and metro networks, **packet switching and routing are still conducted with electronics in most instances, except for quasi-static routing**. Optical packets must, therefore, be subjected to OEO at the switch or router level and then converted for further transmission to the optical field. The OEO conversions needed make switching, one of the fastest-growing energy consumption areas [8] and vulnerable to contention leading to high Packet Loss Rates (PLR) [16, 17]. Contention arises when one or two signals choose the same output port at the same time. Despite a lot of studies in that field, fast optical switching technology has not yet been able to see the light till the day.

## 2.1.1 Optical networks Overview

### 2.1.1.1 Telecommunication networks structure

Optical fiber is now emerging in various sections of the network. Indeed, as shown in Figure 2.1, from the point of view of their geographical scope, three principal categories of telecommunications networks can be differentiated : access, metro and core network. Basically, a node in each level aggregates and forwards the traffic coming from the immediate lower level producing, thus, a higher stages of traffic aggregation.

- **Access network (Last mile)** : The access network is the closest stage of the telecommunication networks to the end user. It is responsible for connecting the subscribers to the network operator (or service provider) over a distance of a few (less than or equal to 10) kilometers. Based on the operator point of view, the access network is also called the last-mile network. Typically, different kinds of links have been used for the access networks, namely twisted pair and xDSL technologies for copper wires and WiFi and WiMax for wireless links. Thanks to these characteristics of optical transmission (low loss, wide bandwidth, noise isolation ...) [18, 19], optical technologies present a fierce competitor to other technologies. Fiber access networks bear also Fiber-To-The-x (FTTx) system. As its name suggests where "x" can be "home", "building", "curb"... depending on how deep in the field fiber is deployed or how close it is to the end user. In a fiber to-the-home (FTTH) system,



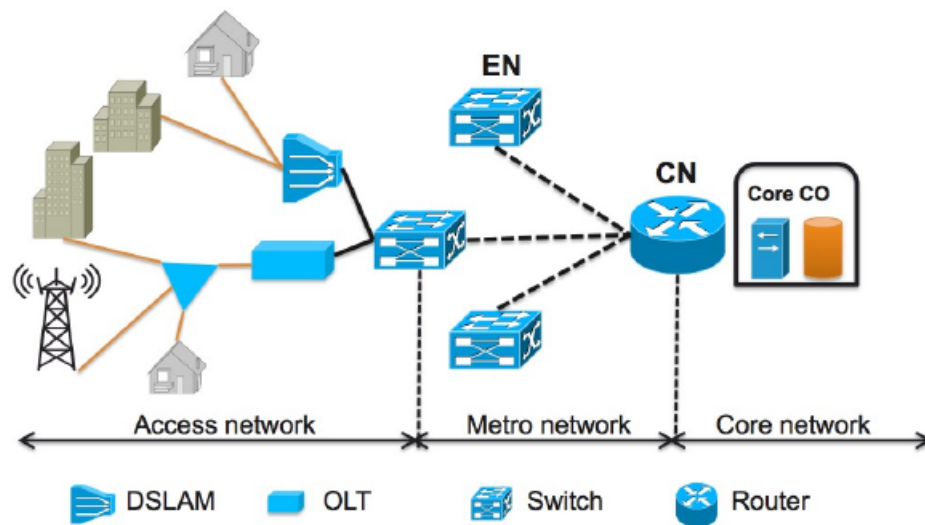


FIGURE 2.1: Telecommunication network architecture : core, metro and access networks.

fiber is connected all the way from the service provider to household users. On the way to the user, local routers transport the traffic from the access network to the metro network. The local routers are also called access routers. Their capacity are relatively low as such Cisco 3850 local switch allows to connect up to 48 Ethernet ports with a rate of 1 Gb/s per subscriber and up to 40 Gb/s of wireless capacity [2].

- **Metro network :** The metropolitan network (MAN) also carries the name Backhaul or regional network, which typically includes large metropolitan areas (up to 200 km according to [20]). It represents the network's intermediate portion connected to the core network from one side and to the access part from the other side. As depicted in Figure 2.1, they are classified into two types mainly Edge Nodes (ENs) and Concentration Node (CN). ENs aggregate flows coming basically from the access part i.e. the DSLAMs and OLTs. All aggregated traffic in the ENs are subsequently transmitted to the CN, also known as the Point of Presence. This latter is accountable for connecting the metro to the core network. Ring is the most common topology used to interconnect ENs [13] as it has inherited several advantages such as fast restoration in case of failure and spatial reuse. Regional network can be presented in the form of several interconnected rings in the case of a large metropolitan area. In this case, a primary ring connected through the CN to the backbone network, collects traffic from multiple secondary rings. The architecture described above requires an enormous buffering capacity and a large amount of computing resources in the CN to filter and handle all the traffic flows

passing through it in general. Indeed, although the transmission focuses completely on optical fibers; amplification, consistent detection and switching remain electronic. Even though the shift from electronics to optics is in the process of covering all of the network's parts; there is no electronically done radical solution for switching and routing. Therefore, OEO conversions are required. Conducted researches at metropolitan networks paid specific emphasis on two associated problems, namely the cost-effectiveness and simplicity of optical switching technologies. The main objective is to deal with the growing quantity of information transmitted over fixed and mobile networks and to increase optical transparency as much as possible. Roughly, all the conducted researches performed in this thesis take this part of the network into account among others 2.3.

- **Core network** : Also identified as backbone or long-haul networks, are used between long distance nodes such as continents providing thereby the access to the international networks. The core network is central part of a telecommunication network and it is built over very high bitrates transmission links, connecting the principal nodes of the network. Each service provider designs its network architecture taking into account some factors such as the covered area, the traffic load and the geographical characteristics among others. Information from metro networks is aggregated [21] and then transmitted to the core one. It may also provide the gateway to other networks. The transmission is generally based on IP/MPLS over WDM. Currently rolled out core have Optical Transport Network (OTN) (i.e. ODU4) interfaces of 100Gbit/s. Thanks to ROADM and WSS technologies, intermediate nodes operate at complete optical capability without electronic buffering and processing. Recently, systems with a greater bit rate i.e. 200Gbit/s or 400Gbit/s began to be assessed. Therefore, it raises two significant difficulties that are spectral and effective network. Moving to a flexible WDM grid using the so-called Flex Grid may rise the first challenge. This WDM grid may be based on a multiple integer of a 12.5 GHz frequency slot. The second challenge could optimize network effectiveness by incorporating a layer 2 i.e. OTN between the ROADM and the switch/router.

Within N-GREEN, three network segments are considered. Metro-access considering future 5G traffic, metro-core considering the evolution of traffic sources, such as the creation of distributed information centers and core networks by proposing innovative multi-terra-class router architectures.

## 2.2 Traffic evolution in terms of volume and distribution

This part reviews prediction and identifies factors that affect traffic growth significantly. A comparison between forecasted traffic in different part of the network has been

made. Indeed, Cisco's white paper [2] was often used as a fundamental reference to extrapolate future developments in traffic. As a consequence of the increasing number of connected end-user terminals (smartphones, tablets, connected TVs) and the race toward higher definition content; traffic growth across all parts of the transport network has been steadily increasing in recent years. This growth of fixed, mobile and video traffic is expected to continue leading evidently to significant bandwidth utilization.

An analysis of the Cisco white paper [2] demonstrates that IP traffic will expand from 2016 to 2021 at a 24% Compound Annual Growth Rate (CAGR). It has been estimated to have increased by about five times and for the next three years it will be multiplied by three. As shown in Figure 2.2, the annual growth rate will reach almost 23% between 2014 and 2019. It is worth to note that the peak-hour traffic growth is anticipated to exceed 28.5%. This is consistent with the quantity of video traffic compared to the overall traffic. Global mobile data is supposed to increase by a factor of ten to 2019, and the latest Ericsson confirms the same trends.

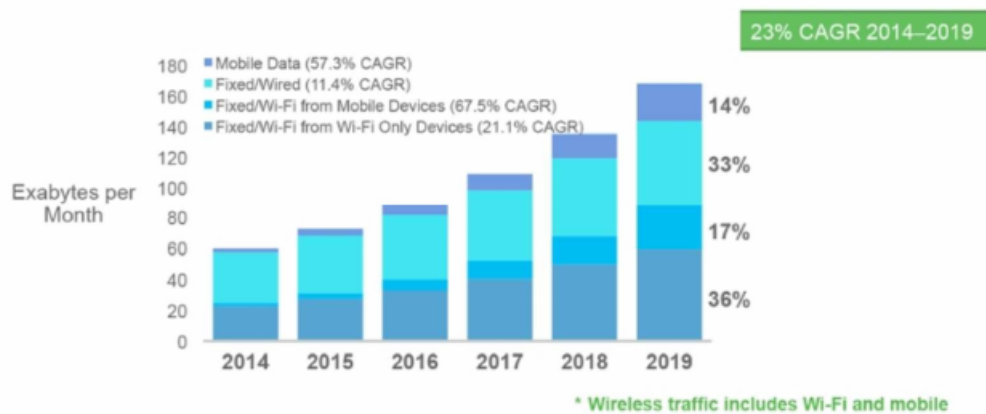


FIGURE 2.2: Forecasted global fixed and mobile traffic growth (from CISCO-VNI [2]).

Another interesting observation is that by the beginning of 2019, the MAN network will account for 66% of complete IP traffic leading to a grow by double of the metropolitan traffic intensity (see Figure 2.3). The trends in metropolitan flow are growing as a consequence of the increasingly important role of video caching and servers to the distribution over the edge nodes (i.e. deployment of CDN networks), will bypass long-haul connections and deliver flows straight to the metro. Moreover, CDN traffic is anticipated to be 62% of total data circulating in Internet by 2019, representing 80% of Man's flow. According to this trend, the metro core is expected to support small data centers or some simple units for local caching and processing.

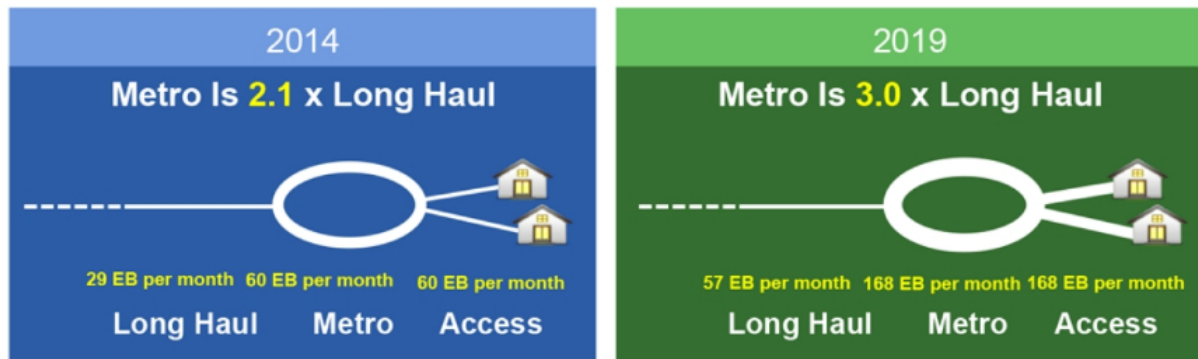


FIGURE 2.3: Forecasted growth rates of the different network segments (from CISCO-VNI [2]).

## 2.3 Optical Switching Technologies

In general, optical networks can be classified into two groups by the degree of optical packet transparency that is :

- **Opaque optical network** : In opaque optical networks all the point to point links are fibers, however OEO conversion is conducted at each intermediate node. Indeed, to drop or forward some flows, the traffic obtained from the converted channel is processed. In the case of forwarding, the electrical signal is converted back into an optical domain, electrical-to-optical conversion, and sent to its destination in fibers. In these networks, the function of optics is mainly restricted to data transmission.
- **Transparent network** : In transparent networks, optical data channel/signal bypass intermediate node optically, thus staying in the optical domain from source to destination. Furthermore, multiplexing and add/drop functions are all done optically. An optical switch, for example, does not matter if it switches an Ethernet signal of 10 Gbps or an OTN signal of 40 Gbps.

There is another type that bears the translucent network name. It is a compromise between opaque and transparent network. Using this method, network traffic continues on the optical format until it needs to be regenerated i.e. attenuation and signal degradation are much greater, then it is required for conversion and regeneration [22].

The degree of transparency is not the only defining factor in the networks in hand where the degree of granularity can also be used, particularly in the scope of the MAN network. In fact, based on the degree of granularity, two main methods were defined. Their operational principles are described below.

This part provides a brief background review of optical switching and transportation technology.

- **Optical Circuit Switching (OCS)** : The simplest way to provide connectivity in a WDM network is by assigning a particular wavelength channel to each pair of source-destination. This first switching technique is referred to as Optical Circuit Switching(OCS). Nodes are interconnected in an OCS via an end-to-end statistical or dynamic communication channel called lightpaths. Dynamic wavelength routing is feasible only when the nodes in the network integrate a wavelength converters such as Optical Cross Connect (OXC). Therefore, the allocated wavelength can be changed within the same communication. Otherwise, all the connections along which the communication is transmitted use the same wavelength. The main advantage of OCS is the ability to eliminate the need for costly OEO conversions and the capacity to provide high-level Quality of Service (QoS) links. Despite these substantial benefits, OCS has two major disadvantages : First the insufficient use of the available bandwidth and the absence of its flexibility. Second, providing full connectivity in a large OCS network that hampers interconnecting  $N$  nodes which requires  $O(N^2)$  different lightpaths. OCS therefore suffers from problems of scalability.
- **Optical Packet Switching(OPS)** : Proposed OPS solutions [23–25] is based in a finest granularity. It does not handle lightpaths as for OCS, but rather fixed or variable size optical packets. It tends to perform the entire processing of packets in the optical domain. The idea of optical packet switching mimics electronic IP networks as it takes routing decisions based on the information contained in the packet header. Using the optoelectronic approach, the header is extracted and converted to the electrical domain while the payload is stored optically in Fiber Delay Lines (FDL), see Figure 2.4 during header processing. FDLs are optical buffers used to delay the signal by sending it through a fiber. They therefore provide only fixed delays and have very restricted capacity for storage. As a consequence, contentions are highly susceptible to optical packets. We remind that contention takes place if two (or more) packets are to be forwarded to the same output port at the same time. Although the main objective of OPS technology is to enable high capacity and transparency, OPS networks do not seem to have achieved what was expected of them after several years of development. The main problem in implementing OPS is the absence of optical random access memory (RAM) and the restricted electronics processing power. Some believe that the future of OPS networks is in the wise integration of optical and electronic networks. The future of optical WDM networks is actually in Optical Burst Switching technology (OBS) [26] which is explained in the following section.

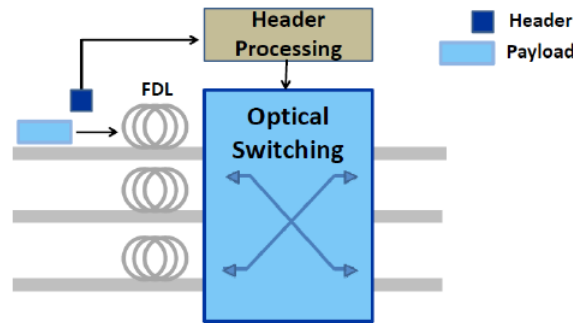


FIGURE 2.4: Optical Packet Switching.

- **Optical Burst Switching (OBS)** : OBS [27, 28] is a suggested solution that results from the need for an OCS-OPS compromised solution. It is a technology that provides less granularity than OPS and a greater granularity compared to OCS. However, it is usually considered as the most viable alternative to OPS, as it does not necessarily require optical buffering of payload and has decreased overhead processing and less restrictive switching. Since a burst is handled instead of packets then burst creation techniques are considered in the input node of the network. Multiple IP packets could be collected to form a burst along with a common header. This header is, at first sent, extracted and processed before the burst in order to determine the suitable pattern. After some delay, called offset time, the burst crosses the network as shown in Figure 2.5. At that moment, all switches and nodes in the route are configured for transfer to route the burst without needing OEO conversions. By forming a burst larger than an individual packet, the required switching speed needed in OBS is lower than the switching in an OPS network. Added to that, since common headers are formed for a burst, header overhead is lower than that in the case of optical packet switching. OBS is a great candidate for the next-generation of optical networks thanks to these favourable features.

There are several key components, other than the switching techniques that contributed to the opaque switch emergence. We provide an overview of some of these components in this section while highlighting their advantages :

- **Optical Add/Drop Multiplexers (OADMs)** : To set the requirements of bandwidth flexibility and operational efficiency, the OADM (Figure 2.6) was introduced to multiplex and route different channels of light into or out of a single fiber. An OADM drops and adjoins a number of wavelengths selectively chosen from a WDM signal while allowing, simultaneously, the remaining wavelengths to pass through transparently. A different range of OADMs exists with different capabilities based on the number of wavelengths they can add or drop along with the easiness degree

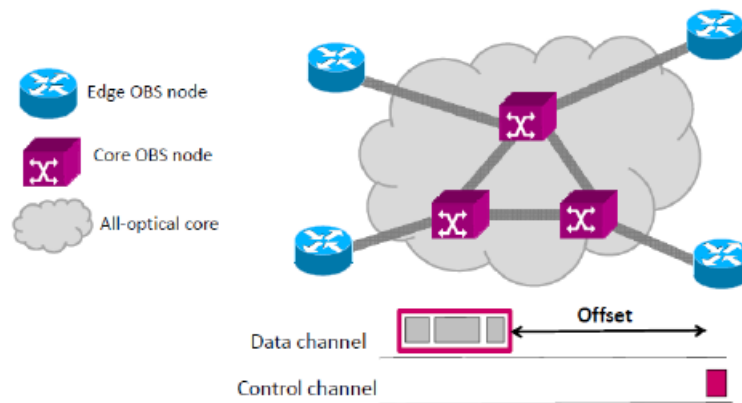


FIGURE 2.5: Optical Burst Switching (OBS).

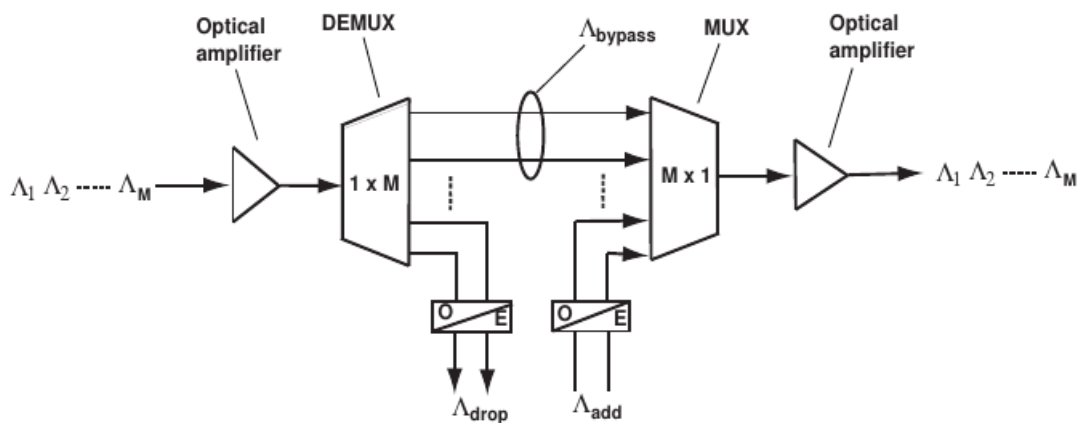


FIGURE 2.6: Optical Add/Drop Multiplexer (OADM) (according to [3]).

of dropping and adding additional wavelength. All the lightpaths that directly pass through OADM are termed cutthrough lightpaths, while those that are added or dropped at the OADM node are termed added/dropped lightpaths [29]. OADM, however, is generally deployed to handle simple network topologies, such as linear topology or ring topologies. For large number of wavelengths or complex topologies i.e. mesh topology or interconnection of multiple rings, OXC is deployed.

- Reconfigurable Optical Add-Drop Multiplexer (ROADM) : As its name suggests, a ROADM 2.7 is simply a configurable OADM which service providers can reconfigure remotely. By adding the flexibility that specifically characterizes the network infrastructure mode any-wavelength-to-anywhere (directionless) using any available port on the network node (colorless)[30]; ROADM can help to improve



the transparency of optics. ROADMs are primarily used in the metro and long-haul networks to optimize operating costs and reduce travel to update and maintain networks. Since their invention, ROADM has experienced a number of innovations and improvements [31, 32].

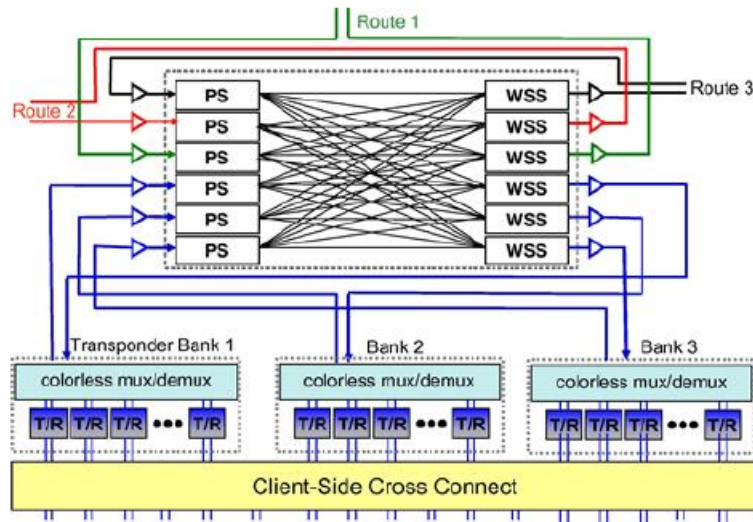


FIGURE 2.7: ROADM Reconfigurable Optical Add-Drop Multiplexer.

- Optical Cross Connect (OXC) : Optical Cross Connect (OXC) (Figure 2.8) can be based on distinct techniques and executes distinct tasks as main components of the optical network. OXC's main characteristics are : optically switching paths, configuring optical topologies and last but not least adding and dropping generated and terminated client layer traffic. This can allow the network to be dynamically reconfigured at the wavelength level, thus, ensuring simple restoration or accommodating changes in demand for bandwidth. They presented interests primarily for a mesh network or interconnecting WDM ring in metro networks. They are based on three main components : ports of input/output, fabric of the switch and control unit. At network level between all OXC's control unit there must be a communication and control to setup and tear down an end to end lightpath. In particular, N-GREEN OXC's are used to ensure protection in case of failure and to balance the load.
- Wavelength Selective Switch (WSS) : is another device that has been invented to ensure optical transparency. It is used primarily to dynamically reconfigure, route or block certain wavelengths, Figure 2.9. The selective switching of the NxN wavelength can be done by a MUX/DEMUX to spectrally or spatially separate the incoming light input, and then by an OXC switch or any spatial switch to change/swap the route of the wavelength ports. The WSS reconfiguration time



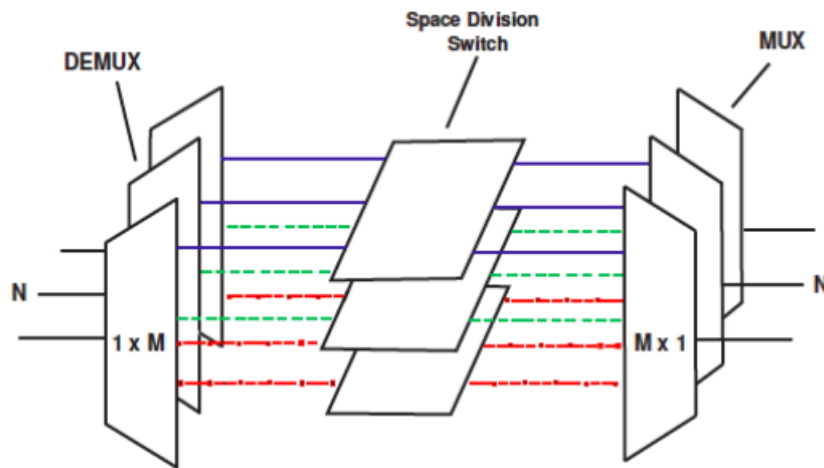


FIGURE 2.8: Optical Cross-Connect (OXC) (according to [3]).

determines the average switching velocity. Currently, the available industrial WSS is based on Micro Electro Mechanical Systems (MEMS) [33] and Liquid Crystal On Silicon (LCOS) [34] technologies, both of which represent no less than  $\mu s$  switching time.

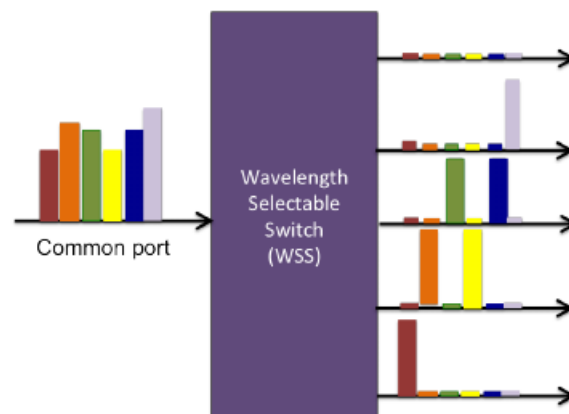


FIGURE 2.9: Wavelength Selective Switch (WSS).

In summary, the main and only brake for the emergence of fast optical switching schemes in products was and remains **the absence of optical memory**; slowing down their replacement to the electronic switch.

This part, summarizes the evolution over the years of transparent optical networks while defining the adopted technology. As it is mentioned above, the first introduced solution in the OPS is the FDL Fiber delay line. It seeks to resolve contention in real

time by imitating electronic memory while taking into consideration the weaknesses and constraints of optical technology, e.g. skimpy optical buffer [35].

Although this technology provides the advantage of being quiet easy to implement, it can not provide complete electronic memory flexibility because of the high restrictiveness of FDL size.

Two significant study lines were subsequently considered :

- Hybrid NxN switching schemes : persuaded that it is totally essential to incorporate a memory to fix the contention issue; a mixture of fast optical space switching and electronic memories was therefore at the focus of most scientists. In fact, a supplemented switch by an electronic shared buffer has been studied extensively [6, 27]; this ensures transparency for packets that do not have to cross the electronic buffer. For instance, the ROMEO[36, 37] and HOPR[38] study projects are among the most notable early study projects that adopt this structure. However, using this strategy, it is mandatory to pass through the buffer once the system is heavily loaded. Several approaches and methods were tested and suggested in this context. The objective is to guarantee maximum optical transparency while ensuring an acceptable rate of packet loss (PLR).
- Fast Optical add/drop Multiplexers : An important marking step in the evolution of transparent optical network is the development of fast optical add/drop multiplexers. Performance analysis of the system shows that OADM decreases significantly the contention. Within the architecture, there still an electronic buffer for the add and the drop part of the system, however, a large part of the traffic can cross in a transparent manner. A  $N * N$  system is built by connecting different OADM boards with an electronic switch. Due to the electronic memory used to store packets in case of conflict, the contention gives the same efficiency as complete electronic systems. Packets pass through the electronic buffers only when we switch the fiber. Otherwise, all packets that pass through the node do not need to be demodulated as they stay in the same fiber until achieving their destinations. Within this context, a series of interested successive projects and papers came out to light. We found, in this context, RINGO, DBORN and lately Packet Optical Add/Drop Multiplexer Technology (POADM) and Time-Wavelength Interleaved Network (TWIN). All these techniques are outlined in more details in the next sub-section 2.3.1.2.

### 2.3.1 Concurrent technologies

The following is an up-to-date survey of main forgoing used or promised technologies suggested for the next generation of optical metro networks. It describes also how they came to suggest N-GREEN network and highlights the components and technologies that should be considered when designing cost-effective and energy-efficient networks.

Among opaque architectures, two competing applicants as optical modes of transportation are to be regarded. The first is defined by using OTN over WDM and the second describes the Ethernet technology concept once used in the network's metro part and is described in detail in 2.3.1.1.

As for the transparent networks, a number of different architectures have been studied over the last few years. These were used as a basis for the suggestions of N-GREEN. In our dissertation, we outline the most known architectures in a chronological order in the section 2.3.1.2 : RINGO, DBRON, POADM and TWIN. The main difference between them is the amount and type of transmitters and/or receivers that the stations are using.

All these proposed architectures could be used as optical transport layer, as an alternative, to e.g. OTN or Ethernet as it is depicted in the Figure 2.10).

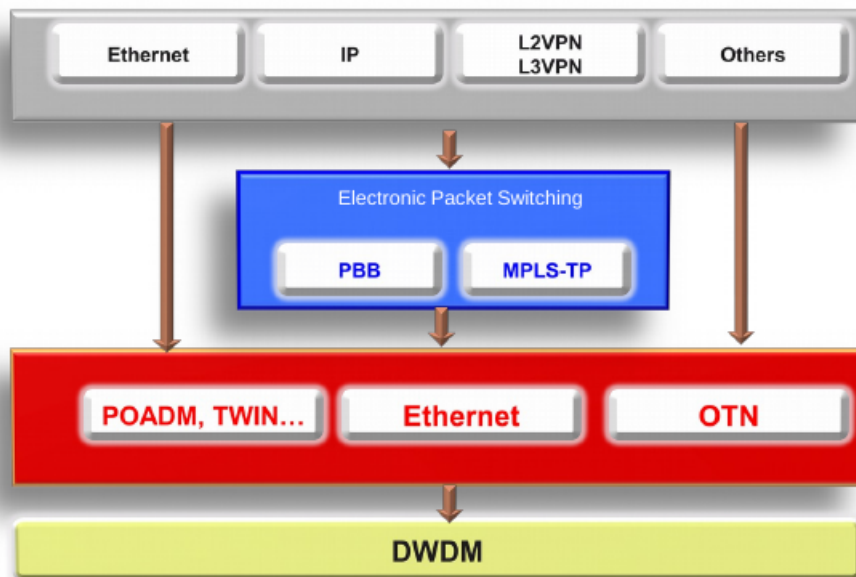


FIGURE 2.10: Layer model displaying N-GREEN competitor applicants.

### 2.3.1.1 Opaque Packet Networks

- **OTN over WDM** : The Optical Transport Network (OTN) [39] technology is based on circuit switching and relies on a connection oriented paradigm. It has been already rolled out in large operators' backbone networks and starts gradually to get more interest for access part. Typically, a generic OTN node consists of an OTN switch, supplemented by a ROADM (Figure 2.11). The latter guarantees that data is inserted, extracted or transferred transparently. Thanks to this combination, OTN node provides features linked to the transport, multiplexing, switching, management, monitoring and survivability of optical channels. The paths between nodes' source and destination are pre-established as OTN is based on circuit switching. Optical switching is achieved either by passing optically transit nodes by ROADM or electrically by the OTN electrical switch. Consequently, this architecture's deployment cost and power consumption are still higher. Although that the cost of the network can be reduced by decreasing the amount of transponders, as it constitutes the main cost of an optical network ; savings are not systematic. It obviously relies on many factors such as, traffic matrix distribution and its evolution ; network topology specifically for mesh network and flow granularity [7].

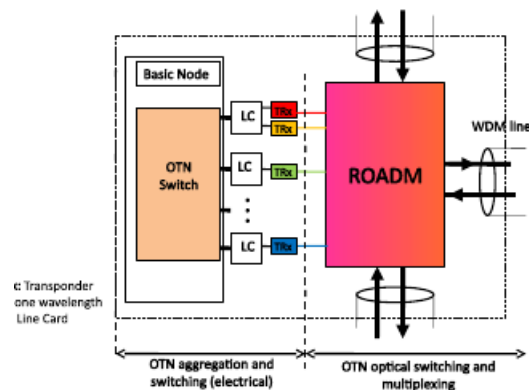


FIGURE 2.11: Node architecture of OTN.

- **Ethernet** : The overwhelming success of Ethernet technology in LANs has prompted a continuous effort among research communities in migrating Ethernet technology into MANs and WANs. It presents a good candidate that could replace some traditional technologies like SDH/SONET [25]. A typical network based on Ethernet technology is made up of opaque nodes capable of aggregating traffic. Opaque nodes are equipped with one or multiple client cards (CCs) and transponders (TRXs) at different rate. At each intermediate node, L2 frames are switched in the electronic domain and received at the destination node. Therefore, a TRX is required at each

node for each wavelength to send and receive traffic over the Ethernet ring. Statistical multiplexing is achieved thanks to the OEO conversion and the possibility to retransmit the Ethernet frames on any wavelength, i.e thanks to packet switching performed in the electronic domain which offers wavelength conversion for free. However, Ethernet has a scalability problem. This scalability concern arises from the fact that the MAN/WAN are equipped with WDM/DWDM fibers. In order to support full traffic switching, the number of OEO transceiver ports needed by an Ethernet switch has to be proportional to the number of wavelength channels per fiber multiplied by number of fibers incoming to the switch. This makes Ethernet neither scalable nor cost-effective.

### 2.3.1.2 Optical Packet Switched Networks

In the past few years, several architectures for optical-packet ring have been suggested. Here, we expose a short summary of these technologies.

- **RINGO** : Ring Optical network [4] belongs to the series of Italian initiatives centered on the development of various metropolitan optical packet architectures. Within the RINGO project, developers are attempting to bring the logical complexity at the electronic stage; while at the same time aiming to achieve an effective use of the optical bandwidth. The very first version of the proposed architecture considers a unidirectional ring that operates in a slotted mode with fixed-duration frames.  $N$  nodes compose the architecture along with at least one wavelength ( $W = N$ ) per node. Fixed-size packets are formed and stored in the electronic format in each node and then sent to the ring later. An example of the RINGO station's overall architecture is shown in Figure 2.13.

It is based on the following :

- An array of tunable transmitter used for packets insertion.
- A fixed tuned receiver that operates on a specified wavelength assigned to each node. A node must therefore tune its transmitter to  $\lambda_X$  in order to communicate with node  $X$  as shown in 2.12.

Packets are transmitted in a slotted way in time and synchronized with all wavelengths. The monitoring method  $\lambda$  ensures that free slots are detected while this prevents collision. The upstream transit packet has the priority for accessing to time slots and the packets to be sent are stored electronically in each destination's Virtual Output Queuing (VOQ) structure. This is used to avoid the effect of blocking the head of line (HOL).

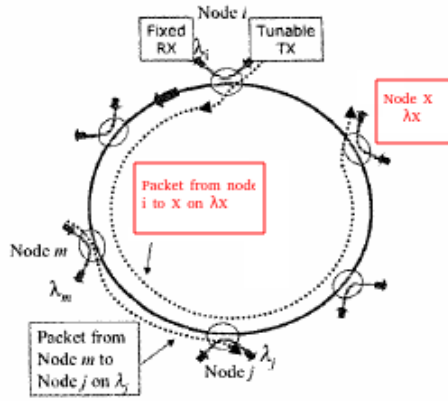


FIGURE 2.12: RINGO Optical network.

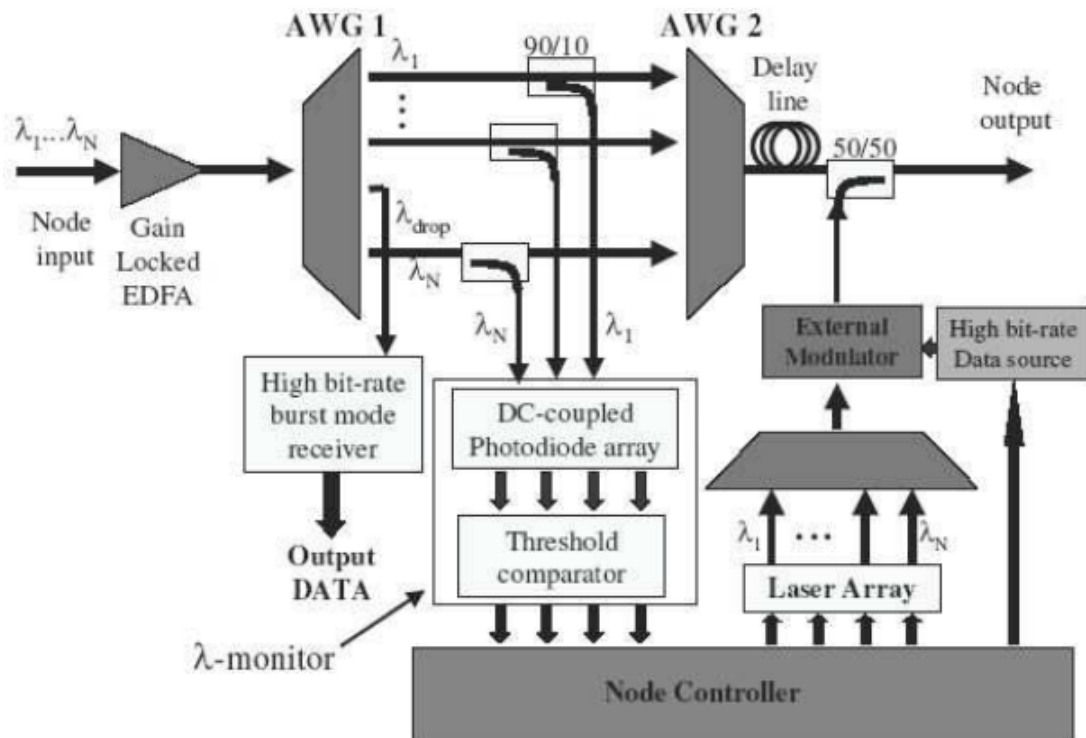


FIGURE 2.13: Structure of the first version of RINGO node (from [4]).

RINGO subsequently evolved into a more sophisticated framework as a complement of RINGO project called WONDER [40] without the prior restriction  $N = W$ . Unlike the first version, the transmission resource is segregated from the receiving resource. As it is based on a bidirectional ring, packet transmissions are in one direction and receptions occur in the opposite direction. The weakness of this technique is the loss of space reuse; this can boost the network's throughput considerably if it was

allowed. It should be noted that recovery can only be achieved with a single failure. One of the extremity nodes named master is chosen to loop the ring. Therefore, the failed link is isolated and is a new master node for each remaining bus network.

- **DBORN** : stands for Dual Bus Optical Ring Networks ; a technology that has been designed by Alcatel [5]. It has been studied in several projects as instance NOBEL and DAVID. It can be considered as an extension of the Passive Optical Network PON concept to the metropolitan network.

In fact, the 2.14 architecture consists of a bidirectional ring that is connected to others via a particular node called the **Hub node**. It can logically be viewed as two unidirectional buses ; the upstream and downstream buses that transmit information to/from the access nodes to the hub. Access nodes in the upstream bus share a common transmission medium to carry their traffic to a centralized node (Hub node), while the downstream bus carries traffic to all access nodes from the Hub node. For the cost effective solution, each ring node possesses passive components, resulting in not being able to drop any transit packets in the upstream line. In order to ensure optical transparency, each access node integrates Fiber Delay Line (FDL) in order to store packets in transit optically instead of storing them in the electronic buffer as within the well known RPR architecture [25]. This ensures optical transparency for the transit line upstream.

DBORN adopts optical unslotted CSMA/CA 2.15 as protocol to access to the transmission channel for detecting vacuum between two successive optical transit packets. CSMA/CA protocol can measure the size of voids and notify the node to insert a local packet into the detected void as all transit packets pass through the FDL.

As indicated in the Figure 2.15, the transit signal is divided into two identical signals thanks to an optical coupler : the primary signal goes straight to the next node and its copy is received by a photodiode. Using the FDL with a storage capacity of approximately 1500 bytes (the maximum size of an Ethernet packet), the collision between a packet to be inserted and the packet in transit is avoided based on the photodiode information. Two critical issues arise when combining CSMA/CA protocol with an asynchronous-based bus network that bandwidth fragmentation and "position priority" [41]. A centralized traffic control mechanism (TCARD) has been developed [42] to enhance fairness between nodes on the upstream bus. However, two access mechanisms were then suggested for fairness and bandwidth segmentation in DBORN. The first, Modified Packet Bursting (MPB)[43], is intended to improve network transmission effectiveness (i.e. resource utilization) by removing unnecessary optical headers. In fact, MPB with the same destination are concatenated and sent with a single optical header. The second mechanism called Dynamic Intelligent

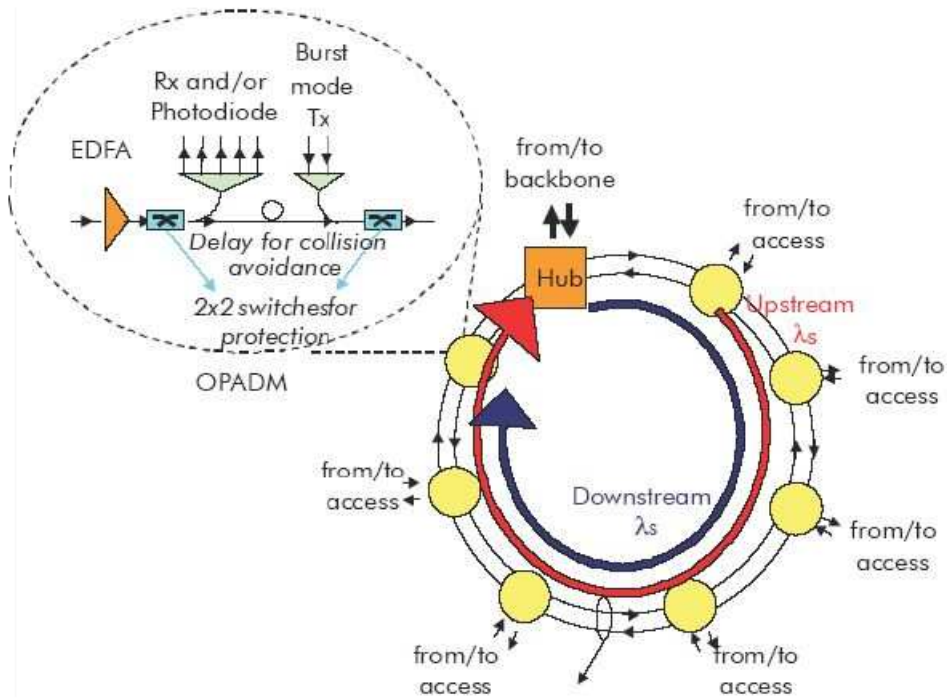


FIGURE 2.14: Schematic representation of DBORN architecture and node (according to [5]).

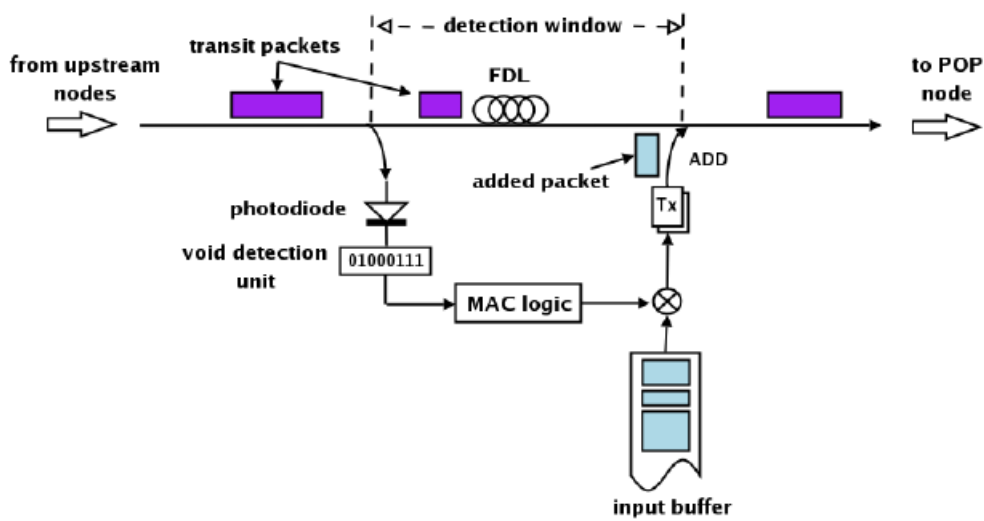


FIGURE 2.15: Optical asynchronous protocol CSMA/CA.

Medium Access Control(MAC-DI) where the [41] solves the above-mentioned issues. DI-MAC is based on a distributed algorithm that dynamically spaces the transmission of packets to prevent inefficient bandwidth fragmentation. Ensuring thus more



usable bandwidth for downstream nodes. These mechanisms' performance assessment has shown that they considerably enhance network performance in terms of fairness between nodes and resource utilization compared to OU-CSMA/CA while enhancing the rate of packet loss and delay. They also make the network more stable and more adaptable to traffic changes.

- **POADAM Packet Add/Drop Multiplexing (POADM)** POADM based on WDM ring networks was suggested by the same N-GREEN project group as part of the ECOFRAME project [44]. The considered network consists of unidirectional or bidirectional slotted ring, as shown in Figure 2.16, using [45–47] Optical Slot Switching OSS technology. The early version defines a WDM ring network that operates over 40-wavelengths at 10 Gbit/s. Subsequently, advanced studies [45] demonstrated the feasibility of a bit rate transparent ring based on POADM up to 100 Gbit/s.

For network control purposes, the nodes are connected with a single out-of-band control channel. The data channel is switched all optically. However, the control channel must undergoes OEO conversion at each node in order to be processed. This process is necessary since control information relative to each data channel and to the global ring (e.g. Operations, Administration, and Maintenance (OAM) messages) is carried within. The channel of data and control are synchronized and has slots of fixed size. The data slot is 10  $\mu$ s long and can carry only one burst; the value of 10  $\mu$ s is deducted from previous studies [48].

The POADM node ensures the emission, the transit and the reception of bursts. The simplified node architecture of POADM [6] as illustrated in Figure 2.17 is equipped with four key components are :

- Tunable optical transmitter.
- Optical multiplexer and demultiplexer.
- SOAs as optical fast gates.
- One or multiple receivers.

Once a node receives an incoming WDM line; it is demultiplexed by the optical DEMUX. The SOA gates are reconfigured based on the data obtained from the control channel. The SOA gate is in the "OFF" position if it only passes through the optical packet transparently; otherwise, it is suppressed. Therefore, only packets that need to be dropped or added are processed and the remainder crosses the gates are then multiplexed into the exit fiber all optically. Each node can obtain one or more wavelengths in accordance with the amount of receiver considered in the architecture. However, once an empty time slot is identified; only one burst can be introduced by a fast tunable transmitter at any wavelength. In a nutshell,

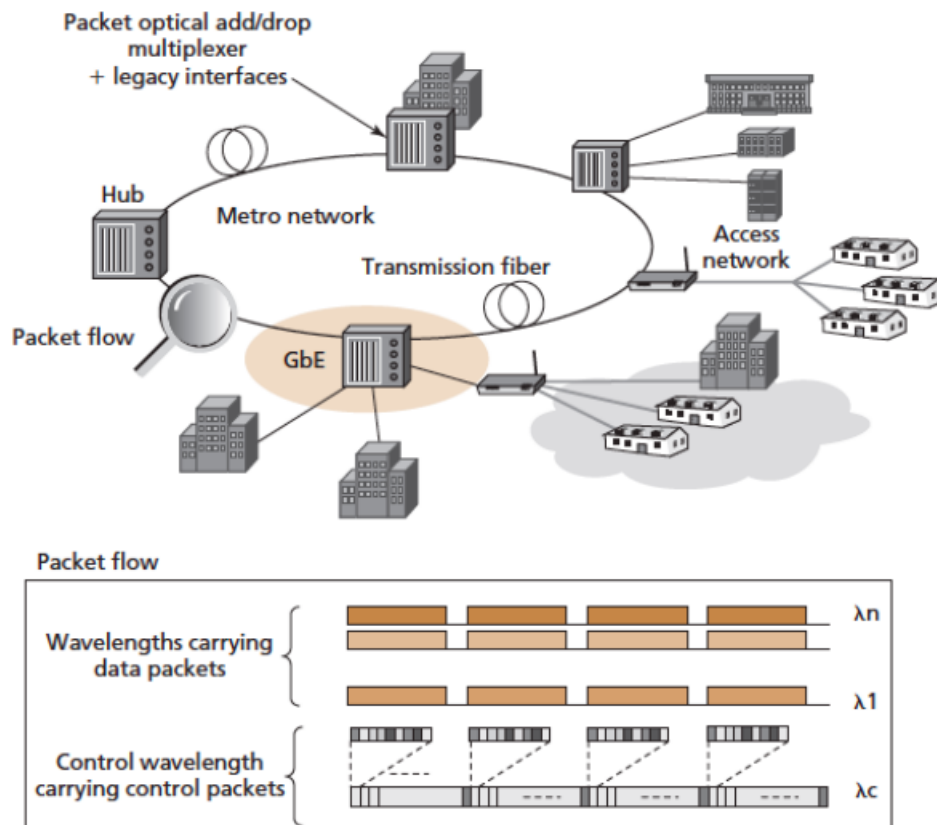


FIGURE 2.16: Metro Network based on Packet-OADM Ring Model (according to [6]).

the POADM ring provides optical transparency and granularity of sub-wavelengths, making it an appealing solution for future metropolitan area networks. Nevertheless, the architecture utilizes complicated optical equipment, such as fast tuneable lasers that are still expensive and hard to use in operating systems. Moreover, the notion of POADM includes cascading many de-multiplexers, which needs very powerful demands on the precision of the channel wavelength. Finally, as they operate on a single wavelength, many SOA-based optical gates are needed.

- **TWIN** : The Time Domain Wavelength Interleaved Networking originally designed by Bell Labs [49, 50]. TWIN is an optical transport network architecture that provides an all-optical sub-wavelength granularity without incorporating either [49] optical fast switching or buffers. The use of passive components such as wavelength selective switch (WSS) incorporated in the inner network nodes ensures optical transparency. The complicated processing is driven to the nodes' edges incorporating **receivers in mode burst** and **fast tuneable lasers**.

TWIN's mode of operation is articulated shortly as follows : Giving that each edge node has its specific wavelength data receiver and while any specific source

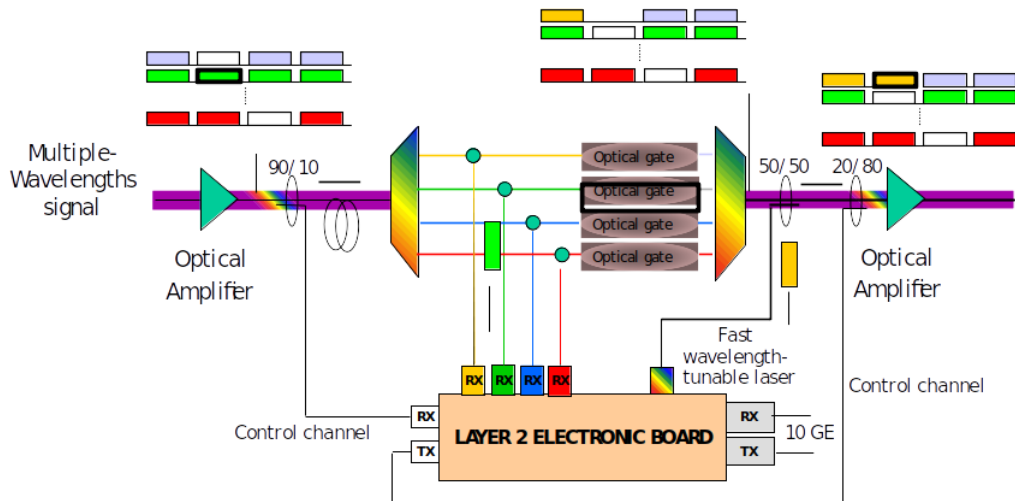


FIGURE 2.17: Packet Optical Add Drop Multiplexer Node Architecture.

has a burst to be sent to a given destination ; that source tunes its laser to the already assigned wavelength. A Selective Wavelength Switch (WSS) in each internal node guarantees the best possible path for the incoming wavelengths. The latter is directed to the appropriate outgoing ports without the need for OEO conversion, based on the burst color. As viewed in Figure 2.18, it is possible to consider TWIN's virtual formed topology as overlaid multi-point to point trees. Within TWIN, it is regarded that a dedicated wavelength performs an automatic discovery of resources, routing and signaling. The cross-connect configuration remains the same within a very long time scales as reconfiguration is needed only when a failure occurs or when a fresh link needs a fresh tree branch to be created. Since several nodes share the same medium to reach a specific destination ; collision could occur at each tree merging point. In order to avoid this situation ; TWIN relies on a complicated scheduler to coordinate transmission between source nodes. The transmission to each destination is organized in repetitive cycles. A cycle in this case refers simply to a set of slots used by a given source node. The scheduler's function is to assign the suitable slot(s) within each cycle to the pair source destination, thus avoiding collisions.

Two scheduler variants were suggested :

- The first is a centralized version with a single control entity. This latter is installed within the network in a particular point. By collecting and processing all the necessary information (e.g. traffic demand matrix) in a relatively long time interval ; the scheduler can efficiently attribute slots to each source/destination couple. The scheduler's decisions are sent to the edge nodes via an out of band control channel.

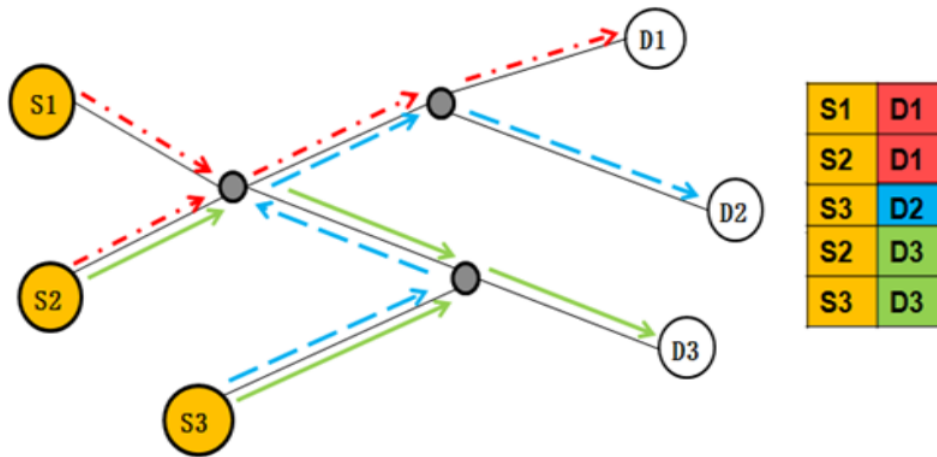


FIGURE 2.18: Illustration of TWIN principle.

- As for the second one named distributed; a control entity per destination is taken into account. The distributed scheduler is more appropriate for asynchronous traffic with dynamic bandwidth requirements. To speed up the scheduler's response time; each destination is assigned to a control point that assigns independently slots to sources. As it is based on a distributed scheme; decisions are taken upon the request of the source's resource. A source can therefore obtain a set of numerous grants and requesting, at the same time, to be transmitted which may causes conflicts. Several [51, 52] algorithms were suggested for a congestion control protocol.

Authors present a novel TWIN version in [53] based on assigning a wavelength per source instead of the destination. Source, thus, becomes the root of a multipoint lightpath shared by all destination nodes. The variant replaces tunable transmitters and fixed wavelength receivers with fixed wavelength transmitters and coherent tuneable receivers. TWIN concept looks interesting in terms of fast switching and providing all functional characteristics for carrier-grade operation (no loss, low latency, limited jitter, and fast restoration), at least in metro networks. It also guarantees transparent grooming without the need for buffers or collision in intermediate nodes due to a robust control plane. Nevertheless, as for the POADM network, TWIN requires complicated optical equipments such as fast tunable lasers. In addition, assigning a certain number of wavelengths to each egress node may lead to scalability issues and to fiber link underutilization due to the lack of wavelength reuse.

The properties of the optical packet architectures are compared in the table below 2.2.

Name	Type of Topology	Slotted	Control Channel	No Type for Transmitters per node	And for receivers per node	Packet Removal per Destination
RINGO[4]	unidirectional ring (vers.1). 2-fiber bidir. ring (vers.3).	Slotted	in-band	1, tunable	1, fixed (laser array)	vers. 1 : yes vers. 3 : no
DBORN [5]	2-fiber bidirectional. ring with hub.	Slotted Unslotted	in-band	$\geq 1$ ([54]) fixed	$\geq 1$ ([54]) fixed	no
POADM [44]	unidirectional . or bidirectional ring	Slotted	out-band	1, tunable	1, fixed (laser array)	yes
TWIN [49, 50]	mesh topology	Unslotted	out-band	1, tunable	1, fixed (laser array)	yes

TABLE 2.2: Optical Packet Ring Architectures.

## 2.4 Conclusion

Through this chapter, we reviewed a few optical transport systems in the scope of metropolitan area networks while highlighting the main broken of emergence of all optical networks. In fact, the deployed/proposed network architectures and protocols are the result of a gradual accumulation of improvements and developments aimed at maximizing the capacity to transport optical networks by proposing fast optical switching.

Implementing optical switching techniques has excellent potential to improve the energy efficiency of future network switching nodes. Despite several remarkable laboratory tests of optical packet switches; optical switching takes place only at the wavelength channel level, e.g. in ROADMs in current operational networks. N-GREEN aims to capitalize on mature technologies (mostly derived from next-generation optical access network designs). The suggested method will be based on WDM optical packets allows gaining the best benefit from the wide bandwidth of optical gates and switches. It becomes cost-effective thanks to the progresses of opto-electronic integration of the transceivers.

In the next chapter, we will present the novel architecture named N-GREEN while emphasizing its specificities in comparison to competitive architectures.

# Chapter 3

## N-GREEN Architecture

### 3.1 Introduction

As stated in chapter 2, the need for fresh network architecture becomes inevitable. In response to the traffic evolution highlighted in chapter 2, and to react to emergency demands for a cost-effective and energy-efficient network ; N-GREEN project was introduced. The purpose of this project is to design and validate a versatile, scalable capacity, low cost and low energy consuming network architecture as well.

Two innovative concepts were proposed :

- A WDM Slotted Optical Add-and-Drop Multiplexing (WSADM) : that can be viewed as an accumulation and deduction of numerous researches and experiments done within Packet Optical Add Drop Multiplexing (POADM) that is described in detail in the previous chapter 2. As the deployment of WSADM equipment relies on the deployment of a new optical networking technology ; exploiting a WDM slot concept, as a novel specification of new network architectures became mandatory. This will be defined through this chapter.
- A modular high-capacity backplane inside a switch/router to interconnect line cards. As this feature is not connected to networking issues ; it is rather connected to node one ; therefore, it is not discussed in this thesis.

Given that this work analyzes the efficiency of the N-GREEN network ; this chapter is entirely devoted to describe this new concept. As a first step, we define the functional and physical specificities of N-GREEN node in Section 3.2.1. Subsequently the details of the working mode of WSADM, processes of insertion and extraction, reservation and information about the data channels considered in N-GREEN network are presented in

section 3.2.2.1. The network architecture and the technological hypotheses considered in this thesis are pointed out at the end in section 3.4.1.

## 3.2 N-GREEN concept

N-GREEN node concept combines sophisticated optical technology with electronic strength while considering mature and available components. The main purpose is to suggest a scalable architecture while addressing problems such as cost and energy efficiency and wavelength capacity facing traffic evolution.

The chapter is started by a specification of the N-GREEN node functionally and physically while highlighting the impacts of some components in the network operation mode.

### 3.2.1 N-GREEN Functional and Physical Description

Functional scheme of an N-GREEN station is shown in Figure 3.1. Globally, it includes five building blocks.

- The optical add/drop multiplexer denominated WDM Slotted Add/Drop Multiplexer (WSADM) : is used primarily to manage optical slots in the physical layer. The main functionalities for a WSADM is
  - Drop and erase : The node receives the optical packet and strips it off.
  - Drop and continue : The node copies the optical packet and enables to continue its path optically.
  - Drop and add : The node drops the optical packet ; fill with another set of packets and insert it into the network.
- The line cards of the switch/router : Their main function is simply to process and schedule the data before and after the switching.
- The backplane of the switch/router : Its main function is to switch the data to dynamically interconnect the different line cards or electronic cards of the switch/router.
- The protection system : used for the purpose of ensuring the continuity of operation in case of failure. It includes the required elements to protect the global system managing thus the data in case of both cable or node failure.

Nonetheless, the mechanism of protection depends on the topology implemented, which in turn, depends on the network considered segment. As it will be detailed a little further in the report ; this thesis considers a bidirectional ring where one ring



is used for transmitting data and the second is used for protection. For the same reason, the node is also duplicated.

It is important to note that N-GREEN nodes are connected to a Software Defined Network (SDN) controller that is used to provide protection in some scenarios, but also for other purposes.

Considering this scheme, two separate protection scenarios are proposed ;namely, a completely hierarchical one where the SDN controller manages protection and restoration in a fully distributed system or locally, where all decisions are made by the nodes based on data extracted from the control channel. The last option allows a very brief time protection and recovery ; approximately defined by the time of propagation. Nevertheless, the nodes of the routes taken by the flows that traverse them depend on extensive knowledge. Using a Fast ReRoute FRR method [55] defined to be an effective trade-off as it offers rapid protection without needing the dissemination of information per stream ; while the SDN controller is set up to restore the optimal route.

- The client boards : Thanks to the client boards data, coming from the client layer are collected and sent later to the switch/router for switching or routing.

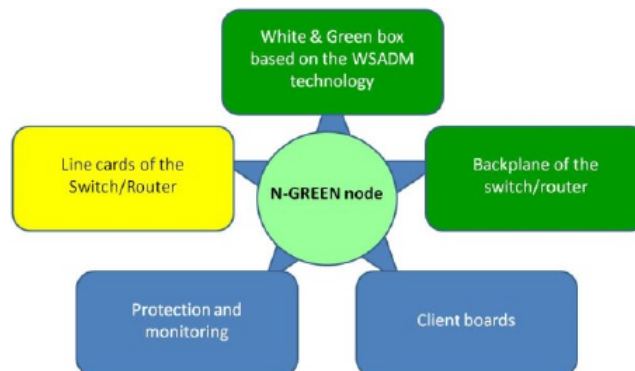


FIGURE 3.1: Main sub-blocks of the global node functional structure.

These features could be provided by traditional components used in the optical node such as a set of transmitters TRx, Variable Optical Attenuator (VOA) and optical coupler.... etc except some of a specific components used in the context of N-GREEN which are briefly described in the following :

- Semiconductor Optical Amplifier (SOA) : SOAs are very appealing optical components thanks to their linear features, their large nonlinear coefficients and the compact size as they can be monolithically incorporated with other optical components. As for space switches, signal re-generators and wavelength convectors become

significant players in ultra-high bit rate optical networks. They have less than 1 ns of switching time with 45dB extinction ratio as active space switches [56]. The high speed response of the SOA switch and its implementation in different architectures has made it a sub-wavelength granular switch for OPS or OBS switching node structure.

Within N-GREEN, SOAs are controlled by SDN (Software Defined Network) controllers and they are mainly used as :

- A simple optical amplifier in some usage cases or simply for an upgrade operation.
- An optical gate; compared to POADM dedicating one SOA per wavelength. N-GREEN utilizes one single SOA per 10 wavelength waveband ( $10 \lambda$ ) to optimize network costs. This, however, has the impact that slots can only be re-used when all packets are transmitted while using the B&S transmission mode.
- A power equalizer, calibration of the operating point of the SOA plus a driver to reach a correct operation.
- Fixed laser source : as the name indicates; fixed Laser source is an optical source with fixed wavelength. In brief, the choice of wavelength is not allowed at the insertion time of the optical packet. As a rival, we found fast tunable laser [57] where wavelengths could be tuned and switched from one to another in less than a few hundreds of ns for a channel spacing as low as 12.5 or 50 GHz. Although that the latter has gained considerable attention thanks to these features; it has the disadvantage of being less stable and more costly, especially in packet switched optical networks. The choice was therefore concentrated on fixed lasers within N-GREEN.

The Figure 3.2 shows a descriptive instance of N-GREEN node.

## 3.2.2 Overview of N-GREEN specificities

### 3.2.2.1 Insertion processes

In short, N-GREEN concept combines optical transparency and electrical packet granularity. Emitted electrical packets, including for example Ethernet frames, are gathered into containers named colored optical packets. Each colored optical packet, sized of  $10 \mu s$ , is encoded over 10 wavelengths (from  $\lambda_1$  to  $\lambda_{10}$ ) via a shift register mechanism during  $1 \mu s$  time slot, as it is presented in Figure 3.3, with 50 GHz or 100 GHz frequency

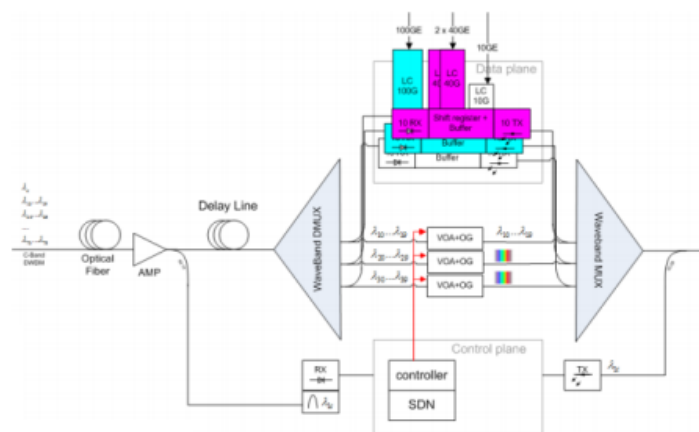


FIGURE 3.2: Physical N-GREEN node architecture.

spacing. The container duration of  $10 \mu\text{s}$  corresponds to, at most 12500 bytes at a bitrate of 10 Gbps without taking into account guardband, preamble and framing overhead. The duration of WDM slot of  $1 \mu\text{s}$  leads to a trade-off between the maximum time a client frame waits before being sent for insertion in an optical slot and the mean filling ratio of the container. A WDM slot of 10 wavelengths has been chosen to be compliant with the conventional data rate evolution of legacy and next generation architectures (10 and 100 Gbps). These packets of small sizes are switched transparently in the optical domain.

As data and control information are sent separately, their control fields are carried by a dedicated wavelength  $\lambda_{11}$  at a moderate bitrate; reducing, thus, the constraints of electrical processing. Note that control channel carries information on the data packets: if they are intended for this node, if they will have to be dropped etc.. Each node is equipped with a fiber delay line on the data path to absorb the processing time of the control channel. This control channel is regenerated at each intermediate node to guarantee the self-synchronization of the network in particular.

Within N-GREEN, Switching granularity is moving from Optical Packet Switching (OPS) to Optical Slot Switching (OSS) where we consider WDM Slot Switching. N-GREEN node uses WSADM multiplexers to insert and extract WDM slots. Compared to POADM architecture, where new traffic demands are processed by adding new transponders [46], the N-GREEN node is overdimensioned since it uses 10 wavelengths at a rate of 10 Gb/s independently of the traffic. New demands, as such, are processed by adding new electrical client cards ensuring, thus, a very high scalability. However, the over-dimensioning cost due to 10 wavelengths initial provisioning is reduced thanks to

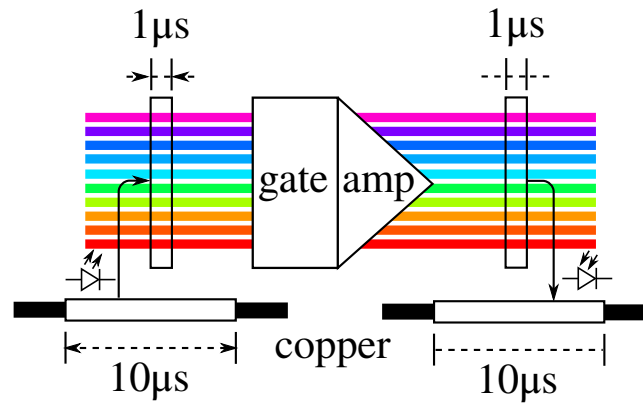


FIGURE 3.3: A symbolic presentation of a N-GREEN node connected to a 10Gbps Ethernet. There is set of fixed lasers, an optical gate, an amplifier and a receiver.

photonic integration and the use of 10 fixed lasers instead of a tunable one at the level of the transponders 3.2.1.

Besides, thanks to the shift register mechanism and the smaller time granularity ; the insertion delay for N-GREEN packet can be as small as  $1 \mu\text{s}$  when the optical container is constructed, compared to (at least),  $10 \mu\text{s}$  for other optical slot switching technologies, such as POADM.

For the rest of this report, we denote an PDU (Packet Data Unit) the information structured by an N-GREEN station that aggregates several « SDU » (Service Data Unit, typically Ethernet frames) to form container(WDM slot) and insert them later through the network. A PDU consists, in some overhead information, of a set of complete SDUs and in some stuffing used to reach the fixed container size which equals to 12500 bytes as mentioned earlier.

### 3.2.2.2 Reception and extraction process

Packet extraction and drop depends on the queuing policy considered in the network under evaluation. Indeed, two different modes could be used to benchmark N-GREEN network based on the enabled queuing policy at source nodes which depends in its turn on to the scenario and segment of the network under evaluation :

#### — Queuing policies

- **Destination based mode :** One PDU contains SDUs for either one or several destinations. This mode supports point-to-point (or unicast), as well as one-to-many (or multicast) communication schemes, based on label switching. It requires the sending station to take into account the destination of each SDU

when building the PDU and marking it with its label. This work takes only into consideration the point-to-point (or unicast name is used for the remainder of this dissertation) mode. It uses a different queue for each destination implying that grooming at the source node is not allowed. Resources are, therefore, well shared between nodes but containers will not be well filled specifically for low and medium loads. In particular, if their paths do not overlap; two different nodes can have simultaneous access.

The slot release process is guaranteed using **destination release mode** where the **last** destination station of a PDU deletes it. Note that filtering is performed on the PDU label part of station configuration. In a label-switching mode, it is easily implemented by associating to a label (either PDU or SDU) the appropriate action to be performed.

Actions which can be carried out on a packet could be :

- Drop-and-continue : It consists of retrieving the local copy of an optical packet and enabling it to travel transparently through it.
- Drop-and-erase : It consists of dropping and erasing packets so that WDM slot can be instantly re-used.
- **Broadcast and select mode (B&S )** : A set of SDUs with different destinations may be included in the same PDU. An emitted PDU will be read by each station it passes through and which will only copy the SDUs that are destined to it. This mode facilitates the constitution of PDUs as packets are not even treated in the entrance node but requires SDU filtering at each station in order to receive the appropriate flows (this is similar to the handling of downstream traffic in Passive Optical Networks). The policy considers one queue and therefore creates one common container for all destinations. Therefore, the containers are more likely to be well filled when they are sent. However, this policy reserves the ring for only one node each time. The use of the resource may be ineffective for heavily loaded networks. A specific feature of N-GREEN is that there is only one Semiconductor Amplifier optical (SOA) [58] for all wavelengths (see Fig. 3.3) which implies that a PDU can only be removed in its totality if all packets are either transmitted or suppressed.

### 3.3 N-GREEN network scenarios

The new designed versatile and modular node architecture could be used mainly in :

- **In the metro access/aggregation network** : N-GREEN is appropriate for the wireline part as well as for the fronthaul/backhaul links for the wireless

part. It provides a sustainable cost-optimized alternative to traditional electronic transportation, namely Ethernet [59]. Basically, N-GREEN architecture nodes could be used as an example in an aggregation network for an Internet Service Provider (ISP). In this case, Ethernet nodes i.e. switches Optical Line Terminal (OLTs) or a Digital subscriber line access multiplexer (DSLAMs) could be attached to the N-GREEN bridge nodes. Whereas, an N-GREEN switch node is attached to the IP edge named PoP Point of Presence. Mostly, a ring is used to interconnect bridge/switch nodes to each others. Several circles could be interconnected together with one given PoP, depending on the region enclosed.

- **Metro backbone network** :It could be used ,as well, as a solution for the metro core and the backbone, as an example for the metropolitan/Regional IP network. In this case, the network may be either a single ring, or an interconnection of rings or even a mesh network. Within this context, N-GREEN guarantees high-capacity dynamic bypasses, thus, providing an effective interconnection channel for communication between data centers.
- **Xhaul** : It is worth to note that the proposed architecture could be used as well as in the Xhaul networks. An Xhaul transport network interconnects Remote Radio Heads (RRH), macro or femto cells, BaseBand Units (BBU) and the IP edges of one or many ISPs [60]. As the next generation considers centralized/cloud radio network C-RAN instead of the distributed one ; they may confront the problem of controlling the latency in the transfer process. Evidently, low latency is one of the main challenges to raise specifically for some services where End to End (E2E) latency have not to exceed 1 to 10ms. Another critical problem to consider in the C-RAN context is the periodicity of the data transfer between RRH and BBU.

Some researchers were interested in the performance of this architecture once used in the Xhaul networks [61–63]. A cost optimized and deterministic scheduler supporting the time-sensitive CPRI traffic with zero jitter has been proposed [64]. The performed studies have shown that significant cost and energy consumption reductions were obtained when compared to a same capacity state of the art Ethernet technology.

## 3.4 N-GREEN Optical Packet Switched Ring

### 3.4.1 Studied Network Architecture

Since the research focuses mainly on the metro part of the network; the studied architecture in this dissertation considers a bi-directional ring where one ring is used for data transmission and the other one for protection. An N-GREEN network includes two types of nodes as it is the case for the metro network part : those on the ring termed bridge nodes while the node that closes the ring by an electrical bridge termed optical switch node (PoP). Transit traffic bypasses intermediate nodes in a transparent way, i.e. it does not need to be demodulated inside the nodes' electronic structures. Indeed an optical switch node connects the ring to other rings where Optical OEO conversions occur at the level of this node.

The architecture in question is shown in Figure 3.4

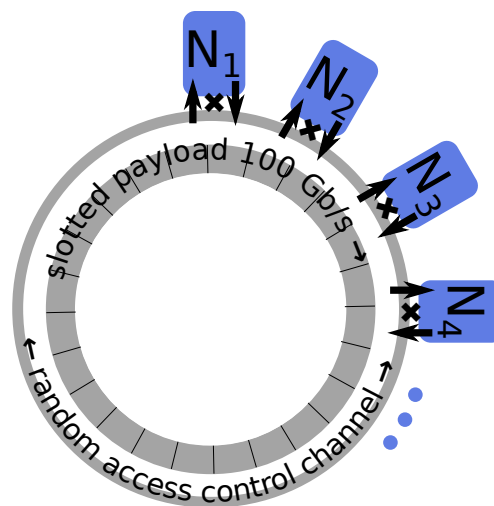


FIGURE 3.4: Optical ring topology.

As the applied transmission modes 3.2.2.2 depend on the targeted network segments; it will be specified before each contribution 4, 5.

### 3.4.2 Scenarios

The process of inserting optical packets into the ring varies depending on the network's operating mode. In fact there are three insertion policies that can be used in the N-GREEN network.

- **Opportunistic mode** : Whenever a WDM slot is empty; a node can use it to transmit an optical packet. Note that the node may decide not to use that WDM slot if it considers that none of the PDUs currently built is ready for transmission.
- **Time division multiplexing (TDM)** : TDM is a benchmarking scenario often used in telecommunications in which containers are sent upon a regular interval of time regardless of current network state and container filling level. The interval of time used in N-GREEN network is  $10 \mu s$ . This value permits to fill at most 12500 bytes at a bitrate of 10 Gbps client cards without taking into account guardband, preamble and framing overhead. In fact, the impact of optical fixed packet creation on optical network performance was studied in [65]. Performance analysis of such systems has allowed to determine certain values, such as, time slot length and mean waiting time... etc. According to [65, 66], the best choices are assigned to the use of a fixed size optical packet (WDM slot) with a regular length of  $10 \mu s$  which explains the value used in the N-GREEN project.
- **Timer based mechanism** : The notion of timer-based mechanism has been introduced in [67] for burst assembly for optical burst switching (OBS) networks. The main purpose behind timer scenario is to guarantee the best trade-offs between latency and packets loss. Using this method, during the optical packet creation, incoming electronic packets are buffered inside a filling buffer. These packets remain memorized until the moment when sufficient information is collected for the optical packet creation. Even when the following slot is available, electronic packets must wait until the arrival of the packet that triggers the optical packet creation. In this experiment, the main reason for using this technique is to ensure the best trade-offs between two competing variables including latency and energy efficiency. Only constant value of timer [65] and CoS-wise [68] have been used to the best of our knowledge, so far. We use optimization in this research to dynamize this value and to adjust it according to circumstances[69]



## 3.5 Conclusion

This chapter has introduced the N-GREEN network's structure and outlined its features.

We started by presenting a new optical networking architecture introduced through the N-GREEN project focusing on a WSADM slotted WDM Optical packet concept. A global functional and physical description of the N-GREEN node are given. The choice of some components such as fixed lasers instead of tunable one and SOA are justified.

In its second part, this Chapter presents a brief overview of the basic characteristics of the insertion and extraction mode for each distribution mode. The size and the value of the unit structure are defined, a functional organization of the typical N-GREEN station is shown and queuing policies possible were pointed out. The presented work contributes to the definition of the basis of the operating mode of N-GREEN layer and to the concept of different entities belonging to it.

Finally, we wrapped up by mentioning potential assumptions we have taken into account in the following work dealing with different angles in the N-GREEN project. Aside from presenting an example of a network architecture to evaluate N-GREEN ; the scenarios that can be studied within this architecture are pointed out.

## Chapter 4

# Adaptation of the N-GREEN Architecture for a Bursty Traffic

### 4.1 Introduction

In this chapter, we display the steps we are going through to adjust N-GREEN network to bursty traffic.

The first part of this chapter features the performance criteria considered when studying N-GREEN's performance. Preliminary results from node-level simulations show that the architecture is overdimensioned, hence advanced method for packet management and transmission for colored optical packet switching has been proposed and evaluated [4.2](#). Results obtained by exploiting wavelength granularity and sharing the different wavelengths are addressed in section [4.2.1](#), while in the second section [4.2.2](#), we display results once a smaller time granularity is utilized.

The second step includes designing, simulating and testing more complicated traffic models. The simulation results show N-GREEN inability to support a highly variable traffic pattern. As a solution, we suggest a dynamic timer adaptation that is dedicated from the sizes of the local and/or global queues. The relation is found using a direct optimization method named Nelder Mead Simplex. The results obtained substantially decrease latency without a need to update the proposed architecture. We only need a way for nodes to inform each other about the momentary size of the data in their output buffers. This is possible as N-GREEN already has a control channel that could be used for this purpose.

The fourth section ends the chapter while outlining the limit of the proposed method and provides some insight into the theory of the proposed scheme to surpass those limits

## Performance criteria

The main performance criteria, defined below, are the mean access delay and the resource's use efficiency. The latency is important for the user, specifically in the context of the 5G where End to End (E2E) which for some services must not exceed 10  $\mu s$ . Nonetheless the resource efficiency is an indicator for both energy and cost efficiency that are of a great importance for service providers.

### Resources use efficiency

Resource efficiency is an indicator of network use performance. It is calculated as follows :

$$R_{efficiency} = \frac{\sum_{i=1}^N x}{12500 \times N} \quad (4.1)$$

where  $x \in [0, 12500]$  is a mean of filling ratio of the WDM slot and  $N$  is the sum of WDM slot used during the whole simulation. This value is an indicator for the resources utilization efficiency.

It is proportional to the energy efficiency. Indeed, it is computed with respect to the different equipment crossed which is estimated by the N-GREEN designer to 0.8 nJ per byte. As we dispose of optical packet of 12500 bytes within the slotted ring studied model ; the energy consumption is computed as follows :  $12500 \times 8 \times 0.8$  nJ. The energy efficiency represents the ratio between 80 nJ and the payload of the optical packet which depends evidently on the filling ratio.

### Mean access delay

Another important performance criterion is the mean access delay, called also buffering time. It refers to the time for which client traffic must wait before being inserted into the ring. Two processes may have impact on the insertion delay. The first one is the queuing policy considered 3.2.2.2 in the architecture which depends on its turn on the network segment under evaluation. The second process is the waiting time for container full filling which is impacted by the scenarios considered 3.4.2. Note that this insertion

time can be as small as 1  $\mu s$  if the ring is free when the container is constructed. This is specific to N-GREEN node whereas this time is at least equal to 10  $\mu s$  for other optical slot switching technologies like POADM.

## Packet Loss Rate (PLR)

The PLR is the ratio between the number of packets lost due to contention, and the number of all circulated packets. It is calculated at a certain system load ( $\rho$ ). The **system load** depends on the mean idle time per source ( $\tau$ ), which is simply the average time interval separating two consecutive packets arriving to a node, and the packet duration ( $\gamma$ ). The system load is expressed as :

$$\rho = \frac{\gamma}{\tau + \gamma} \quad (4.2)$$

The system is called “fully loaded” ( $\rho= 1$ ) when packets are sent one after another unceasingly ( $\tau = 0$ ). This is the most critical operating case.

## Simulation conditions and setup

In order to assess the efficiency of the proposed mechanisms ; we conduct simulation studies using different traffic model, as input. As already discussed in the previous chapter, a basic instance of an N-GREEN network consists of a uni- or bidirectional optical ring which transports colored packets. We have simulated a unidirectional ring with 10 nodes along with line cards at 10Gb/s, as it is defined in the N-GREEN specification. We considered that the second ring is dedicated for protection.

Our simulator is written from scratch for N-GREEN taking as input, among others, the time slot assignment, the operating scenario and network configurations then, returns detailed statistics along the simulation time such as mean access delay 4.1 and network uses efficiency 4.1.

It is worth to note that in all studies, we do not include the travel time through the ring, as this path is all optical and thus, predictable and very fast. We assume that the ring contains  $M = 1000$  WDM slots at a given time which is realistic in the metro area applications.

Various traffic models were considered :

- As for the first part where we attempted to improve N-GREEN’s performance ; we consider a randomly drawn traffic matrices according to a uniform distribution.

At the same time, we assume simultaneously that Ethernet frame arrivals follow a Poisson random process.

- In the second part, when we tried to adjust the network to other potentially interesting uses; we experimented different traffic patterns presented in details in 4.3.2.

## 4.2 Performance improvement of N-GREEN network

We begin by evaluating the network's performance taking into account the typical benchmarking scenarios outlined in 3.4.2. Preliminary results published by our partners depicted in Figure 4.2 (a) consider different values of timer such as  $40 \mu s$ ,  $30 \mu s$ ,  $20 \mu s$  along with T++ where containers are sent only when they are fully filled. Results obtained pointed out a paradoxical behavior of N-GREEN network. Indeed, the higher delays are exactly where the ring is low loaded; revealing that the architecture is over-dimensioned. Therefore, WDM slot sharing was introduced and tested to take advantage of this particular N-GREEN node feature.

### 4.2.1 WDM Slot Sharing

The proposed approach considers a timer with a fixed duration and operates in an opportunistic way. Applying **WDM slot-wavelength**, each node can benefit from the entirely free time WDM slots. It allows WDM slots that are partially used, where the free space is higher or equal to the size of the newly constructed optical container, to benefit from the free time as well [7]. The possibility of the container segmentation was also evaluated along with class of service differentiation (CoS). Three CoS were considered named respectively Gold, Silver and Best Effort (BE). At each time WDM slot of  $1 \mu s$  distributed over 10 wavelengths, some of them may be occupied by the optical packets of a node  $i$  and others by the packets emitted by another node  $j$  while favoring packets with highest priority. This is particularly possible when the system is low loaded ( $\rho \ll 1$ ). An illustrated example is shown in Figure 4.1 composed of 4-node ring topology with 7-  $\lambda$  band and 4 time WDM slots initially affected to the four nodes. Without node-4 container segmentation, the free wavelengths corresponding to Node-3 are lost due to node-4 container size. They can be used however, if container segmentation is allowed and the container is scheduled (e.g., it is filled or timer has before the time WDM slot T3).

Results obtained while applying **WDM slot sharing** in both scenarios; First In First out (FIFO) and with CoS distinction policies are presented in Figure 4.2 (b). In

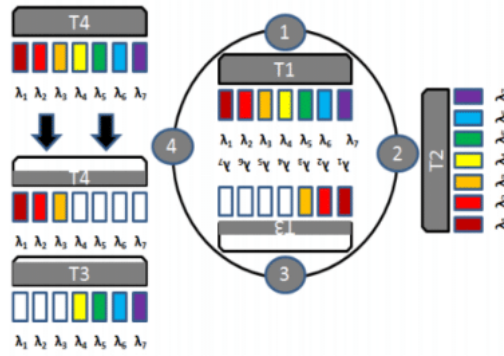


FIGURE 4.1: Packets insertion as WDM slot-wavelength method.

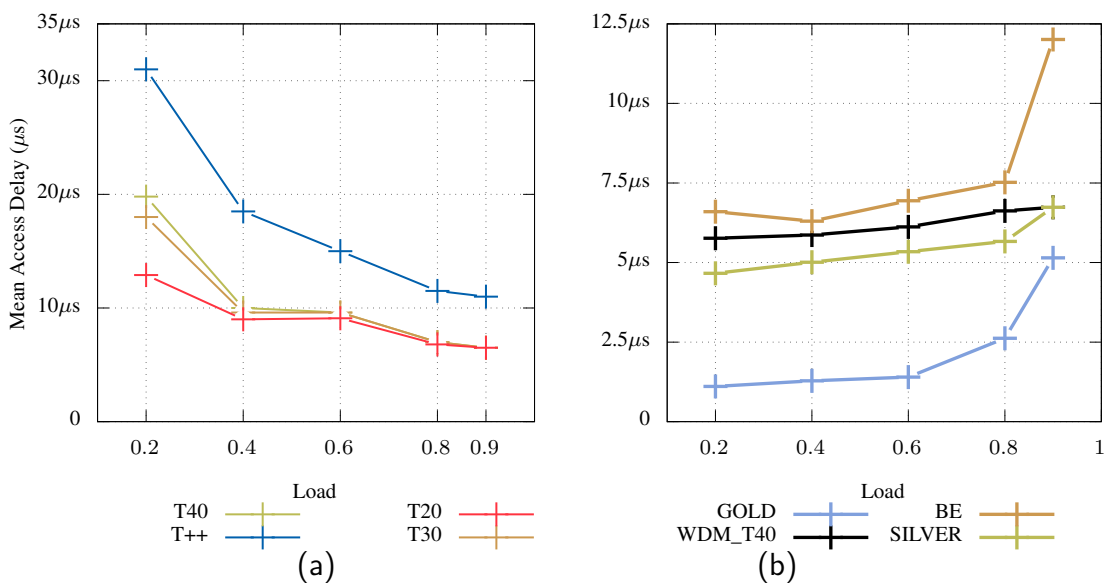


FIGURE 4.2: Mean Access delay for different scenarios in N-GREEN network while considering B&S mode [7]

addition to decreasing significantly the mean access delay by up to 70% for low load cases as seen in 4.2 (b) for the curb WDM-T40; it shows a very good latencies for Gold frames and acceptable results for Silver frames whereas Best Effort frames are not strongly penalized. In spite of an overall improvement of N-GREEN performances; **WDM slot-wavelength** can be done only during one time WDM slot cycle. This is necessary in order to seize the opportunity of packets' reception during the next cycle. Furthermore, it is only restricted to the B&S mode as the label switching mode operates on lambda granularity. The capitalization on the results of **WDM slot-wavelength** gives birth to the proposition of Time Slot Sharing described in the following section 4.2.2.

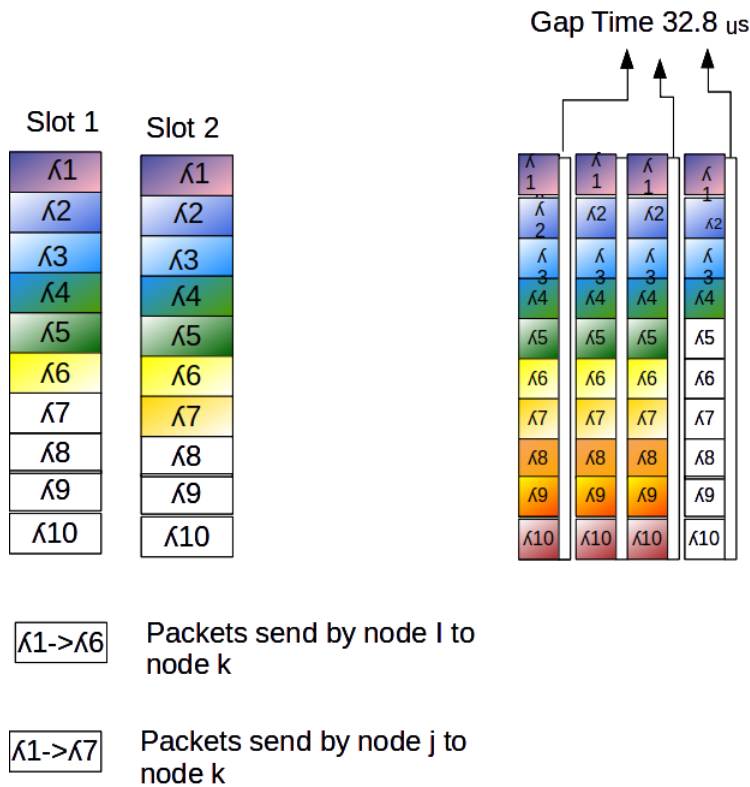


FIGURE 4.3: Packets insertion as Ssh-time method.

### 4.2.2 Time Slot Sharing (Ssh-time)

In Ssh-time [70], instead of sharing the wavelengths; we go down to a smaller granularity. Indeed, each node always sends its packets in a sub WDM slot over all the 10 wavelengths. A partially filled WDM slot can be re-used by another node which will place its packets over the 10 wavelengths but after the used part of the WDM slot, yet a guard time must be added in between. This margin or gap is required for lasers and other electronic components to be readjusted as well as in order to avoid collisions with the fragment already in the fiber. Technically, the guard time has an incompressible value consisting of zero bits of a minimal duration of 32.8 ns per sub WDM slot. As it is specified in N-GREEN; a guard time comprises : bits at '0' around 200 and 128 bits of clock giving the sum of 328 bits  $\Rightarrow$  32.8 ns). In our simulation, the WDM slot is divided into four sub WDM slots in order not to lose more than 18% of its capacity. Figure 4.3 presents an example of a shared WDM slot encoded according to the two different methods : with and without Ssh-time.

The obtained results following the implementation of Ssh-time will be described in the next paragraph and addressed below.

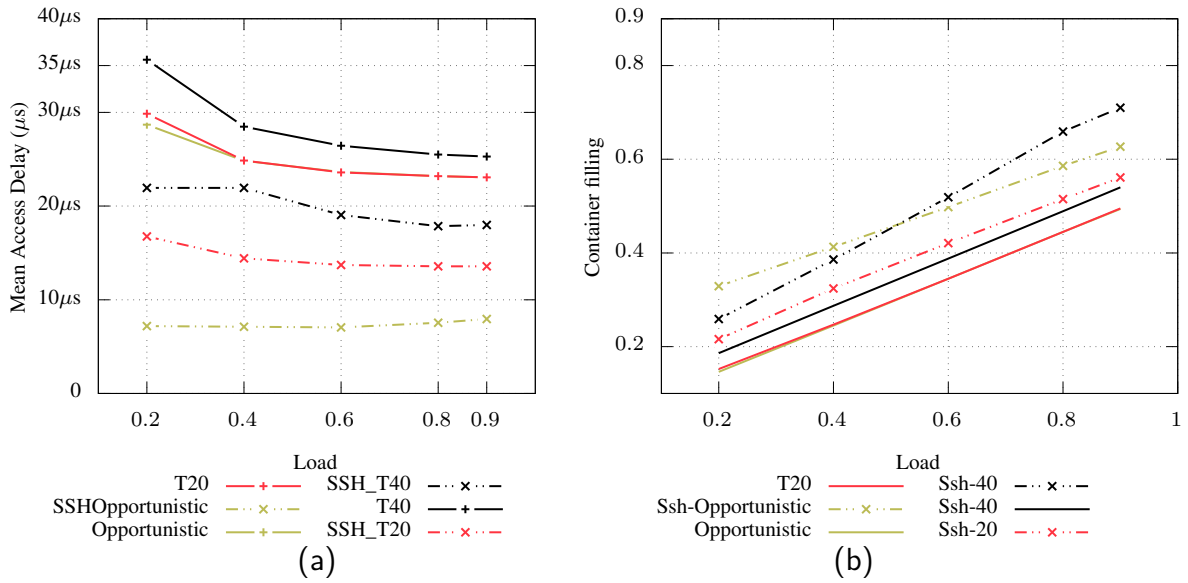


FIGURE 4.4: Mean Access delay and container filling within unicast mode (Note that Ssh-20 and Ssh-40 stands respectively for 20, 40  $\mu s$  timer based mechanism with sharing)

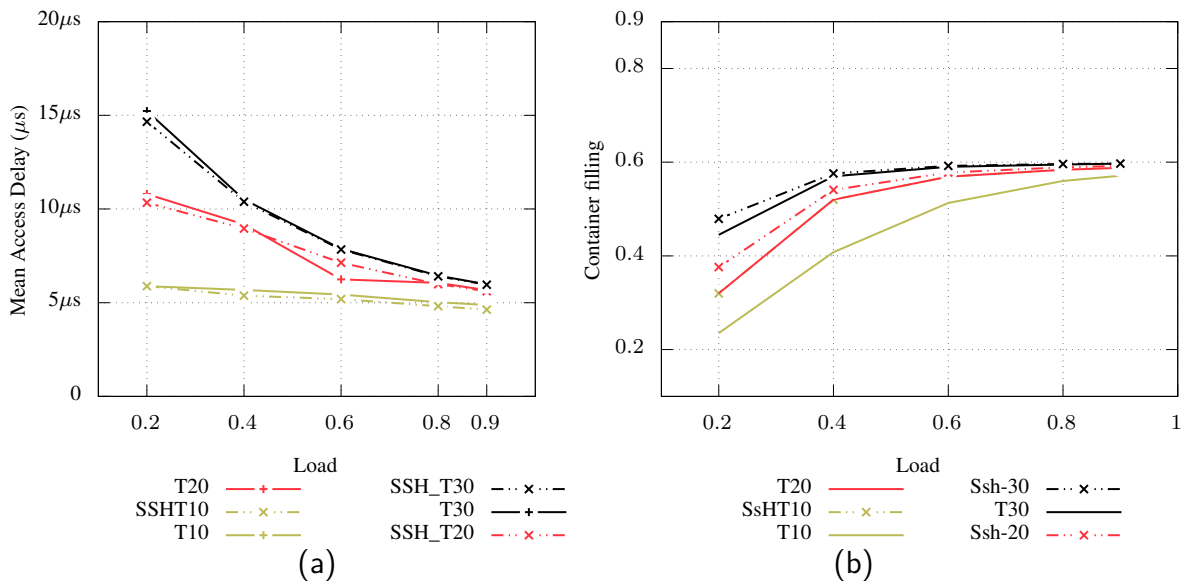


FIGURE 4.5: Mean Access delay and container filling within B&S mode (Note that Ssh-10, Ssh-20 and Ssh-30 stands respectively for 10,20 and 30  $\mu s$  timer based mechanism with sharing)

The timer values are chosen according to the applied transmission mode respectively 20  $\mu s$ , 40  $\mu s$  for the unicast mode and 10  $\mu s$ , 30  $\mu s$  for the B&S mode. Contrary to the B&S mode in which a guard time has to be added; unicast mode requires more packets to fully fill the WDM slot, hence, we assign a greater timer value to it. The results of our



simulation within the unicast transmission mode are presented hereafter in Figure 4.4 (a) and (b). The Figure 4.4 (a) displays the network load as a function of mean access delay for opportunistic mode and timer based mechanism (i.e. T20, T40) with and without sharing. The Figure 4.4 shows the container filling progression for the various scenarios. As expected, the opportunistic mode and one-aside timer 40 (i.e. T40) are the highest and lowest access delay respectively. Nevertheless, within the opportunistic mode, the WDM slot filling rate remains too low and thus, resources are not well used. Therefore, various timer values are evaluated to tackle this problem. Increasing the timer value significantly improves the container filling yet at the expense of the access delay. This is due to the packets clustering that engenders their waiting until the timer is elapsed. As such, it is obvious that timer duration value has significant impact on resources utilization, especially for low and medium loaded network cases. To increase this filling without affecting latency; we propose and evaluate Ssh-time method that benefits from the existing free resources in N-GREEN overdimensioned nodes. As shown in Figure 4.4 (a) and Figure 4.4 (b), implementing Ssh-time in the opportunistic mode greatly improves the access delay of about three folds; it also enhances the resources utilization by factor of 15%. Similarly, applying Ssh-time on a timer-based mechanism improves the mean access delay as shown in Figure 4.4 (b). Generally speaking, Ssh-time improves significantly both the mean access delay and resources utilization; more particularly, for low and medium load cases compared to scenarios without sharing.

The same scenarios with different value of timer were tested while applying the B&S mode. Figure 4.5 (a) and (b) represent respectively results in terms of mean access delay and container filling within the second architecture. As we can see in the Figure 4.5(a); the Ssh-time in combination with the B&S distribution mode does not improve the access delay. Ultimately, we consider it to be beneficial since it improves the resources use efficiently without affecting the access delay. The required gap time induces a resource loss of approximately 18%.

### 4.3 Adaptation of N-GREEN to bursty traffic

We extended our survey by including other more concrete types of traffic, such as CAIDA traces [1] models. Figure 4.6 provides an example of the dynamism of flow taken from CAIDA traces; in contrast to the well known theoretical Poisson model. We observe that the real traffic fluctuates more than Poisson flow with an instant average number of packets that could be multiplied by three.

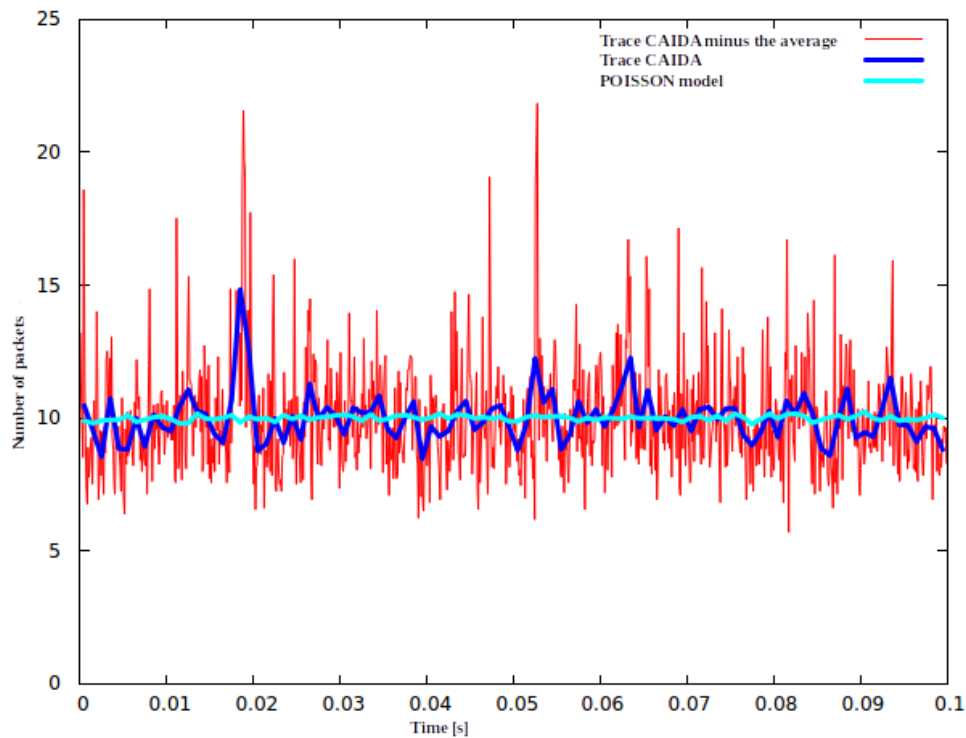


FIGURE 4.6: Real and Poisson traffic variations of one traffic flow.

Based on the results acquired and taken from our simulator; we get degradation in performance specifically for latency when considering CAIDA traffics. We notice that N-GREEN is normally equipped and adjusted to a predictable traffic with low burst rate, found e.g. in the metro aggregation as shown in Figure 4.7. As a demonstrative example, below we see a momentary network state where a low yet bursty traffic triggered an output buffer overflow in Node 5 due to low fill ratios of buffers. It highlights **the absolute need for proper packet management**.

The main goal is to adapt the network to other, potentially interesting applications, where the traffic is more bursty. Due to its reduced upfront, maintenance and energy cost; N-GREEN seems to be attractive in a number of applications requiring extreme data transmission rates with a substantially diverse traffic profile, such as big data centers or commercial centres. Nevertheless, contrary to what we find in the current metro aggregation network, where traffic is statically averaged (See Figure 4.7 (a)); traffic considering new future applications is characterized by a very variable fluctuation (See Figure 4.7 (b)). Taking into account other applications such as expected data center traffic exchange where the traffic is more bursty; we notice that 4.7 (b), the network needs to be updated. Normally in N-GREEN, a capacity increase request is managed by adding

more resources. Here we try to adapt the architecture to more applications without any upgrade in the network design by simply integrating a new scheme of packet management.

The suggested model takes into account the B&S mode while trying to reduce the mean access delay as much as possible. The main reason for not considering the resource use efficiency is that within the B&S mode, its value is sufficiently optimized.

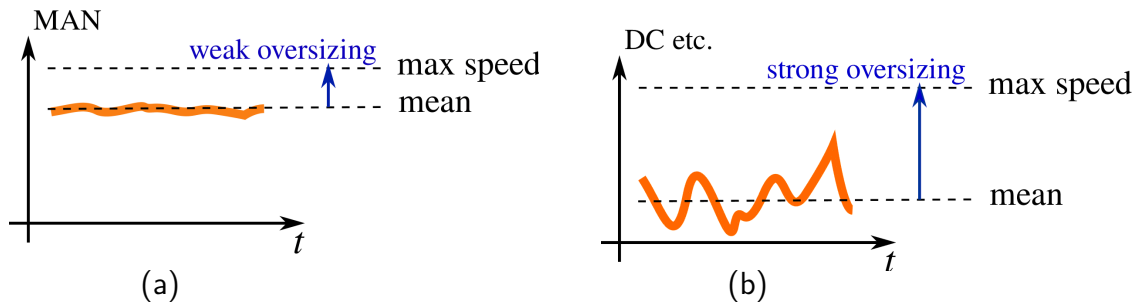


FIGURE 4.7: Difference between overdimensioning with smoothie traffic and burtsy one.

A list of symbols used in this study are summarized in this Table 4.1.

### 4.3.1 Optimization Methods

Convinced that the timer value is a crucial factor affecting the efficiency of the network mainly, the latency; a new packet management scheme optimizing this value is defined. The idea is to find the optimal timer value that minimizes latency considering the instant network state. This optimal value is calculated based on the Nelder Mead Simplex [71] optimization method. The latter has a proven efficiency and is easy to implement [71–73]. The Nelder Mead Simplex is a commonly based on a numerical used to find the minimum or maximum of an objective function in a multidimensional space. It is also known under the name of "Downhill Simplex". This iterative method may found the optimal value by searching in a neighborhood of a given initial condition. At the beginning of the iteration, a "simplex" polytope is created. If the dimension of the problem is  $n$ ; which is also the number of variables, this simplex is composed of  $n + 1$  vertices. Each vertex constituting the simplex corresponds to a solution. The defined objective function is used to drive the direction of the variables to optimize. For each iteration, vertex movements are deformed according to values returned by the transmission quality estimator. If the value of the function at this new point is lower in the case of minimization or higher in the opposite case; then, the simplex is stretched in this direction.

symbol	value if constant	description
$A$	$10 \cdot 10^6$	number of packets, whose statistics is collected in a simulation for a single element of $L_s$
B&S		mode broadcast&select
SDU		electronic packet
$d$	$10^{-5}$	scaling factor which increases the isotropy of the optimization space
$C_i$		accumulation of the expiration timer
$I_C$	1ms	constant which limits $C_i$
$L$		mean input load of a ring
$L_s$		set of typical loads
$N$	10	total number of nodes in a ring
$N_i$		$i$ th node in a ring, $i = 1, 2 \dots N$
PDU		optical packet
$O_{\text{load}}$		an optimization of a single element of $L_s$
$O_{\text{univ}}$		an optimization of all elements of $L_s$ at once
$S$	12500	size of a WDM slot in bytes
$S_{\text{max}}(N_s, N_t)$		maximum queue size between nodes $N_s$ and $N_t$
$S_{\text{mean}}(N_s, N_t)$		mean queue size between nodes $N_s$ and $N_t$
$t_{\text{lim}}$		equation for limiting the expiration timer and modifying its accumulation
$t_{\text{max}}(N_s, N_t)$		expiration timer for a packet travelling from an emitter node $N_s$ to a destination node $N_t$
$t_{\text{max}}^L(N_s, N_t)$		optimized equation of an expiration timer for an element $L$ in $L_s$
$t_{\text{max}}^{\text{univ}}(N_s, N_t)$		common optimized equation of an expiration timer for a whole $L_s$
$t_r$	1 sec	packet resend time

TABLE 4.1: List of symbols used in section 4.3.

The size of the simplex is a criterion that can be followed to verify the convergence of solutions. When this simplex becomes small enough ; it means that solutions are quite close to each other, so they converge on the optimal solution. Moreover, like all iterative algorithms, this method is very sensitive to initial conditions. In our simulation, we consider a very large number of iterations for the convergence of the function.

### 4.3.2 Traffic models

As we aim to adapt the network to different situations, we tried to define three different traffic patterns : an exponential traffic (Poisson model) and two trace-based

traffics which use a CAIDA data set [1], respectively called **raw** and **balanced** for the rest of this dissertation.

- Within the exponential traffic, in order to put accent on its smoothness, all packets are of an equal size which is equal to the mean packet size in the discussed trace.
- In the case of the raw traffic, the anonymized address space [74] is simply divided into equal parts; one for each N-GREEN node  $N_i$ ,  $i = 1, 2 \dots N$  for the number of nodes  $N = 10$ .
- In order to balance the traffic without affecting its bursty characteristic; we iteratively relax the said equidistant parts. The resulted model can be seen, as a symmetric distribution, as compared to the raw one. This is done by minimizing the following penalty equation :

$$P = \sum_{i=1}^N \min \left( D, \left| \log \frac{v_i}{\bar{v}} \right| \right), \quad \bar{v} = N^{-1} \sum_{i=1}^N v_i \quad (4.3)$$

where  $v_i$  is a traffic in bytes emitted or received by  $N_i$ ; depending on whether the address space to divide is the source or the target one. The logarithm and  $D = 10$  together moderate penalty contributions where a node receives a very small or a very large amount of data relatively to the mean; so that their respective importance is not dominating over the rest of the contributions to the penalty. This is relatively important as the division is grainy where there are boundaries between addresses with the same two least important IP bytes. The probability that such addresses belong to a single local network is elevated and we want N-GREEN to primarily transport data having relatively distant destinations.

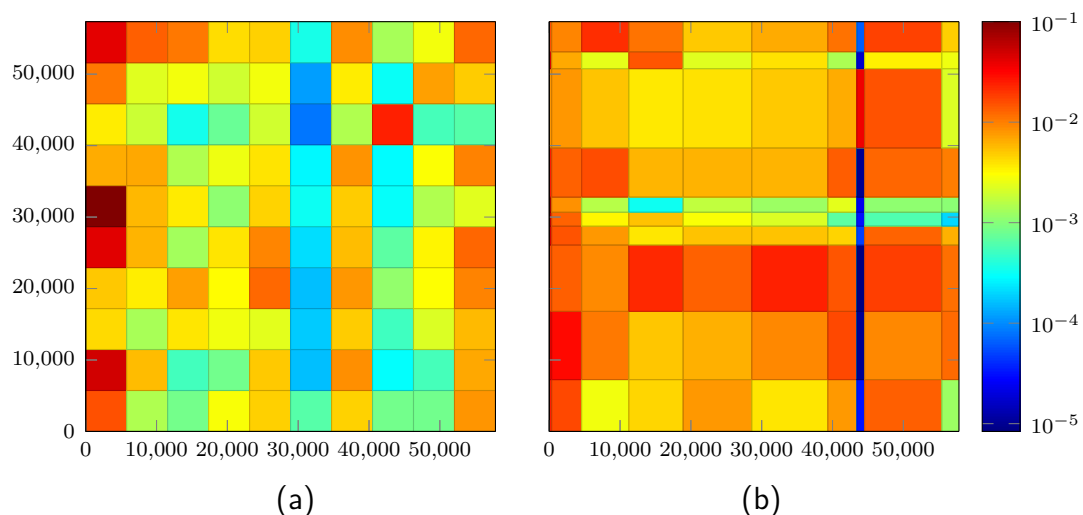


FIGURE 4.8: Normalized histograms of the traffic models raw and balanced. Addresses represented by their two MSB.

In the Figure 4.8, the respective normalized histograms of the amount of traffic in bytes for both trace-based models are scrutinized. The x-axis represents the sources and the y-axis represents the destinations while the tiles between the two couple of source-destination are just a representation of the amount of traffic between nodes. Unlike what you can see in the histograms; packets with the same origin and destination are never allowed in the simulation.

Any of these traffic patterns can be further regulated by changing the timescale represented by the load.

$$L = \frac{\bar{s}}{10\text{Gbps}} \quad (4.4)$$

where  $\bar{s}$  is the average stream rate emitted by a statistical node. In the original metro aggregation architecture with Ethernet cards of 10Gbps,  $L = 1$  would represent a theoretical limit where all the cards transmit data to the ring at their full duty. As in our case, we assume a bursty traffic and we allow the input buffers to be filled at a momentary rate larger than 10 Gbps while ensuring that the average does not exceed the allowed limit which is the 10 Gbps.

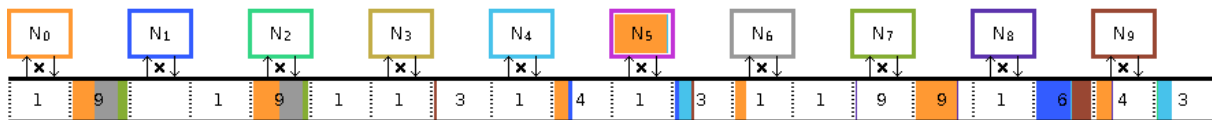


FIGURE 4.9: An example state of input buffers and of the ring (displayed as a bar for brevity). Colours show the number of bytes of packets destined to a given node; a number in the WDM slot depicts the emitter node. Network interfaces symbolize a node that can read a WDM slot; then delete it and later insert new contents into the just-emptied WDM slot. In the visualised state,  $N_9$  produced a burst of WDM slots containing packets to  $N_6$ ,  $N_7$  and  $N_8$  causing a packet loss in the input buffer of  $N_5$ .

An analysis of the shown results proved that even  $N = 10$ ; the network can be no longer overdimensioned. Indeed, the speed limit of  $10\text{Gbps}/100\text{Gbps} = 10\%$  of ring capacity inserted by a single node can be temporarily exceeded; which may overload the ring.

Figure 4.9 shows an example of a momentary state at  $L = 0.4$  where a rare coincidence led to temporary congestion.

Despite the increase in traffic for N-GREEN is simply processed by adding new resources in this dissertation; we show that a new advanced packet management is effective enough to meet user needs in terms of latency.

### 4.3.3 Packet management

A timer based mechanism designs a scheme where once the value of waiting time expires; an unconditional formation of a WDM slot occurs. All studies until to date considers either timer is constant [65, 75] or CoSwise [68].

In the case of N-GREEN, only a constant expiration timer has been studied [7, 70]. Further, we will discuss a variable expiration timer  $t_{\max}$ , used in the following buffer management scheme :

Each node has  $N - 1$  separate First In First Out (FIFO) input queues filled with Electronic Packets (EP). Typically, Ethernet frames are called Service Data Units (SDU) as defined in the previous chapter 3 considering one queue for each possible destination. The EPs can be arbitrarily segmented and merged into a flat payload (container). To each segment, a preamble is added with the organisational data. Given that EPs already contain headers; we concluded that it is enough to have a preamble of 8 bytes that holds values like a unique packet identifier (4 bytes), a byte offset of the segment which is relatively to the SDU data (2 bytes) and finally the length of the segment (2 bytes). A number of segments together with their preambles, form an PDU which is never larger than a single WDM slot of the mentioned size of  $S = 12500$  bytes.

As mentioned earlier, the network operates in the B&S mode which allows a single PDU to include fragments of SDUs with various destinations. When an SDU is fragmented into different PDUs; their fragments must be transmitted in the internal order but they can be interspersed by other payloads. Each node looks into every passing PDU for segments with fragments of SDU along with its destination address, recovers these fragments if any and merges them back into SDUs. When all the WDM slot's data is received at a  $N_i$  node; the WDM slot is emptied by simply turning OFF the optical gate (SOA).

If a payload ready to be sent by a node can form an PDU of the size of  $S$ ; the first available empty slot will be used to send, straight away, that formed PDU from the oldest SDUs. Otherwise, an oldest SDU is found iteratively; for which the timer  $t_{\max}(N_s, N_t)$  is expired, where  $N_s$  and  $N_t$  are respectively the source and the target node. Fragments of such SDUs are iteratively merged until an PDU of the size of  $S$  can be formed. When no more SDUs with expired timers are found, but at least one SDU with expired timer has been identified so far (i.e. must be forwarded); then, the remainder of the PDU is built from any of the oldest remaining SDUs on the buffers to optimize the slot's use ratio.

Thanks to the fragmentation, a large SDU packet is taken – the only restriction here is the maximum size of an PDU.

A new SDU which does not fit into its input buffer is immediately considered lost. In our study, we consider a "resend time"  $t_r = 1s$ , a large value in comparison to an average insertion time found in N-GREEN, which is normally of the order of tenths of microseconds. Thanks to this, lost packets do decrease considerably the transmission quality. On the other side, the assumed  $t_r$  tends to be very small, given the real values used in computer networks [76]. This is deliberately done in order to maximize further the said quality using a direct optimization method. Too large values of  $t_r$  might produce gradients in the optimization space which would be difficult to handle by that method. The low  $t_r$  does not seem to be a problem though; if we assume that PLR should be very low or even that there should be virtually no packet loss in a properly configured N-GREEN ring. Any SDU that is already within the input buffer which is older than  $t_r/2$  is also lost; this removal process is taken in order to prevent a potential dominant effect of packets. In this case; no longer considered valid by the destination application – a latency of  $t_r/2 = 0.5$  s is considered very large in the realm of N-GREEN. We see that  $t_{\max}(N_s, N_t)$  can be sensitive to the state where a ring fragment through which it is transferred. It could be important if for instance a part of the ring is busy and thus an increased WDM slot fill ratio is recommended in order to maximize resource usage.

#### 4.3.3.1 Adaptation of $t_{\max}$

As mentioned earlier, we use Nelder Mead Simplex as a direct optimization method which repeatedly runs simulations in order to evaluate a quality function at different points of the optimization space. The coordinators of the space are constant coefficients in the equations representing  $t_{\max}(N_s, N_t)$ .

Two variants has been proposed :

- **Local strategy** : The expiration timer of an SDU in the input buffer of a node  $N_i$  uses only the statistics concerning  $N_i$ ; more clearly uses only its local conditions.
- **Global strategy** : Each node has access to some global statistics about the other nodes. The latter solution is more powerful necessitating only transmission of some statistics. This is feasible in N-GREEN where a control channel is sufficiently large to transport such statistics.

**4.3.3.1.1 Parameters of the optimization method** Nelder-Mead optimization method [71] : has been used along with a relative convergence criterion of  $1 \cdot 10^4$  and a starting point at the origin. The method is not predestined to work with a noise optimization space; yet due to large  $A$ , it turned out to work better compared to e.g. [77], theoretically adapted to noise but requiring a bounded space. As we do not have any



idea about the optimal values and we do not want to restrict them by random values ; we have preferred to use Nelder Mead Simplex with enough large iterations essential for results convergence.

In order to avoid overfitting [78] or convergence difficulties and for practical reasons like a temporal performance of the packet management in a real device ; we will avoid general equations for  $t_{\max}(N_s, N_t)$  where the argument would consist of a large number of randomly selected parameters that would have a major impact on the optimization process. Rather, the equations will have a concrete substantiation in relation to the architecture of the network.

#### — Estimation of a transmission quality

As mentioned in 4.3.1, in each iteration there is a direct optimization that provides a transmission quality. Given that the results are very sensitive to noise ; the quality of the transmission is estimated by several simulations.

Within each simulation, statistics of the first  $A = 10 \cdot 10^6$  packets are collected. The constant  $A$  turns out to be high enough for the noise in the gathered statistics to be averaged out sufficiently, given a resistance to noise of the used optimization method. We have chosen a maximum total size of input queues per node of  $B = 10 \cdot 10^6$  bytes which seems reasonable ; given the current technology.

As an estimation of the transmission quality ; we use the mean latency of an insertion of a packet into the ring.

A set of loads  $L_s = \{0.01, 0.1, 0.2, \dots, 0.9, 0.95, 1.0\}$  which covers a usable range of traffic intensities was considered. It is worth noting that the extra value of 0.95 is used to improve a region with a high probability of losses where small differences may affect latencies leading to its remarkable modification due to a relatively large  $t_r$ .

The method of optimization has two different modes :

- $O_{\text{load}}$ , which finds separately a set of optimized  $t_{\max}^{L_s}(N_s, N_t)$  for each  $L_s$ . In this case, the simulator is ran independently for each load value and returns a set of adjusted coefficients determining the optimal timer value for that specific load value.
- $O_{\text{univ}}$ , where a single quality optimization covers all  $L_s$  and the resulting transmission quality is given by an arithmetic means of mean latencies for each  $L_s$  ; thus, there is only a single optimized equation  $t_{\max}^{\text{univ}}(N_s, N_t)$ . More specifically, the simulator takes the average returned transmission quality value and does the same for the coefficients for each iteration.

Obviously, the function found by  $O_{\text{univ}}$  is what is expected in practice : an equation appropriate to all loads.  $O_{\text{load}}$  is not practical simply because the mean load is only known during the simulation as it is defined by the designer. It can only be estimated by  $t_{\text{max}}^{\text{univ}}(N_s, N_t)$  in a real network. This  $O_{\text{load}}$  is mainly used to estimate if  $t_{\text{max}}^{\text{univ}}(N_s, N_t)$  adapts well to different network conditions. If a latency for a given  $t_{\text{max}}^{L_s}(N_s, N_t)$  is substantially better than the one given by  $t_{\text{max}}^{\text{univ}}(N_s, N_t)$  for the same load  $L_s$ ; then, it implies that there is room to improve the estimation of the expiration timer.

The simulator achieves an average of 1 million packets transmitted per a second of physical time; yet, the convergence speed of the optimization method still turned out to be a major limiting factor.

- **Accumulation of  $t_{\text{max}}$**  : As stated earlier, there are no boundaries on the coefficient values that define the timer value; therefore, the values returned by the simulator may be illogical. Nevertheless, only a range of  $t_{\text{max}}$  values has a significance. For example, negative  $t_{\text{max}}$  has normally no interpretation and  $t_{\text{max}} \geq 100\mu\text{s}$  degrades the quality overly for N-GREEN; such elevated values were not even previously considered in the case of this network [7] as they degrade significantly the performance of N-GREEN.

The following formula is defined in order to ensure a reasonable value of  $t_{\text{max}}$  :

$$t_{\text{max}}(N_s, N_t) = t_{\text{lim}}(t_{\text{opt}}(N_s, N_t)) \quad (4.5)$$

Where :

- $t_{\text{opt}}(N_s, N_t)$  is one of the optimized equations considered later.
- $t_{\text{lim}}(t)$  limits  $t$  by  $t_l = 0$  and  $t_h = 100\mu\text{s}$  where the maximum is deducted from previous study [7, 70].
- $t_{\text{max}}(N_s, N_t) =$  the resulting value as the effective timer expiration.

Different techniques can be used to obtain reasonable value of timer. For instance; for a simple order, we can merely clamp  $t$  to get  $t_{\text{max}}$  by taking only positive values.

Two reasons preventing us from doing this :

- It might cause a flat quality regions in the optimization space as different values of the optimized coefficients might lead to the same effective value of  $t_{\text{max}}$  and hence, the same value of the quality of transmission that caused the optimizer's assumption to be the optimal value.
- Instead, we could find a new application for these regions i.e. a temporal accumulation of  $t_{\text{max}}$ .

In order to ensure this, a set of an accumulation value  $C_i$  for each node  $N_i$  has been defined while considering the following interpretation; allowing an optional inertia when estimating  $t_{\max}$  :

- Negative  $C_i$  means that  $t_{\max}$  should also be small for some short period in the future; i.e. the node buffer that attempts to transmit data may be largely full which implies that there will not be a need for larger  $t_{\max}$  in the near future.
- On the contrary, positive  $C_i$  indicates a strong predictor that a large  $t_{\max}$  will be required for some time. The node does not have enough packets to fill the WDM slot as it needs a longer timer value.

The  $t_{\lim}$  value controls  $t_{\max}$  as follows :

$$\begin{aligned} C'_i &= \max(-I_C, \min(I_C, C_i + t)) \\ t_{\max} &= \max(t_l, \min(t_h, C'_i)) \\ C_i &= C_i - t_{\max}. \end{aligned} \tag{4.6}$$

Using these equations, we ensure that  $t_{\max}$  consumes a maximal part of  $C_i$  given the limitations  $t_l$  and  $t_h$ . Additionally,  $I_C = 1000 \mu s$  limits the inertia of  $C_i$  as we assume that is unsafe to consider a predictability of the network state for periods larger than  $I_C$ .

### 4.3.4 Performance achieved in terms of latency

To find an exact relation between the optimal timer value and the parameters of the network guaranteeing the minimum latency value; two functions have been defined named respectively Local and Global.

#### 4.3.4.1 $t_{\max}$ as a function of local conditions

We started with an estimation of a variant  $t_{\max}$  further called *local*. The name comes from the fact that nodes do not need to share their statistics with the others. The results obtained while applying this function will be compared later on to an optimized constant expiration timer i.e. a variant further referred to as *const*.

The expiry time of SDUs in  $N_i$  depends only on the total size  $S_i$  of input buffers in bytes in the local node. Given that we do not have any indication about the shape of the function; thus, we started with a second degree polynomial function :

$$t_{\max}(S_i) = a_0 + a_1 \frac{S_i}{d} + a_2 \left( \frac{S_i}{d} \right)^2 \tag{4.7}$$

where the optimized coefficients  $a_0, a_1, a_2$  are common for all nodes and  $d = 1 \cdot 10^5$  being 10% of  $B$ , is meant to improve better the performance of the Nelder Mead method by increasing the isotopy of the optimization space parameterization.

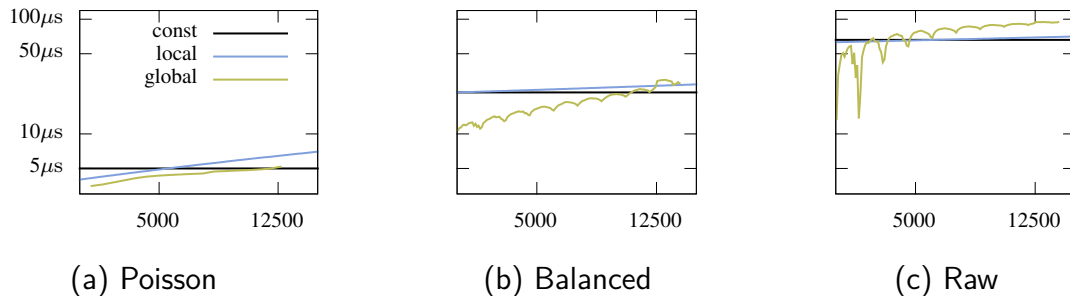


FIGURE 4.10: Timer expiration  $t_{\max}$  against sizes of buffers' input considering the variants const, local and global against  $S_i$ .

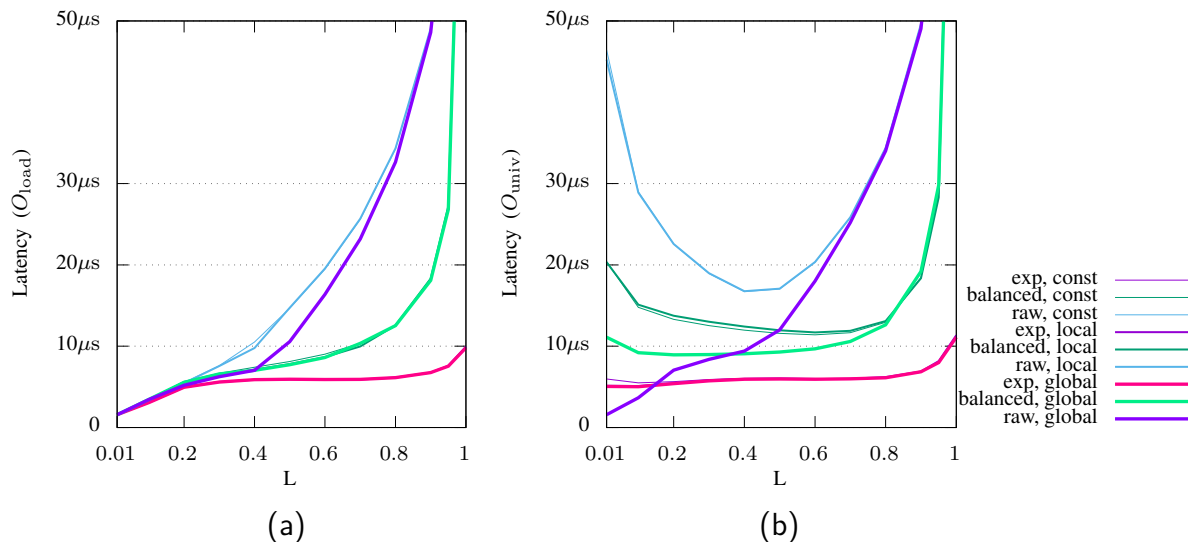


FIGURE 4.11: Latency after optimizations (a)  $O_{\text{load}}$  and (b)  $O_{\text{univ}}$ , against  $L$  using the variants const, local and global. Latency values out of scale are caused by packet loss.

The resulting  $t_{\max}$  and insertion latency are shown respectively in Figure 4.10 and Figure 4.11.

In the latter Figure 4.11, we see practically no improvement in latency values for any traffic type when comparing the variant local to the variant const. This is confirmed in Figure 4.10 where both variants give similar  $t_{\max}$  for all loads.

Conversely, their  $t_{\max}$  varies once the traffic type changes. These two traits together may indicate a problem for the traffic raw which can be seen as a mixture of different

traffic patterns; thus, requiring a specific packet management of  $t_{\max}$ . We can as such, expect both variants const and local to perform poorly in this case. It is confirmed when comparing Figure 4.11(a) and (b) that  $O_{\text{univ}}$  works almost as good as  $O_{\text{load}}$  for the exponential traffic; yet, there is a large performance drop for  $O_{\text{univ}}$  in the case of the traffic raw as large as ten times for  $L = 0.01$ . The balanced traffic gives here a more moderate performance drop.

#### 4.3.4.2 $t_{\max}$ as a function of global conditions

Given that the local variant was not useful and did not give the desired result; we opted, then, for another variant named Global. The analysis started by comparing  $t_{\max}$  (Figure 4.12) and a mean  $\bar{S}$  of  $S_i$  over all nodes during a whole simulation (Figure 4.13). This has revealed that  $t_{\max}$  are the lowest for the traffic exponential model and the highest for the traffic model raw. That similarity was a hint for making  $t_{\max}$  dependent on different values related to buffer sizes.

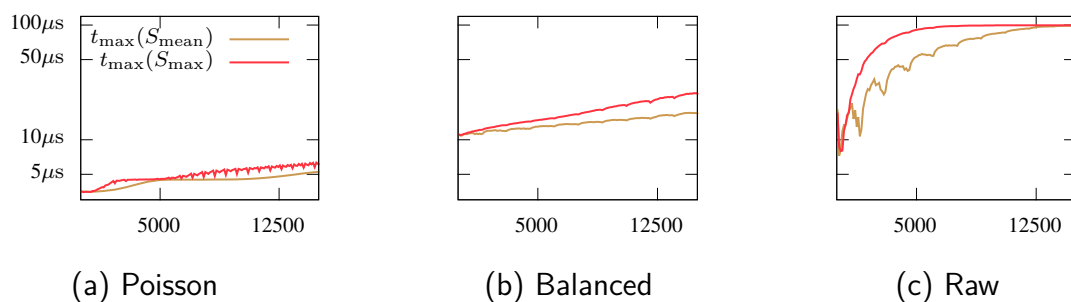


FIGURE 4.12: Timer expiration  $t_{\max}$  against sizes of input buffers considering the variant  $O_{\text{univ}}$ . It shows the variant global against  $S_{\text{mean}}$  and  $S_{\text{max}}$ . For the variant global, only a mean value of an underlying PDF is shown. Columns depict traffic models exp, balanced and raw.

Consequently, we considered more global sizes of buffers to estimate  $t_{\max}$  (a variant *global*). However, using queue sizes  $S_i$  from different nodes requires their transmission through the network. Given that N-GREEN has a special control channel; this set of information goes through this channel. In order to reduce their propagation time; we consider a bidirectional one where each node sends data about their buffers sizes in both directions.

To keep the dimensionality of the optimization space small; we restricted ourselves to a linear equation that will enable us to insert three values representing the following buffer sizes :

- The already discussed  $S_i$  ;

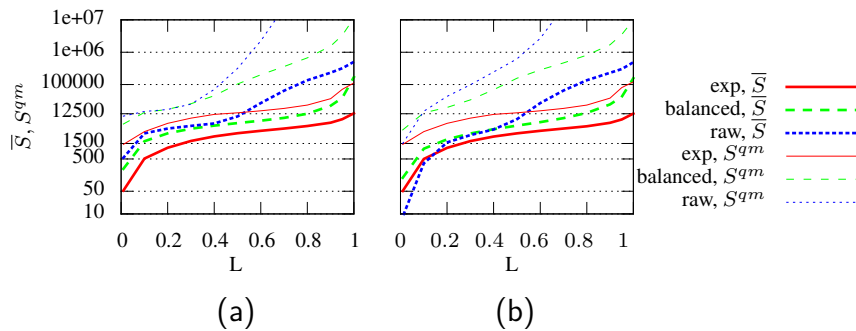


FIGURE 4.13: Dependency between  $L$  and  $S_{\text{mean}}$  for different traffic models using the variants (a) local and (b) global.

- A mean queue size on midway nodes between the source and the target node  $S_{\text{mean}}(N_s, N_t)$  where  $N_s$  and  $N_t$  are, as in  $t_{\text{max}}(N_s, N_t)$ , discussed in the packet management algorithm in section 4.3.3;
- A maximum queue size on midway nodes  $S_{\text{max}}(N_s, N_t)$ .

Considering these new parameters ; the equation to optimize  $t_{\text{max}}$  is defined as follows :

$$t_{\text{max}}(S_i) = a + a_S \frac{S_i}{d} + a_{\text{mean}} \frac{S_{\text{mean}}(N_s, N_t)}{d} + a_{\text{max}} \frac{S_{\text{max}}(N_s, N_t)}{d} \quad (4.8)$$

Looking at latencies Figure 4.11, we see the desired effect : with the exception of the exponential traffic where the latency was already very low for the variants const and local ; the variant global gives a considerable improvement. Additionally, for the traffic raw,  $O_{\text{load}}$  and  $O_{\text{univ}}$  give comparable results.

#### 4.3.4.3 Discussion

The increased unpredictability of a bursty, asymmetric traffic may be seen in the quality of the results : if the nodes do not share their statistics ; it is not possible to estimate correctly the global situation in the ring within a single node. Consequently, the quality of the packet transmission is not optimal. Indeed, within an unpredictable traffic ; it is mandatory to define a proper packet management.

These factors are well clear in the diagrams 4.10 and 4.12 as the variability of the traffic increases (i.e. the traffic exp, balanced and then raw) :

- The variant local becomes more and more insensitive to the local buffer size thus, approaching the variant const (Figure 4.10) ; it shows that  $S_i$  alone is an unusable predictor for  $t_{\text{max}}$  ;

- The latency increases and becomes problematic (Figure 4.11); this may lead to losses. As instance, when the system is not loaded; the latency of traffic raw using the local variant reaches almost  $20 \mu s$  (i.e.  $L = 0.2$ ).

The improved performance of the global variant is due to its responsiveness to the new considered statistics. A four-dimensional surface of (4.8) is practically difficult to use, specifically while visualizing the relationship between the parameters on which  $t_{\max}$  depends. Therefore, within the simulation, a mean  $t_{\max}$  against  $S_i$ ,  $S_{\text{mean}}$  and  $S_{\max}$  has been computed; the obtained results pointed out a non-linearity behavior proving the interdependencies between the three arguments (Figure 4.10). As depicted in Figure 4.10, we notice that for the traffic raw where the variant global is especially advantageous; the said relations are strong.

In order to estimate a practical advantage of the variants global versus constant; we consider a plot of an indicator  $S^{qm}$ , as the minimum queue size of the top most 1% of the PDF of  $S_i$  during a whole simulation. This allows us to detect if there are sporadic congestions that may not show in  $\bar{S}$ . We see that, if the network should be prepared for traffics like the model raw; the load then, should not exceed 0.6. This is also the value where the expiration timer becomes less important, as the criterion of filling a WDM slot is more readily due to the more filled input buffers. Hence, the three variants in question behave similarly (see Figure 4.13(a) vs (b) for larger loads). There are clear differences for a bursty traffic at small and moderate loads where the variant global is capable of sensing how much  $t_{\max}$  should be decreased to increase the latency. The calculated value is a compromise between an earlier packet expiration and an increased risk of congestion due to a lower fill ratio of WDM slots. This is the situation where the variants const and local show their inflexibility which leads to even a tenfold increase of latency compared to the variant global (See Figure 4.11).

The short expiration periods in the case of the latter variant can be risky, because a sudden growth in traffic intensity that is unpredictable by the adaptation method of  $t_{\max}$ , which might cause a packet loss. Const and regional variants are more secure with their larger average expiry timers. Considering this effect, we analyzed the mean PLR for  $O_{\text{univ}}$ , i.e. the optimization which produces an adaptation expected to adjust well the network to heavy to changes. For the most uneven traffic case raw, as well, it turns out that the global variant gives a smaller PLR for the loads  $L_s$ , as  $3.21 \cdot 10^{-5}$  vs  $4.26 \cdot 10^{-5}$  and  $4.24 \cdot 10^{-5}$  for respectively the variants const and local.

## 4.4 Concluding remarks and future works

The N-GREEN network performance are evaluated and discussed in this chapter. In the context of a metro/aggregation network ; we were interested mainly in the resource's use efficiency and latency under the two communication modes : Destination Based Mode (DBM) (only the unicast mode) and B&S mode. Both models were analyzed while considering different insertion mode such as TDM and timer based mechanism. The approaches suggested include WDM optical slot size and insertion mode strategies.

As for the second part, we focused on adjusting N-GREEN design for other applications where traffic is more bursty. To this end, we began with a local variant where the timer value depends only on the size of the source node. According to the results obtained ; we introduced further parameters as minimum and maximum queue size for the source and destination node. An adaptive expiration timer with an equation, considering this two parameters, was enough to adjust the architecture to different traffic type. This substantially decreases the latency for lower loads and slightly decreases packet loss for higher traffic loads.

Within this work, the traffic type to be studied is defined by the designer at the beginning of the simulation which is not the case for real network. In order to adapt the network to different traffic types ; we focused on replacing the one-time approximation of the coefficient  $a_S$  that represents one of the coefficients determining the strategy (See 4.8) with an off line simulation by a constant adaptation of these new variable coefficients in a production network. The scheme suggested and the results obtained were presented in the next chapter of 5.



## Chapter 5

# Analysis of a frequency response of a telecommunication network for its self-adaptation

### 5.1 Introduction

In the previous chapter 4, a strategy has been suggested to adjust the N-GREEN structure to bursty traffic and results have been discussed.

This was achieved through specifying an advanced method to determine the optimal timer value i.e. time at which a set of packets are inserted into the ring regardless of the network conditions. The calculated value returned by our simulator is composed by a set of optimized coefficients calculated using the Nelder Mead Simplex Optimization method. These coefficients are specific for each type of traffic apart i.e. the model of the traffic is specified in the beginning by the designer. Nevertheless in real network traffic models change over time, hence, we need a way to keep track of these changes.

In this chapter, we display the steps we are going through in order to replace the one time adaptation of  $a_S$  of one of the coefficients affecting the strategy. In an off line simulation, we attempt to adapt the coefficients on which  $t_{\max}$  depend in a production network.

For that purpose, we study the quality of frequency response of N-GREEN network making use of frequency-domain industrial loop controllers [79, 80]. Indeed, we analyze

a step or a frequency response of N-GREEN as a simulated computer network where the stimulus is one of the coefficients which regulates the network's strategy of packet transmission and the response is the network's momentary performance. Hence, we found a frequency range where an instantaneous dependency between these two parameters can direct a self-adaptation scheme, taking into account the changing network conditions such as traffic models.

The chapter is divided into two large parts and organized as follows :

- **Section 5.2** : In that first part, we define briefly the principle of loop controllers while focusing on frequency modulation as it is the basis of our work. Some examples are given while defining some key concepts in relation with the topic.
- As for the second part **section 5.3**, in order to test our proposed methods, we are introducing a specific traffic models defined and simulated in 5.3. Then we display the steps we are going through to find the relation between the stimulus and the network response.

Finally, we present the conclusions of this chapter in section 5.4.

## 5.2 Background and Related Work

### 5.2.1 PID (Proportional Integral Derivative) controllers

As previously pointed out, it is important to note that network parameters i.e. the further discussed timer value will be independent of external conditions. These conditions include : the traffic models or the initial configuration and will be able to adapt itself to a new network change. To overcome this situation, PID systems can provide a robust way to control network parameters automatically. The subsequent research was influenced by the basic theory of PID controllers.

PID is based on a control loop mechanism that adjusts the system's controlled parameters according to the returned feedback. It measures an error value continuously and simply representing the difference between the desired setpoint (SP) and the measured process variable (PV) and applying the adjustment based on proportional, integral and derivative factors (denoted P, I and D respectively). PID controllers are used primarily for the electronic control systems of chips and that are lately integrated into the telecommunications domain. Although the implementation of this concept is still restricted within the optical networks; some few examples do exist. It has been introduced in the

field of telecommunication networks by proposing a GA-based PID active queue management control (AQM) design for a class of Transmission Control Protocol (TCP). This guarantees both high usage and low packet loss rate by regulating the queue length of an internet router [81, 82]. It has been used later in dynamic optical burst-switched networks [83] to model a wavelength locking loop in order to stabilize the output of tunable lasers. In Refs [83, 84], the authors designed some controllers in order to manage both computing and network resourcing. This is possible via managing certain tasks in optical grid networks and establishing dynamic lightpaths in Wavelength Division Multiplexing networks. Also in [85, 86], we can find PID controllers where authors manage the allocation of bandwidth in order to minimize delays in passive optical networks (PONs). The suggested strategy [85, 86] demonstrated better performance and robustness than previously existing Dynamic bandwidth allocation (DBA) algorithms.

The technique used to define controllers within PID systems is defined in accordance with the need and the considered system. In this context, we propose the development of an expert and intelligent PID controller based on a frequency modulation to define timer value facing traffic changes.

## 5.2.2 Key Concepts

Important key terms used in this analysis are described in this section. As described in the previous section 5.2.2.1, the study sets a specific focus on the frequency modulation scheme. Thus a definition of this concept will therefore be introduced at the beginning of this section 5.2.2.1. Furthermore, we define in the second part, the main term in relation to this approach.

### 5.2.2.1 Frequency-domain adaptation

Frequency domain adaptation methods in industry loop controllers [79, 80] are rarely found in computer networks [87, 88] even though the topic of self-adaptive computer systems [89] is getting increasingly discussed through years. The main factor preventing their emergence in the network could basically be the strong noise generated as a result of the changes in the environment. The reliability of the frequency response is diminished by a non-linear and undeterministic network behaviour. Adding to this the requirement of a proven reliability of a computer network may lead to a preference of precise, proven, hand-crafted methods, like the many TCP flow control techniques.

Encouraged by the results obtained in chapter 4 where despite of the noisy system caused by a very complex traffics design ; we managed to find a way to change the network parameters in real time. Based on loop controllers, a model of a system can be any type of abstract description that captures a process. We consider frequency domain systems among the most well-known models used in adaptive loop controllers. The system may be composed of an oscillator and a regulator which senses and compares data input signal such as phase and amplitude to the output. Such a comparison is defined to determine the relation between the signals. Within N-GREEN, a sinusoidal perturbation of the system constantly introduces small modifications into a main hand-crafted strategy found to be reliable [69] and which contains its own feedback mechanisms. Possible resulting oscillations in the quality of the behaviour of the system are then detected as a useful response in loop control algorithms like the widely known Ziegler–Nichols method. In short, the stimuli is one of the coefficients that regulates the packet transmission strategy of the network while the response is the network’s momentary performance. In view of the noise impact described above and in order to maintain the network more secure, we sought to weaken the stimulus.

As a concrete example in the formula defined in section 4.8, a sine wave of low amplitude may be used to define some technique parameter making  $a$  oscillating in the original value. We assess then, the quality of the response in order to test if it can find an optimal  $a$ . When the reaction is not postponed, for instance ; no interference is presented and the mechanism is constant, as it is explained by the principle of regulation. One may simply look at the phase difference between  $a$  and a similar sinusoidal frequency in  $q$  if they fit, both  $a$  and  $q$  are positively correlated and thus ; may be slightly increased by  $a$  to improve the quality and repeat the process.

To test the limits of obtaining a useful response ; we use a highly variable noisy traffic generation that is specifically defined and applied as part of this study 5.3.1.

### 5.2.2.2 Bode Diagram

The diagram of Bode is a way to represent the frequency behavior of a system under evaluation. His name comes from Hendrik Wade Bode, his inventor. In general, it allows a simplified graphic resolution, in particular for the study of the transfer function of a slave system.

Generally, the Bode diagram of a frequency response for a system while assisting the response of a frequency modulation  $T(j\omega)$  is a graphical representation composed

mainly by two plots :

- The gain (or amplitude) in decibels (dB). Its value is calculated from  $20 \log_{10} (|T(j\omega)|)$ . This provides us with primarily information about the degradation ; it is useless to analyze the phase change if the signal is too deteriorated.
- The phase in degree, given by  $\arg (T(j\omega))$ . A phase change close to zero gives us a clear idea of the relation between the  $S_{\text{mean}}$  and  $a_{\text{mean}}$ . This actually reflects the level of noise in the network.

The pulse scale is logarithmic and is expressed in rad/s (radian per second). The logarithmic scale allows a very readable trace as it consists mainly of linear sections.

## 5.3 Steps of Auto Adaptation of the Network

### 5.3.1 Traffic Models

In an operational network, traffic models are very variable in metro as well as in the core and access networks[1]. In order to create a real traffic model and test the ability of the proposed method to withstand noise ; we simulated a very variable traffic models ; much more variable than a bare CAIDA trace [1] used in [69]. Indeed, the two different CAIDA traces described in 2 are considered. We made a mixture of two very different CAIDA traces and for contrast ; we consider a node-symmetric traffic given by a Poisson process with packets of an equal size.

All the three sources have the same mean packet size equal to 127 Bytes representing the mean packet size in CAIDA and they are individually processed as described in [69].

Figure 5.1(a) sums up these two traces ; we see a purposely very different occupation of nodes as sources/destinations. In the generated model ; we considered some sources to mix  $s_i, i = 1, 2, \dots, s_{\text{NUM}}$ . At each time instant  $t$ , a *mixing function* provides  $s_{\text{NUM}}$  values  $k_i \in \langle 0, 1 \rangle$ . This is mapped to an *acceptance probabilities*  $p_i^{\text{acc}}$  of packets in each of the sources :

$$p_i^{\text{acc}} = \left( 1 - m_n + \frac{m_n}{\sum_i k_i} \right) k_i \quad (5.1)$$

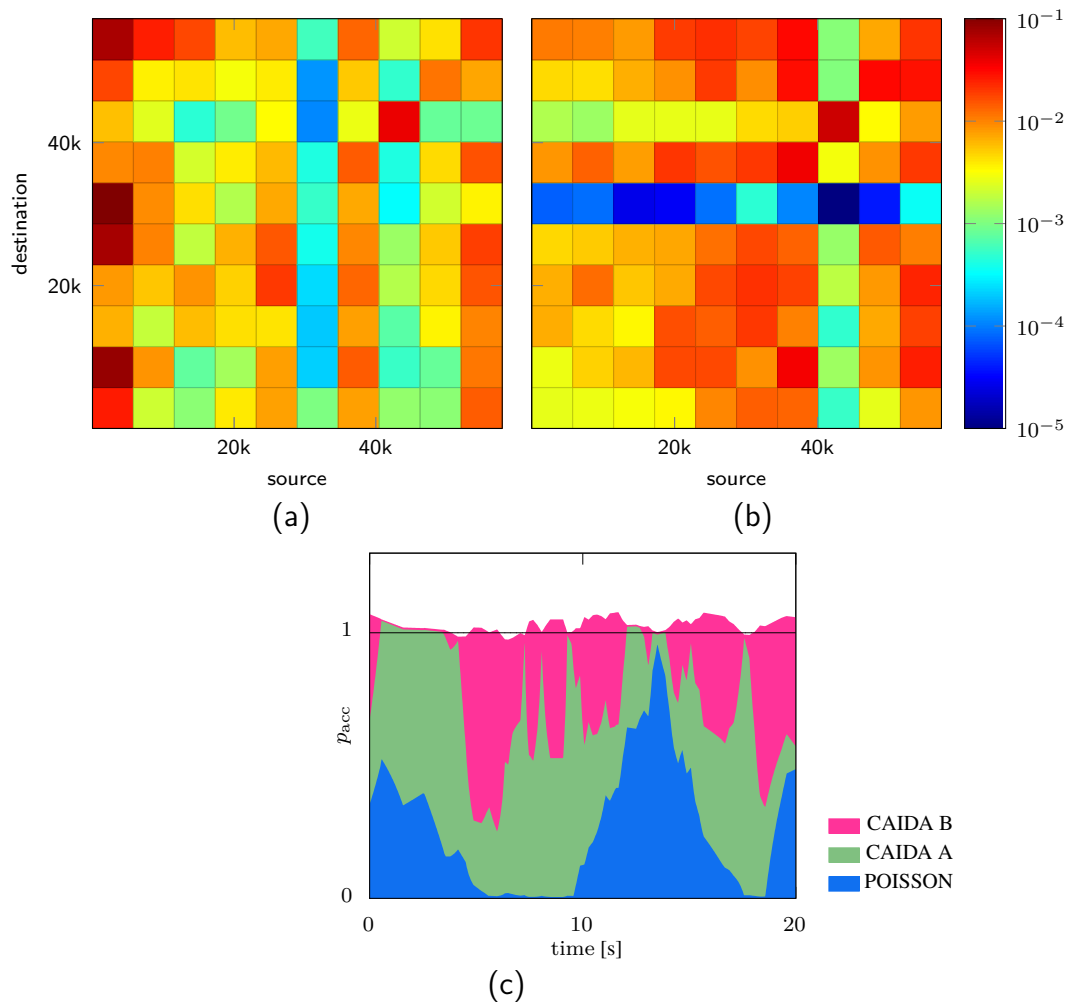


FIGURE 5.1: Normalized histograms (or discrete probability distributions) of the CAIDA traces (a) A and (b) B against a source and a target node found by dividing the two MSB of anonymized IP addresses into 10 equal fragments. (c) A cumulative chart flow showing the probabilities of acceptance of packets in three sources,  $m_n = 0.95$ . Assuming that each of the sources has a mean rate of 1; the upper edge of the colored area shows the effective packet rate.

where  $m_n$  is a normalisation factor, so that  $\sum_i p_i$  is always 1 for  $m_n = 1$  and there is no normalisation at all for  $m_n = 0$ ; see Figure 5.1(b) for an example of the mixing function.

We used a rather high  $m_n = 0.95$  because even such a traffic was difficult to handle by the network at large  $L$ , comparing to a single CAIDA trace. Because of the given different probability distributions in Figure 5.1(a) and the burstiness of the CAIDA sources; the momentary rate of input traffic still varies a lot at individual nodes.

Instead of using a stochastic mathematical equation as a source of  $k_i$ ; we took three more traces, calculated their instantaneous rates and used them later, to create the new

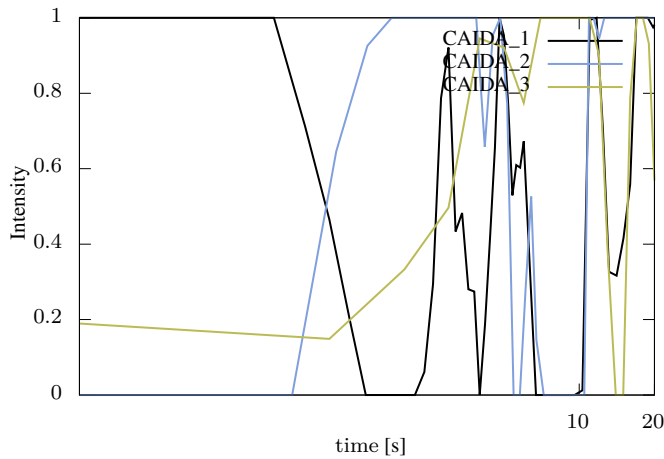


FIGURE 5.2: Intensity taken from three different CAIDA traces

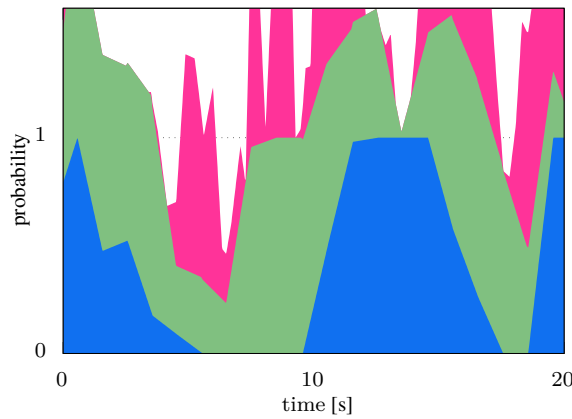


FIGURE 5.3: A cumulative flow chart showing the probabilities of acceptance of packets in three sources,  $m_n = 10$ . Assuming that each of the sources has a mean rate of 1 ; the upper edge of the colored area shows the effective packet rate without normalisation

traffic model. The Figure 5.2 shows an example of curves that reflects the intensity of traffic extracted from three different CAIDA traces. An instance of traffic model while taking intensity from considered sources without any manipulations is presented in the Figure 5.3. As clearly seen in the latter graphic, The sum of mixed produced traffic model may exceed 100%; reason for which, a standardization function is considered. On this point, the time scale multiplied the time by  $m_s = 500$  (i.e. made them  $m_s$  times slower, compared to the three mixed traces) and normalized them then, to have a mean of  $s_{NUM}^{-1}$  each. This hopefully reflects better the phenomena like a self-similarity, found in real telecommunication networks.

The traffic with the varying mixing function applied will further be called MIXED. For contrast, we will also use its homogeneous variant POISSON where all packets from the Poisson source are accepted, the two CAIDA sources ignored.

### 5.3.2 Responses to stimuli

We considered both a rectangular and a sine wave of the frequency  $f$  for the purpose of finding a connection between the stimulus  $a_S$  that reflects one of the coefficients that regulating the network strategy and the response provided by the momentary performance of the network. To gather a mean step and a frequency response of the network, nodes uses local histograms that store  $S_{\text{mean}}$  against  $\text{mod}(t, f^{-1})$  where  $t$  is a time of evaluation of (4.8); a histogram is thus, swept with a frequency of  $f$  similarly to an oscilloscope and for the same purpose to observe a waveform of that frequency. These histograms will then be integrated over all nodes into a response given by  $\hat{S}_{\text{mean}}$ .

In case of the further simulations, we took the total simulated time during the stage of packets' arrival. we take into account statistics of packets arriving during  $T_s=10s$ ,  $T_s =10$  s, otherwise exempted. Actual simulated time lasts until the last of these packets leaves the network.

#### 5.3.2.1 Step response

To get some insights, we started analyzing results while considering waves with a rectangular shape sent through  $a_{\text{mean}}$ . Indeed, the values of  $a_{\text{mean}}$  taken into account vary between 0 and two its optimal predefined value  $a_{\text{opt}}^{\text{mean}}$  found in 4 .

In order to see clearly different elements in the network's behaviour, Figure 5.4(a) we started by a case of a moderate oscillation frequency, a low traffic noise and a moderate  $L$ .

Due to propagation delays along the control channel,  $\hat{S}_{\text{mean}}$  is updated progressively, which is seen in the response's slopes, found directly after each flip of  $a_{\text{mean}}$ . After any of the two slopes occurs; an overshoot followed by a slight ringing, a shape similar to that expected from an electrical serial RLC circuit with a near-critical damping. Several factors play a role here. An instantaneous increase of  $a_{\text{mean}}$  is reflected by increased  $t_{\text{max}}$ ; this slows down the insertion of packets into the ring. This in turn increases the queues, which due to positive  $a_{\text{mean}}$  causes a further increase of  $t_{\text{max}}$  (predefined constants and



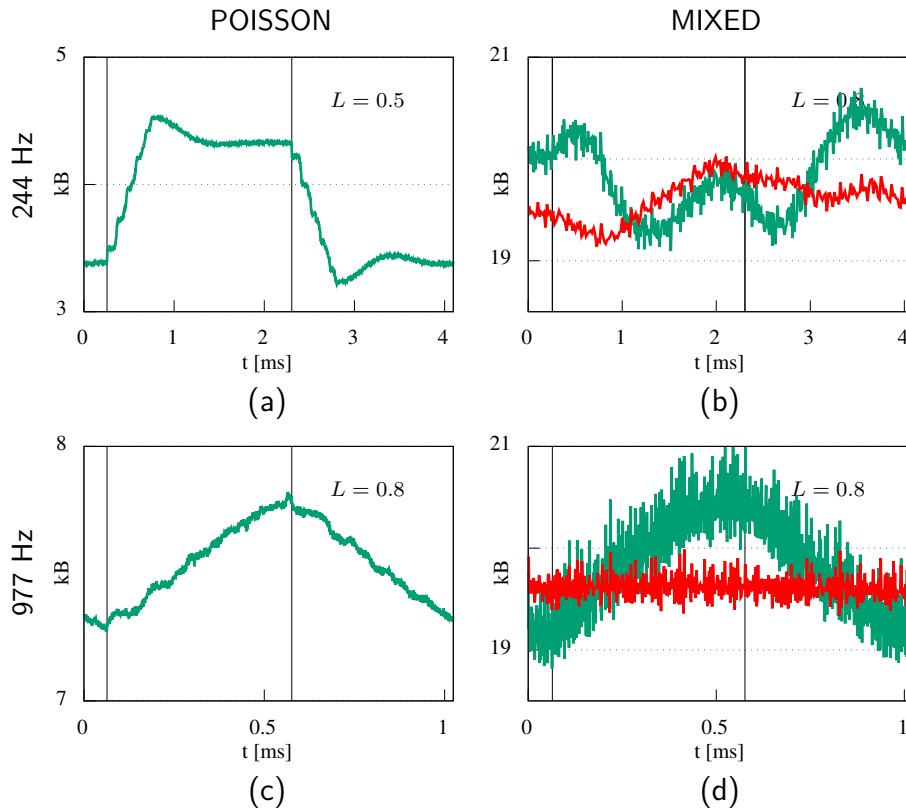


FIGURE 5.4: Step response : optimal  $a_{\text{mean}}$  is multiplied by a square waveform of levels 0, 2 and a given frequency. Vertical dashed lines show respectively the beginning and the end of the higher value of  $a_{\text{mean}}$ .

arguments in (4.8) are positive).

This produces effects which in contrast promotes an increased packet insertion :

- The ring becomes empty, the free WDM slots reach the nodes which follow ring-wise.
- The longer queues allow a more probable 100% fill ratio of a WDM slot, thus, less need for waiting for  $t_{\text{max}}$ .

These factors may evidently decrease  $\hat{S}_{\text{mean}}$  which subsequently decreases  $t_{\text{max}}$  etc. There is a complex set of circular dependencies which hinders the prediction of a better strategy. In a nutshell, we notice that in the analyzed case; a stabilized high  $a_{\text{mean}}$  increases buffer sizes and vice versa. We suppose that larger buffer sizes are expected to be proportional to the mean latency; an essential quality trait of a network. We thus, conclude that for the operating point in Figure 5.4(a); the mean value of  $a_{\text{mean}}$  should be decreased.

In Figure 5.4 (b), compared to (a); the traffic MIXED is used and also the load is increased. Due to the extreme burstiness and traffic heterogeneity; the relationship between  $a_{\text{mean}}$  and  $\hat{S}_{\text{mean}}$  can not be seen directly. It is the reason for which, we superimposed  $\hat{S}_{\text{mean}}^0$  which represents mean buffer size after sending packets who have an expired timer while considering a fixed strategy. This latter is ensured by considering a constant  $a_{\text{mean}}$ . The clear unevenness of  $\hat{S}_{\text{mean}}^0$  showed us that the noise level is very high at this operating point.

The bottom row in Figure 5.4, a higher frequency is considered while using both Poisson and MIXED traffic. Indeed, the results illustrate another problem :

- The two responses look very similar but the mechanism behind them is radically different :
  - In (c),  $a_{\text{mean}}$  and  $\hat{S}_{\text{mean}}$  are positively related. Given that the presented plot displays a small part of the slopes in (a); reason for why the curve changes direction exactly when  $a_{\text{mean}}$  changes as in (a).
  - In (d), similarly to (b),  $a_{\text{mean}}$  and  $\hat{S}_{\text{mean}}$  are negatively related. However, the phase delay between them makes (d) appears to have the same shape as (c). This illustrates, though, potential difficulties in analyzing the character of the response by e.g. an FFT transform. Nevertheless, the relatively high frequency of 977 Hz considered in (d) has also high phase delays, but on the contrary,  $\hat{S}_{\text{mean}}^0$  is almost flat. As a result, the noise, originating from the variable traffic, that is supposed to be low for that frequency is high. This trade-off may signify that there is some optimal frequency where the noise is sufficiently reduced.

### 5.3.2.2 Frequency response

The step response revealed traps that must be avoided also for sinusoidal oscillation of  $a_{\text{mean}}$  and those that we would rather use. Indeed, we should consider the potential abrupt changes triggered in the network by a rectangular oscillation as seen in Figure 5.4. As we all know, a multi-sine wave superposition forms a rectangular wave. Therefore, we expect that a sinusoidal oscillation produces a more focused answer in the further used frequency domain. We considered an amplitude of  $A = 1$  with the coefficient  $a_{\text{mean}}$  oscillating in the same range of  $\{0, 2a_{\text{opt}}^{\text{mean}}\}$  as in the section 5.3.2.1.

Similarly to what we did in section 5.3.2.1 ; we began with low load and POISSON traffic. The corresponding bode diagram at the top row of Figure 5.5 as for 5.4(a), reveals a characteristic similar to the low pass filter for passive electrical components. Due to the high speed of N-GREEN, we estimated that the phase delay should be negligible for very

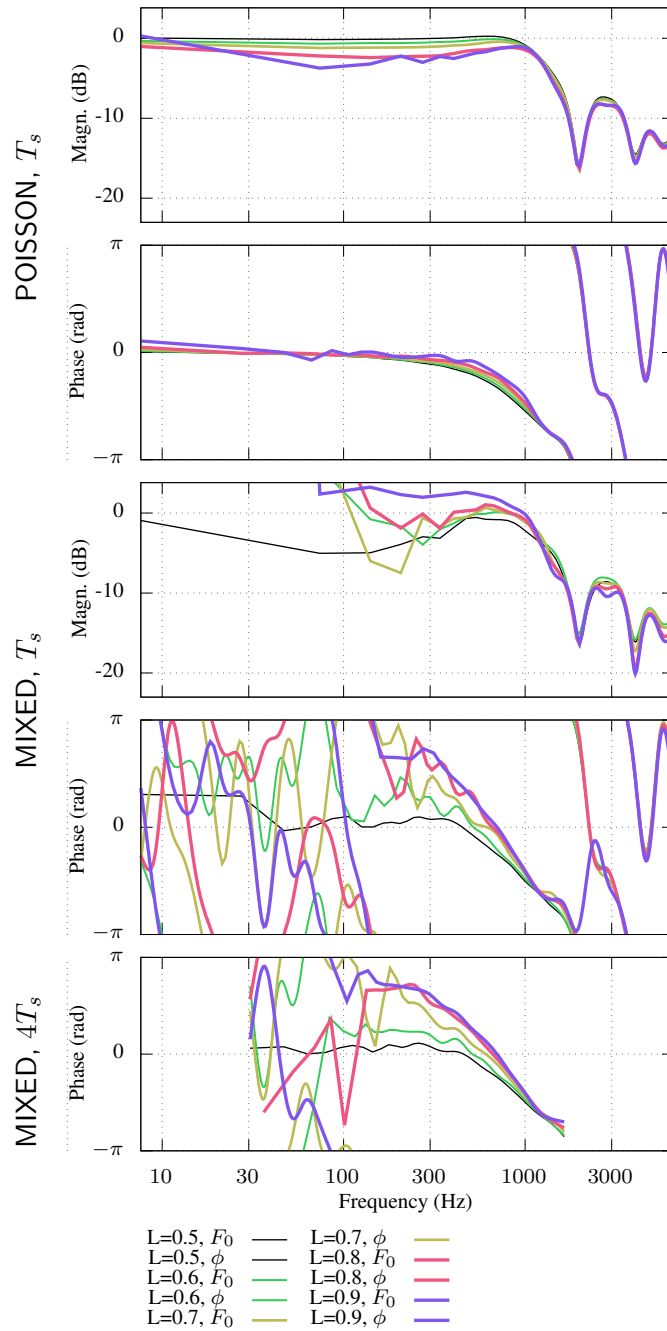


FIGURE 5.5: Bode diagrams of an N-GREEN ring against different  $L$  and traffic models,  $A = 1$ . As the stimulus and the response are in different units, we normalized the magnifications by comparing them at high frequencies and assuming 0 dB at low frequencies.

low frequencies. As depicted in the top 5.5, even with low noise of the traffic POISSON, at low frequencies ( $\in [0 :300]$ Hz); we observed a phase delay of  $\approx 0$  revealing that  $a_{\text{mean}}$  and  $\hat{S}_{\text{mean}}$  are positively related. At around 300 Hz, logically, the relation between  $a_{\text{mean}}$  and  $\hat{S}_{\text{mean}}$  should not change radically due to the small  $D$ . This proves that phase delays

observed are simply the result of network delays. At higher frequencies, besides with an increasing phase delay; we can observe several aliasing effects that are similar to the frequencies of the stimulus because of network delays or ringing frequencies. Nonetheless, the uninterpretability of the phase makes these regions unusable for our ends.

The resulting Bode diagram for MIXED traffic shows major signal distortion at the assumed frequency  $< 100$  Hz for the considered  $T_s$ . This is caused mainly by the noise. This latter can be minimized by longer simulation periods. However, we would like  $a_{\text{mean}}$  to be able to traverse a considerable part of  $D$  within  $< T_s$  in order to get a fast self adaptation. An apparent source of the noise might be the considerably uneven  $\hat{S}_{\text{mean}}^0$ ; compared to the response seen in Figure 5.4(b).

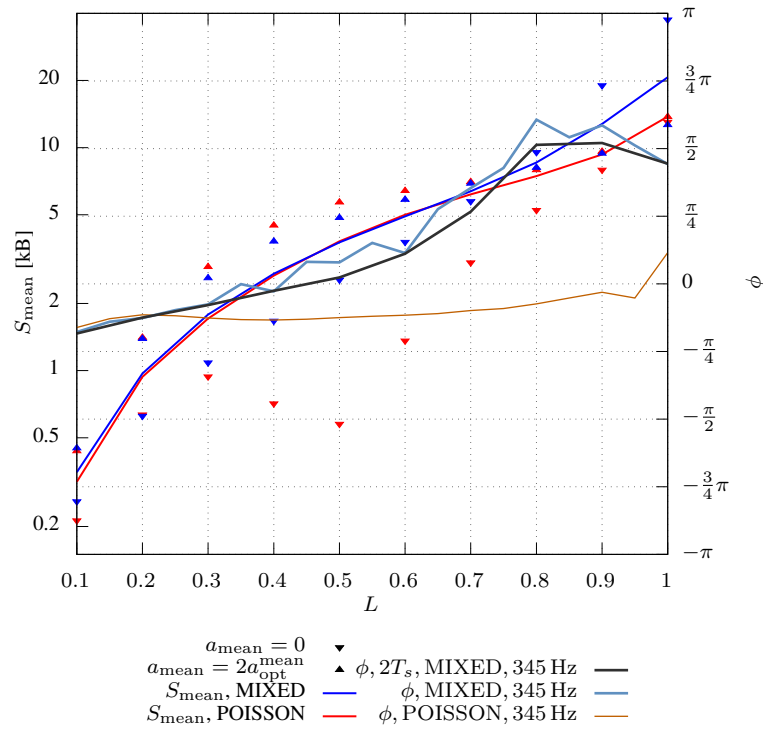


FIGURE 5.6:  $S_{\text{mean}}$  against different  $L$  and  $a_{\text{mean}}$ , both table during an entire simulation : lines for  $a_{\text{opt}}^{\text{mean}}$ , triangles for  $a_{\text{mean}} = \{0, 2a_{\text{opt}}^{\text{mean}}\}$ ; due to the limited effect of  $a_{\text{mean}}$  on  $\hat{S}_{\text{mean}}$ , the actual distance of triangles to the line is exaggerated by a multiplier of 5 for a better visibility. Phase values interpreted as in Bode diagrams.

The other factor could be the disappearing  $a_{\text{mean}}-\hat{S}_{\text{mean}}$  relation as clearly seen in the Figure 5.6 between  $L = 0.7$  and  $L = 0.8$  as starting from certain value of  $t_{\text{max}}$ . This particular strategy has no effect on the network. As a consequence  $a_{\text{mean}}$  oscillates without a significant impact on the network behavior. Regardless of all the obtained results in this case; there can be only noise with no reference to the  $a_{\text{mean}}$  phase.

The noise starts to slowly disappear when the frequency is  $> 250$  Hz. We notice also that at  $\approx 300$  Hz and for larger  $L$ ; the phase delay attends approximately  $> \pi$ . Nonetheless, we can not justify it by network delays since they are low at the same frequencies for POISSON traffic. It is quite impossible that phase delays have changed dramatically, due to MIXED traffic since WDM slots propagate at the same speed and the phase delay for high frequencies is similar.

We consider that it is probable that the phase at  $\approx 300$  Hz is a transition between :

- A mixture of  $\approx 0$  and  $\approx \pi$ , characteristic for  $a_{\text{mean}}$  and  $\hat{S}_{\text{mean}}$  positively/negatively related.
- approximately  $\approx -\pi/2$ , observed at frequencies of about 1000 Hz where the phase delays converge and magnifications decrease almost uniformly for all  $L$  (thus for all relations between  $a_{\text{mean}}$  and  $\hat{S}_{\text{mean}}$ ) which suggests that the oscillation of  $a_{\text{mean}}$  is too fast at these frequencies in order to cause a considerable effect on  $\hat{S}_{\text{mean}}$ .

The assumption that the phases in  $\approx 300$  Hz are not just a random noise residue is confirmed by the Bode diagram for a simulation time of  $4T_s$  where the noise seems to decrease even earlier; at  $\approx 200$  Hz.

The region of 350 Hz seems to be optimal given that the phases are considerably less noisy comparing to the lower frequencies that are not uniform for all  $L$  as in the case of higher frequencies. Their values can be seen while checking the relation between  $a_{\text{mean}}$  and  $\hat{S}_{\text{mean}}$  as mapped in 5.6.

### 5.3.2.3 Optimization

Observing the Bode diagrams in Figure 5.5 and the phases  $\phi$  in Figure 5.6, specifically at the tipping point for the traffic MIXED between  $L = 0.7$  and  $L = 0.8$ ; we define  $\phi$  as follows :

- $a_{\text{mean}}$  is increased by  $a_{\text{step}}$  if and only if  $\phi \in \left(\frac{3}{8}\pi, \pi\right)$ ;
- $a_{\text{mean}}$  is decreased by  $a_{\text{step}}$  if and only if  $\phi \in \left(-\pi/2, \frac{3}{8}\pi\right)$ ;
- otherwise, we will keep the value of  $a_{\text{mean}}$  although we can not decide anything about this range of delays.

In this basic demonstrative scheme, the amplification is not taken into account. Nevertheless, it is worth to note that the strategy can drift randomly if the signal obtained is weak or non-existent.

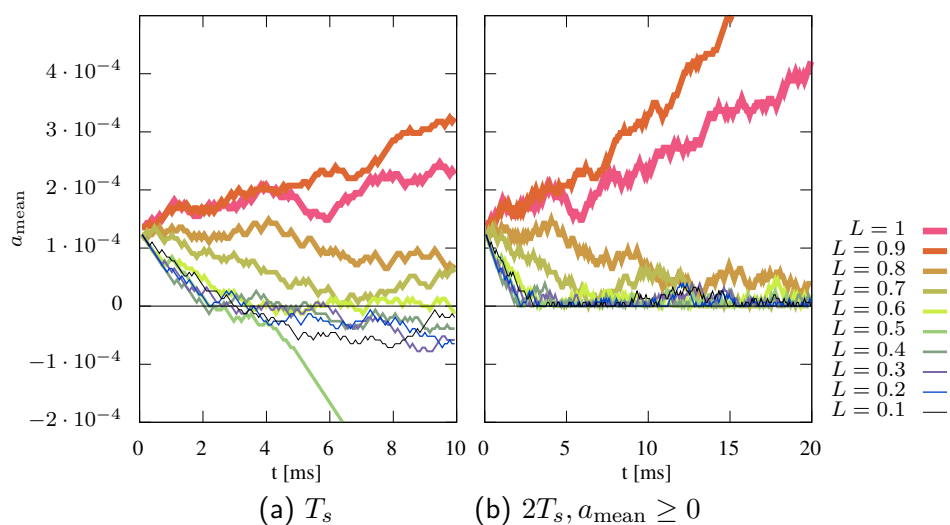


FIGURE 5.7: Adaptation of  $a_{\text{mean}}$  during different optimization processes, the central frequency is always 354 Hz.

Note that we enable an arbitrary  $t_{\text{max}}$  value that obviously exceeds any reasonable  $D$  limit. The goal is to see if the accumulation of  $t_{\text{max}}$  discussed in the 4.3.3.1.1 section ; leads to direct optimization or if it enhances performance when considering  $a_{\text{mean}}$ 's negative value.

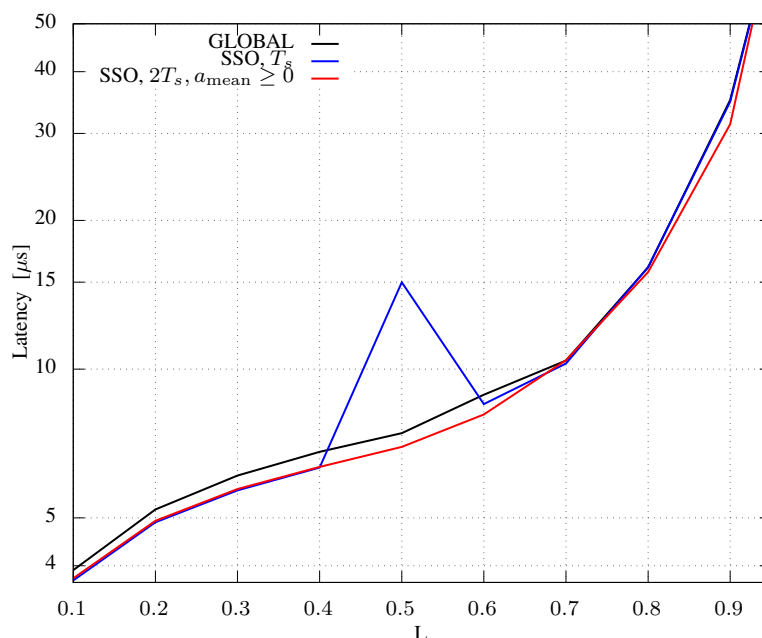


FIGURE 5.8: Quality for different loads and the traffic model MIXED, without and with different types of strategy oscillation. See that an extended simulation time  $2T_s$  is important for larger  $L$ .

Figure 5.7(a) shows an optimization process where after each  $F = 27$  oscillations of 354 Hz; an averaged response is processed with a Fast Fourier Transform. Then  $a_{\text{mean}}$  is modified with a step of  $a_{\text{step}} = a_{\text{opt}}^{\text{mean}}/20$  depending on the phase.  $F$  and  $a_{\text{step}}$  were found experimentally as providing an adaptation time of the order of  $T_s$ ; so that the level of noise which previously considered in the averaged responses is more or less apt. Longer adaptation times would likely to be effective in decreasing the noise as seen  $\phi$  for  $2T_s$  in Figure 5.6, where the phase increases the most between the two borderline cases of  $L = 0.7$  and  $L = 0.8$ . We also reduced the oscillation amplitude from  $A = 1$  to 0.5 in order to be able to keep a better minimally intrusive modification of strategy.

The adaptation of  $a_{\text{mean}}$  roughly follows the direction to smaller  $\hat{S}_{\text{mean}}$  depicted by the triangles in Figure 5.6 except for the borderline cases where  $a_{\text{mean}}$  changes undecidedly.

Figure 5.8 shows the performance of the frequency-domain strategy tuning compared to the original strategy GLOBAL. Given the limited effect of  $a_{\text{mean}}$  seen in the exaggerated Figure 5.6; the tuning works well as a "tuning of tuning", even for the smaller oscillation amplitude.

Predictably there is no improvement for the borderline cases, i.e.  $a_{\text{mean}}$  is meaningless there. An occasional runaway effect which makes  $a_{\text{mean}} < -2 \cdot 10^{-4}$  for  $L = 0.5$  (compare Figure 5.8 to Figure 5.7) is detrimental. This shows the importance of keeping the strategy within  $D$  in order to keep the system robust – in Figure 5.7(b); we prevent  $a_{\text{mean}}$  from being negative.

The results point to a usefulness of traditional frequency-domain control loop methods in optimizing a noisy telecommunication infrastructure.

## 5.4 Conclusion

In this chapter, we studied the effect of changing one of the coefficients affecting the network strategy on network performance facing a highly variable model of traffic.

Initially, we briefly introduced the principle of the considered method i.e. frequency modulation and the key concepts related to this approach. We then, presented the traffic model considered and used to test the proposed strategy ; thus, a rather variable model thus producing a fairly noisy network. The ultimate outcome model takes into account many statistics taken with some modification from CAIDA traces with respect to the parameters defined in the N-GREEN basic architecture.

As for the last part, the effect of strategy change on network behavior has been shown step by step. We began with rectangular wave in order to determine certain frequency values which implies that the noise is quite large and must be avoided in the next step. We later considered that instead of a rectangular wave ; the value of the coefficient changes following a sine wave. Results show the usefulness of conventional frequency-domain control loop approaches to optimize a noisy telecommunications infrastructure. However, the results obtained are not up to aspirations. The main reason on which we are working on a variant, while considering a machine learning is that IA algorithms are potentially more rapid and stable as compared to the optimal method.

The next chapter 6 concludes this dissertation with a few suggestions for future work.



## Chapter 6

# General conclusions and perspectives

Within the framework of this thesis, we have been interested in the performance analysis of the new architecture of switch/router proposed by the international telecommunication company Nokia Bell Labs. Actually, the proposed architecture is the result of a stepwise accumulation of improvements and developments aiming to meet the forecasted traffic for the next few years taking energy and cost effectiveness into account as decisive parameters.

The new N-GREEN design could be used in multiple network segments and under different conditions. As such, it could be used in the metro access/aggregation network as well as in the backbone for the wireline part and the Xhaul, taking into account the introduction of 5G. Within this thesis, as we were interested in the metro aggregation part of the network; hence, we considered optical ring network which transports colored packets. Our preliminary simulation results show that the architecture suffers from a low efficiency of resource usages, especially when it is used in the destination based mode i.e the unicast popular in the metro aggregation. As a first contribution, we proposed an alternate packet management and transmission schema referred to as Ssh-time [70]. Our results have exhibited that the proposed method improves not only the resources efficiency in case of a metro-aggregation network, but also decreases the mean access delay.

We extended our investigation by considering a real packet traces taken from CAIDA traces. Based on our simulation results, we discovered that N-GREEN is more adapted to a predictable traffic with a low burst rate, found e.g. in the metro aggregation. Hence, we were keen on adjusting the network to other potentially interesting applications. In this study where the traffic is more bursty ; we handled the system by proposing a new packet management schema with adaptive expiration times, determined in response to local and/or global queue sizes. The exact relation is found using a direct optimization method simulated and optimized via Nelder Mead Simplex. Our results show that thanks to the regulation of the expiration time, an N-GREEN ring may continuously adapt to a bursty/unpredictable traffic of a varying average load. The nodes notify each other of the momentary data size in their output buffers. The adaptation considerably decreases the latency of the network without needing to add any resources or updating the architecture.

The proposed packet management schema which defines adaptive expiration times are calculated for each type of traffic apart. The traffic type is defined by the designer at the beginning. However, it is desirable to define a network capable of optimally allocating resources and adapting dynamically themselves to the changing operating conditions. To this end, we studied the quality of frequency response for N-GREEN network facing extremely changeable traffic flow model. This latter is designed specifically to test the limit of the proposed method. A generator of flow per node is composed by three traffic models namely, the well-known Poisson model mixed with two models extracted from CAIDA traces. Within this context, we analyze a step i.e frequency response of a simulated computer network where the stimulus is one of the coefficients which regulates the network's strategy of packet transmission and the response is the network's momentary performance. Subsequently, we found a frequency range where an instantaneous dependency between the stimulus and the response directs a self-adaptation schema of the proposed strategy.

As highlighted in our last study [90], the main brake of the emergence of auto-adapting method in networks is their sensitivities to noises. Despite the consideration of an extremely weak stimulus in order to stay in the safe limits of the network's behaviour ; it did not provide the desired output improvement. In a following step, we aim to carry out comparative study with other methods aiming to improve the results obtained while auto-adapting the network to traffic changes. Using the same traffic models, the controller could be represented by an algorithm of machine learning such as Feed Forward Neural Network. Input data could be a set of information about an amount of packets gathered during a short duration i.e mean packet size, source, destination and variance etc... whereas the output could be considered as latency. Latency is represented simply by the size of the

queue. A trained system could be used later to determine an exact relation between the entered data and the received response of the system.

An analytical model should be proposed to validate the obtained results by the achieved simulation. A work already started proposing a diffusion model of the queue management. It defines a system with a periodic loading of optical buffers filled by IP packets as in N-GREEN. Indeed, the modeled system is defined as follows : the electronic packets at each queue are periodically inserted into an optical packet (PDU) of a fixed size  $L$  equal to 12500 bytes which is available within each fixed interval  $\Delta$ . The insertion probability depends on two factors : probability  $p$  that the optical packet is empty and of the applied algorithm.

Two cases are defined within this planned study :

- Each  $\Delta$  we try to put the content of the queue into the buffer  $\Rightarrow$  the probability of event (success) is  $p$ .
- we try to fill the optical packet at the end of  $\Delta$  only if the queue size is larger than  $L$ .

The system will be solved by a diffusion approximation where the size of the queue is represented by the value of a diffusion process [91] and its evolution is given by a defined diffusion equation. Within the first study, we will witness a short study on the performance of a single queue, then, the interactions inside the ring will be considered.

Another perspective of this work is to apply a machine learning that could be used when considering two rings that are meant both for data transfer. As mentioned earlier in this dissertation ; two rings are considered in N-GREEN platform, normally, one is used for data transfer and the second ring is dedicated for recovery in case of failure. In the same axis as for the auto-adaptation of N-GREEN, we can apply a machine learning algorithm that could predict on which ring it is better to transmit data. These predictions and recommendations could achieve the best latency while considering CoS, the possibility that the ring may break down and the intensity of traffic.

# Annexe A

## Synthèse en Français

### Thématique

Dans le cadre du projet ANR/N-GREEN, une nouvelle architecture de commutateur/routeur a été conçue principalement pour répondre aux exigences strictes de 5G telle qu'un délai de bout en bout de moins  $250 \mu s$  pour certaines applications [64], mais aussi pour répondre à l'augmentation des trafics prévus particulièrement dans la partie métropolitaine de réseau (MAN). **Dans le cadre de cette thèse**, nous étudions cette architecture tout en proposant des méthodes qui lui sont adaptées afin d'améliorer ces performances.

### Adaptation de l'architecture aux trafics sporadiques

Nous avons mené une étude de performance de cette architecture par simulation. Pour commencer, nous avons considéré des scénarios des benchmarking traditionnels telle qu'un modèle TDM (Time Division Multiplexing) et des mécanismes d'insertion à base de timer à valeurs constantes appliqués sur un réseau en anneau composé de 10 noeuds N-GREEN. Nos résultats préliminaires montrent un comportement paradoxal révélant ainsi que l'architecture est surdimensionnée.

En prenant en compte cette spécificité, une méthode de gestion de slot optique a

été proposée : Time Slot Sharing (Ssh-Time). L'idée est de descendre à une granularité plus petite dans le but d'utiliser au mieux les ressources disponibles. L'avantage de cette solution ce qu'elle améliore l'utilisation de la bande passante puisqu'elle permet de profiter au maximum des ressources disponibles. En contrepartie, cette approche exige l'ajout d'un temps de garde incompressible en fonction du nombre de sous slots considéré et donc une petite perte des ressources disponibles.

Nous avons étendu notre enquête en considérant d'autres types de trafic réel tirés à partir des traces de CAIDA. Trois modèles ont été considérés : le premier est le modèle théorique de base Poisson et deux autres appelés respectivement Raw et Balanced. Dans la variante *Raw*, l'espace d'adressage anonymisé est simplement divisé en parties égales entre les dix noeuds N-GREEN. Étant donnée que le modèle produit est fortement asymétrique, une fonction d'équilibrage de charge a été proposée. Le modèle de trafics produit est appelé Balanced et représente un modèle plus au moins symétrique. En utilisant quelque algorithme d'optimisation telle que Nelder Mead Simplex, et contrairement à ce qu'existe dans la littérature, une stratégie dynamique permettant de calculer la valeur de timer optimale a été proposée. La valeur retournée optimise au mieux la latence considérons l'état actuel de réseau. Deux variantes ont été suggérées permettant de définir l'équation estimant cette valeur de timer :

- Local : Nous avons considéré que la valeur de timer dépend uniquement des conditions locales d'un noeud, plus particulièrement quantité de trafics en octets dans le noeud source. La fonction à optimiser est définie comme suit :

$$t_{\max}(S_i) = a_0 + a_1 \frac{S_i}{d} + a_2 \left( \frac{S_i}{d} \right)^2 \quad (\text{A.1})$$

- Global : Où la valeur de timer dépend également d'autres informations d'ordre global tel que maximum et moyenne d'octets dans le buffer de noeud source et dernier destination de slot optique en plus que le nombre d'octets dans le buffer de noeud source. La fonction à optimiser est définie comme suit :

$$t_{\max}(S_i) = a + a_S \frac{S_i}{d} + a_{\text{mean}} \frac{S_{\text{mean}}(N_s, N_t)}{d} + a_{\text{max}} \frac{S_{\text{max}}(N_s, N_t)}{d} \quad (\text{A.2})$$

Considérons cette dernière les informations sur les tampons des autres noeuds sont envoyées à travers le canal de contrôle présent dans le modèle de base de l'architecture N-GREEN.

Bien évidemment les résultats obtenus en considérant la deuxième variante sont meilleurs permettant ainsi d'ajuster au mieux les paramètres de N-GREEN en fonction de l'application considérée. L'avantage de cette approche est qu'elle nécessite uniquement d'ajouter quelques informations dans le canal de contrôle.

Les résultats numériques sont détaillés et analysés au chapitre 3.

## **Modulation de fréquence pour l'auto-adaptation de N-GREEN**

Bien que la stratégie proposée permet de répondre aux exigences demandées en matière de latence. Le modèle de trafics considéré est entrée comme paramètre au simulateur et devrait être changé à chaque fois par le designer. Néanmoins, dans les réseaux d'opérateur réels, les modèles de trafic changent constamment, nous avons donc besoin d'un moyen de suivre ces changements. En s'inspirant de l'idée de régulateur PID, nous nous sommes intéressés aux méthodes d'auto adaptation des réseaux en temps réel face aux changements des trafics. Comme on parle d'une adaptation constante de la stratégie dans des conditions bruyantes, nous avons proposé et simulé un modèle de trafic très variable, plus variable que celui tiré de trace CAIDA considéré dans la section précédente. Le modèle produit est formé par un mixage de trois sources CAIDA.

En observant l'effet de changement de fréquence de l'un des coefficients qui régissent sur la stratégie de transmission des paquets sur les performances momentanées du réseau; nous déterminons une bande de fréquences utilisables où une dépendance instantanée entre ces deux paramètres peut définir un schéma d'auto-adaptation.

Deux formes de stimulus ont été considérés afin de déterminer la bonne fréquence de changement de la stratégie :

- Rectangulaire avec différentes fréquences : où on a considéré qu'un des coefficients qui régissent sur la stratégie oscille rectangulairement.
- Sinusoïdal avec différentes fréquences : comme les résultats obtenus considérant le premier variant n'ont pas donné les résultats désirés, nous avons considéré une oscillation sinusoïdale.

Les résultats de cette étude sont détaillés au chapitre 5. Quoique à travers cette étude nous avons trouvé une bande de fréquences qui minimise la latence; nous n'avons

pas pu trouver l'exacte relation entre les stimulus et la réponse de réseau désiré. Cette étude se poursuit actuellement avec un test d'une machine learning qui nous supposons qu'elle sera plus rapide comparé aux méthodes d'optimisation.

## Cadre du travail

Dans le cadre du programme de l'école doctoral de STIC, Science Technologies de l'Information et de Communication de Paris, les travaux de cette thèse se sont déroulés au sein de Télécom Sud Paris, appartenant à l'université de Paris-Saclay sous la direction de Professeur Mme **Tulin Atmaca**. La majorité de ce travail est effectué comme partie de projet ANR/N-GREEN proposé par Nokia Bell Labs. Pendant ces trois années de thèse, j'ai eu l'occasion de faire deux séjours de cours durée à l'académie Polonaise et à l'université technique d'Istanbul pendant laquelle j'ai pu échanger et discuter avec des professeurs de haute calibres. Cette thèse est principalement financée par une bourse nationale délivrée par le Ministère de l'Enseignement Supérieur et de la Recherche Scientifique - Tunisie et basée sur des critères de mérite.

## Bibliography

- [1] CAIDA UCSD. Anonymized internet traces 2012, [http://www.caida.org/data/passive/passive\\_2012\\_dataset.xml](http://www.caida.org/data/passive/passive_2012_dataset.xml), 2012.
- [2] Cisco®. Cisco catalyst 3850 switches datasheet, c78-720918s. *IEEE Tech. Rep.*, Mar, 2016. URL [http://www.cisco.com/c/en/us/solutions/collateral/service-provider/visual-networking-index-vni/VNI\\_Hyperconnectivity\\_WP.html](http://www.cisco.com/c/en/us/solutions/collateral/service-provider/visual-networking-index-vni/VNI_Hyperconnectivity_WP.html).
- [3] Martin Maier. *Optical switching networks*. Cambridge University Press, 2008.
- [4] Andrea Carena, Vito De Feo, Jorge M Finochietto, Roberto Gaudino, Fabio Neri, Chiara Piglione, and Pierluigi Poggiolini. Ringo : an experimental wdm optical packet network for metro applications. *IEEE Journal on selected areas in communications*, 22(8) :1561–1571, 2004.
- [5] Guoqiang Hu, Christoph M Gauger, and Sascha Junghans. Performance of mac layer and fairness protocol for the dual bus optical ring network (dborn). In *Conference on Optical Network Design and Modeling*, pages 467–476, 2005.
- [6] Dominique Chiaroni, R Urata, J Gripp, JE Simsarian, G Austin, S Etienne, T Segawa, Y Pointurier, C Simonneau, Y Suzaki, et al. Demonstration of the interconnection of two optical packet rings with a hybrid optoelectronic packet router. pages 1–3, 2010.
- [7] Djamel Amar, Catherine Lepers, Franck Gillet, Mounia Lourdiane, Cédric Ware, and Dominique Chiaroni. WDM slot sharing of colored optical packets for latency improvement and class of service differentiation. In *Transparent Optical Networks (ICTON), 2017 19th International Conference on*, pages 1–4. IEEE, 2017.
- [8] Daniel C Kilper, Gary Atkinson, Steven K Korotky, Suresh Goyal, Peter Vetter, Dusan Suvakovic, and Oliver Blume. Power trends in communication networks. *IEEE Journal of selected topics in quantum electronics*, 17(2) :275–284, 2010.



- [9] Shun Yao, SJ Ben Yoo, Biswanath Mukherjee, and Sudhir Dixit. All-optical packet switching for metropolitan area networks : opportunities and challenges. *IEEE Communications Magazine*, 39(3) :142–148, 2001.
- [10] Martin Herzog, Martin Maier, and Martin Reisslein. Metropolitan area packet-switched wdm networks : A survey on ring systems. *IEEE Communications Surveys & Tutorials*, 6(2) :2–20, 2004.
- [11] Dominique Chiaroni and Bogdan Uscumlic. Potential of WDM packets. In *Optical Network Design and Modeling (ONDM), 2017 International Conference on*, pages 1–6. IEEE, 2017.
- [12] Catherine Lepers, Djamel Amar, Franck Gillet, and Dominique Chiaroni. On the interest of WDM-colored optical packets in metro aggregation networks. In *Asia Communications and Photonics Conference*, pages M3C–5. Optical Society of America, 2017.
- [13] V Cisco. The zettabyte era : trends and analysis. updated (07/06/2017), 2017.
- [14] Cost to Install Fiber Cement Siding.[online], June. 2016. URL [//www.homewyse.com/services/cost\\_to\\_install\\_fiber\\_cement\\_siding.html](http://www.homewyse.com/services/cost_to_install_fiber_cement_siding.html).
- [15] Unit Cost Entries for Fiber Optic Cable Installation.[online], Feb. 2015. URL <http://www.itscosts.its.dot.gov/its/benecost.nsf/DisplayRUCByUnitCostElementUnadjusted?ReadForm&UnitCostElement=Fiber+Optic+Cable+Installation+%26Subsystem=Roadside+Telecommunications+%28RS-TC%29>.
- [16] Zvi Rosberg, Hai Le Vu, Moshe Zukerman, and Jolyon White. Performance analyses of optical burst-switching networks. *IEEE Journal on Selected Areas in Communications*, 21(7) :1187–1197, 2003.
- [17] Hugo Meyer, Jose Carlos Sancho, Wang Miao, Harm Dorren, Nicola Calabretta, and Montse Farreras. Performance evaluation of optical packet switches on high performance applications. In *2015 International Conference on High Performance Computing & Simulation (HPCS)*, pages 356–363. IEEE, 2015.
- [18] Mohammad Gharaei. *Nouveaux concepts pour les réseaux d'accès optiques*. PhD thesis, Paris, Télécom ParisTech, 2010.
- [19] Ed Harstead and Randy Sharpe. Forecasting of access network bandwidth demands for aggregated subscribers using monte carlo methods. *IEEE Communications Magazine*, 53(3) :199–207, 2015.

- [20] Kostas N Oikonomou, Rakesh K Sinha, Byoung-Jo Kim, and Robert D Doverspike. Performability analysis of a metropolitan area cellular network. In *2015 11th International Conference on the Design of Reliable Communication Networks (DRCN)*, pages 141–148. IEEE, 2015.
- [21] Weiyi Zhang, Balagangadhar G Bathula, Rakesh K Sinha, Robert Doverspike, Peter Magill, Aswatnarayan Raghuram, and Gagan Choudhury. Evolution of the ip-over-optical core network. In *2015 11th International Conference on the Design of Reliable Communication Networks (DRCN)*, pages 227–234. IEEE, 2015.
- [22] Byrav Ramamurthy, Helena Feng, Debasish Datta, Jonathan P Heritage, and Biswanath Mukherjee. Transparent vs. opaque vs. translucent wavelength-routed optical networks. In *OFC/IOOC. Technical Digest. Optical Fiber Communication Conference, 1999, and the International Conference on Integrated Optics and Optical Fiber Communication*, volume 1, pages 59–61. IEEE, 1999.
- [23] Monique Renaud, Francesco Masetti, Christian Guillemot, and Bruno Bostica. Network and system concepts for optical packet switching. *IEEE Communications Magazine*, 35(4) :96–102, 1997.
- [24] Gee-Kung Chang, Jianjun Yu, Yong-Kee Yeo, Arshad Chowdhury, and Zhensheng Jia. Enabling technologies for next-generation optical packet-switching networks. *Proceedings of the IEEE*, 94(5) :892–910, 2006.
- [25] Mike J O’Mahony, Dimitra Simeonidou, David K Hunter, and Anna Tzanakaki. The application of optical packet switching in future communication networks. *IEEE Communications magazine*, 39(3) :128–135, 2001.
- [26] Biswanath Mukherjee. *Optical WDM networks*. Springer Science & Business Media, 2006.
- [27] Chunming Qiao and Myungsik Yoo. Optical burst switching (obs)—a new paradigm for an optical internet<sup>1</sup>. *Journal of high speed networks*, 8(1) :69–84, 1999.
- [28] Yang Chen, Chunming Qiao, and Xiang Yu. Optical burst switching : a new area in optical networking research. *IEEE network*, 18(3) :16–23, 2004.
- [29] Louay Eldada. Optical add/drop multiplexing architecture for metro area networks. *Optoelectronics & Communications, SPIE Newsroom*, 2008.
- [30] Louay Eldada. Roadm architectures and technologies for agile optical networks. In *Optoelectronic Integrated Circuits IX*, volume 6476, page 647605. International Society for Optics and Photonics, 2007.

- [31] Dawei Ge, Juhao Li, Zhongying Wu, Fang Ren, Paikun Zhu, Qi Mo, Zhengbin Li, Zhangyuan Chen, and Yongqi He. Experimental demonstration of roadm functionalities for hybrid mdm-wdm optical networks. In *2016 Optical Fiber Communications Conference and Exhibition (OFC)*, pages 1–3. IEEE, 2016.
- [32] Kenya Suzuki, Kazunori Seno, and Yuichiro Ikuma. Application of waveguide/free-space optics hybrid to roadm device. *Journal of Lightwave Technology*, 35(4) :596–606, 2016.
- [33] Ming C Wu, Olav Solgaard, and Joseph E Ford. Optical mems for lightwave communication. *Journal of Lightwave Technology*, 24(12) :4433–4454, 2006.
- [34] Keisuke Sorimoto, Hiroyuki Tsuda, Hiroshi Ishikawa, Toshifumi Hasama, Hitoshi Kawashima, Kenji Kintaka, Masahiko Mori, and Hisato Uetsuka. A compact high-port-count wavelength selective switch using lcross and a multi-stacked awg. In *21st Annual Meeting of the IEEE Lasers and Electro-Optics Society, LEOS 2008*, pages 376–377, 2008.
- [35] Daniel J Blumenthal, Paul R Prucnal, and Jon R Sauer. Photonic packet switches : Architectures and experimental implementations. *Proceedings of the IEEE*, 82(11) : 1650–1667, 1994.
- [36] Jean-Michel Fourneau and David Nott. Mixed routing for romeo optical burst. In *International Symposium on Computer and Information Sciences*, pages 257–266. Springer, 2004.
- [37] J-M Fourneau, Mouad Ben Mamoun, and A Basic. Modeling fiber delay loops in an all optical switch. In *Third International Conference on the Quantitative Evaluation of Systems-(QEST'06)*, pages 93–102. IEEE, 2006.
- [38] Salah Ibrahim, Ryo Takahashi, SL Pyshkin, and J Ballato. Hybrid optoelectronic router for future optical packet-switched networks. In *Optoelectronics-Advanced Device Structures*. InTech, 2017.
- [39] Timothy Walker. Optical transport network (otn) tutorial. *Capturado em : www.itu.int/ITU-T/studygroups/com15/otn/OTNtutorial.pdf*, 2007.
- [40] Stefano Bregni, Diego Carzaniga, Roberto Gaudino, and Achille Pattavina. Slot synchronization of wdm packet-switched slotted rings : the wonder project. In *2006 IEEE International Conference on Communications*, volume 6, pages 2556–2561. IEEE, 2006.

- [41] Viet Hung Nguyen and Tulin Atmaca. Dynamic intelligent mac protocol for metropolitan optical packet switching ring networks. In *2006 IEEE International Conference on Communications*, volume 6, pages 2661–2668. IEEE, 2006.
- [42] Nizar Bouabdallah, Emmanuel Dotaro, Laurent Ciavaglia, Nicolas Le Sauze, and Guy Pujolle. Resolving the fairness issue in bus-based optical access networks. *IEEE Communications Magazine*, 42(11) :S12–S18, 2004.
- [43] VH Nguyen and T Atmaca. Performance analysis of the modified packet bursting mechanism applied to a metropolitan wdm ring architecture. In *IFIP Open Conference on Metropolitan Area Networks : Architecture, protocols, control and management*, pages 199–215, 2005.
- [44] Dominique Chiaroni, Géma Buforn Santamaria, Christian Simonneau, Sophie Etienne, Jean-Christophe Antona, Sébastien Bigo, and Jesse Simsarian. Packet oadms for the next generation of ring networks. *Bell Labs Technical Journal*, 14(4) :265–283, 2010.
- [45] Ning Deng, Shiyi Cao, Teng Ma, Xiaozhong Shi, Xiaodong Luo, Shuqiang Shen, and Qianjin Xiong. A novel optical burst ring network with optical-layer aggregation and flexible bandwidth provisioning. In *2011 Optical Fiber Communication Conference and Exposition and the National Fiber Optic Engineers Conference*, pages 1–3. IEEE, 2011.
- [46] Dominique Chiaroni. Optical packet add/drop multiplexers for packet ring networks. In *2008 34th European Conference on Optical Communication*, pages 1–4. IEEE, 2008.
- [47] Christian Cadéré, Nora Izri, Dominique Barth, Jean-Michel Fourneau, Dana Marinca, and Sandrine Vial. Virtual circuit allocation with qos guarantees in the eco-frame optical ring. In *2010 14th Conference on Optical Network Design and Modeling (ONDM)*, pages 1–6. IEEE, 2010.
- [48] D Popa and T Atmaca. al. evaluating the performance of an all-optical metro ring network : Fixed-length packet-switching versus variable-length packet-switching technology. *Proceedings of HET-NETs, Ilkley, UK*, 2003.
- [49] Indra Widjaja, Iraj Saniee, Randy Giles, and Debasis Mitra. Light core and intelligent edge for a flexible, thin-layered, and cost-effective optical transport network. *IEEE Communications Magazine*, 41(5) :S30–S36, 2003.

- [50] I Sanjee and Indra Widjaja. A new optical network architecture that exploits joint time and wavelength interleaving. In *Optical Fiber Communication Conference, 2004. OFC 2004*, volume 1, page 446. IEEE, 2004.
- [51] Kevin Ross, Nicholas Bambos, Krishnan Kumaran, Iraj Saniee, and Indra Widjaja. Scheduling bursts in time-domain wavelength interleaved networks. *IEEE Journal on Selected Areas in Communications*, 21(9) :1441–1451, 2003.
- [52] Indra Widjaja and Iraj Saniee. Simplified layering and flexible bandwidth with twin. In *Proceedings of the ACM SIGCOMM workshop on Future directions in network architecture*, pages 13–20. ACM, 2004.
- [53] Giorgio Cazzaniga, Christian Hermsmeyer, Iraj Saniee, and Indra Widjaja. A new perspective on burst-switched optical networks. *Bell Labs Technical Journal*, 18(3) : 111–131, 2013.
- [54] Nizar Bouabdallah, Guy Pujolle, and Harry Perros. Cost-effective single-hub wdm ring networks. In *2006 IEEE International Conference on Communications*, volume 5, pages 2421–2426. IEEE, 2006.
- [55] George Suwala and George Swallow. Sonet/sdh-like resilience for ip networks : a survey of traffic protection mechanisms. *IEEE network*, 18(2) :20–25, 2004.
- [56] Gerlas van den Hoven. Semiconductor optical amplifiers for digital and analog communication. In *OFC'98. Optical Fiber Communication Conference and Exhibit. Technical Digest. Conference Edition. 1998 OSA Technical Digest Series Vol. 2 (IEEE Cat. No. 98CH36177)*, pages 40–41. IEEE, 1998.
- [57] Prince M Anandarajah, A Kaszubowska, R Maher, and Liam P Barry. Wavelength tunable lasers in future optical communication systems. In *2008 10th Anniversary International Conference on Transparent Optical Networks*, volume 2, pages 109–109. IEEE, 2008.
- [58] M Renaud, D Keller, N Sahri, S Silvestre, D Prieto, F Dorgeuille, F Pommereau, JY Emery, E Grard, and HP Mayer. SOA-based optical network components. In *Electronic Components and Technology Conference, 2001. Proceedings., 51st*, pages 433–438. IEEE, 2001.
- [59] Ahmed Triki, Annie Gravey, Philippe Gravey, and Michel Morvan. Long-term capex evolution for slotted optical packet switching in a metropolitan network. In *2017 International Conference on Optical Network Design and Modeling (ONDM)*, pages 1–6. IEEE, 2017.

- [60] Antonio De La Oliva, Xavier Costa Pérez, Arturo Azcorra, Andrea Di Giglio, Fabio Cavaliere, Dirk Tiegelbekkers, Johannes Lessmann, Thomas Haustein, Alain Mourad, and Paola Iovanna. Xhaul : toward an integrated fronthaul/backhaul architecture in 5g networks. *IEEE Wireless Communications*, 22(5) :32–40, 2015.
- [61] Dominique Barth, Maël Guiraud, and Yann Strozecki. Deterministic contention management for low latency cloud ran over an optical ring. *arXiv preprint arXiv :1902.03018*, 2019.
- [62] Dominique Barth, Maël Guiraud, Brice Leclerc, Olivier Marcé, and Yann Strozecki. Deterministic scheduling of periodic messages for cloud ran. In *2018 25th International Conference on Telecommunications (ICT)*, pages 405–410. IEEE, 2018.
- [63] Dominique Barth, Maël Guiraud, and Yann Strozecki. Deterministic contention management for low latency cloud RAN over an optical ring. *CoRR*, abs/1902.03018, 2019. URL <http://arxiv.org/abs/1902.03018>.
- [64] Bogdan Uscumlic, Dominique Chiaroni, Brice Leclerc, Thierry Zami, Annie Gravey, Philippe Gravey, Michel Morvan, Dominique Barth, and Djamel Amar. Scalable deterministic scheduling for wdm slot switching xhaul with zero-jitter. In *2018 International Conference on Optical Network Design and Modeling (ONDM)*, pages 100–105. IEEE, 2018.
- [65] Tuan Dung Nguyen, Thaere Eido, Viet Hung Nguyen, and Tülin Atmaca. Impact of fixed-size packet creation timer and packet format on the performance of slotted and unslotted bus-based optical man. In *2008 The Third International Conference on Digital Telecommunications (icdt 2008)*, pages 99–104. IEEE, 2008.
- [66] Tulin Atmaca and Tuan-Dung Nguyen. Delay analysis and queue-length distribution of a slotted metro network using embedded dtmc. In *2010 IEEE Global Telecommunications Conference GLOBECOM 2010*, pages 1–6. IEEE, 2010.
- [67] Kostas Ramantas, Kyriakos Vlachos, Óscar González De Dios, and Carla Raffaelli. Tcp traffic analysis for timer-based burstifiers in obs networks. In *International IFIP Conference on Optical Network Design and Modeling*, pages 176–185. Springer, 2007.
- [68] Tülin Atmaca and Viet-Hung Nguyen. Optical metropolitan networks : packet format, mac protocols and quality of service. In *Network performance engineering*, pages 808–834. Springer, 2011.

- [69] Tulin Atmaca, Amira Kamli, and Artur Rataj. Adaptation of the NGREEN architecture for a bursty traffic. In *Computer Networks 2018, in press, preview available to reviewers, to appear before Globcom's camera ready date*. IEEE, 2018. URL <http://algstoch.eu/verics/ngb-cn.pdf>.
- [70] Amira Kamli, Tülin Atmaca, Catherine Lepers, Artur Rataj, and Djamel Amar. Performance improvement of colored optical packet switching thanks to time slot sharing. 2018.
- [71] John A Nelder and Roger Mead. A simplex method for function minimization. *The computer journal*, 7(4) :308–313, 1965.
- [72] Michel Bergmann. *Optimisation aérodynamique par réduction de modèle POD et contrôle optimal : application au sillage laminaire d'un cylindre circulaire*. PhD thesis, Vandoeuvre-les-Nancy, INPL, 2004.
- [73] Chinyere Okechi Onwubiko. *Introduction to engineering design optimization*. Prentice Hall, 2000.
- [74] Jinliang Fan, Jun Xu, Mostafa H Ammar, and Sue B Moon. Prefix-preserving ip address anonymization : measurement-based security evaluation and a new cryptography-based scheme. *Computer Networks*, 46(2) :253–272, 2004.
- [75] Nihel Benzaoui, Yvan Pointurier, Thomas Bonald, Qing Wei, and Matthias Lott. Optical slot switching latency in mobile backhaul networks. *Journal of lightwave technology*, 33(8) :1491–1499, 2015.
- [76] Anurag Kumar. Comparative performance analysis of versions of TCP in a local network with a lossy link. *IEEE/ACM Transactions on Networking (ToN)*, 6(4) : 485–498, 1998.
- [77] Nikolaus Hansen. The CMA evolution strategy : a comparing review. *Towards a new evolutionary computation*, pages 75–102, 2006.
- [78] Gavin C Cawley and Nicola LC Talbot. On over-fitting in model selection and subsequent selection bias in performance evaluation. *Journal of Machine Learning Research*, 11(Jul) :2079–2107, 2010.
- [79] Karl Johan Åström and Tore Hägglund. Automatic tuning of simple regulators with specifications on phase and amplitude margins. *Automatica*, 20(5) :645–651, 1984.
- [80] Karl Johan Åström, Tore Hägglund, Chang C Hang, and Weng Kuen Ho. Automatic tuning and adaptation for PID controllers-a survey. In *Adaptive Systems in Control and Signal Processing*, pages 371–376. Elsevier, 1993.

- [81] Naixue Xiong, Xiaohua Jia, Laurence T Yang, Athanasios V Vasilakos, Yingshu Li, and Yi Pan. A distributed efficient flow control scheme for multirate multicast networks. *IEEE Transactions on Parallel and Distributed Systems*, 21(9) :1254–1266, 2010.
- [82] Seungwan Ryu, Christopher Rump, and Chunming Qiao. A predictive and robust active queue management for internet congestion control. In *Proceedings of the Eighth IEEE Symposium on Computers and Communications. ISCC 2003*, pages 991–998. IEEE, 2003.
- [83] Takuji Tachibana and Kenji Sugimoto. Light-path establishment with pid control for effective wavelength utilization in all-optical wavelength-division multiplexing networks. *Journal of Optical Networking*, 8(4) :383–392, 2009.
- [84] Takuji Tachibana, Kiminao Kogiso, and Kenji Sugimoto. Dynamic management of computing and network resources with pid control in optical grid networks. In *Communications, 2008. ICC'08. IEEE International Conference on*, pages 396–400. IEEE, 2008.
- [85] Tamara Jiménez, Noemi Merayo, Patricia Fernández, Ramón J Durán, Ignacio de Miguel, Rubén M Lorenzo, and Evaristo J Abril. Implementation of a pid controller for the bandwidth assignment in long-reach pons. *Journal of Optical Communications and Networking*, 4(5) :392–401, 2012.
- [86] Tamara Jiménez, Noemí Merayo, Ramón J Durán, Patricia Fernández, Ignacio De Miguel, Juan C Aguado, Rubén M Lorenzo, and Evaristo J Abril. A pid-based algorithm to guarantee qos delay requirements in lr-pons. *Optical Switching and Networking*, 14 :78–92, 2014.
- [87] Li Yu, Zibo Shi, Kun Chen, and Yantai Shu. Designing a robust pid congestion controller supporting tcp flows based on  $h_\infty$  optimal control theory. In *Next-Generation Communication and Sensor Networks 2007*, volume 6773, page 67730K. International Society for Optics and Photonics, 2007.
- [88] Noemí Merayo, David Juárez, Juan C Aguado, Ignacio De Miguel, RJ Durán, Patricia Fernández, Rubén Mateo Lorenzo, and EJ Abril. Pid controller based on a self-adaptive neural network to ensure qos bandwidth requirements in passive optical networks. *Journal of Optical Communications and Networking*, 9(5) :433–445, 2017.
- [89] Roberto Sabella and Paola Iovanna. Self-adaptation in next-generation internet networks : how to react to traffic changes while respecting QoS? *IEEE Transactions on Systems, Man, and Cybernetics, Part B (Cybernetics)*, 36(6) :1218–1229, 2006.



- 
- [90] Amira Kamli Artur, Ratay and Tulin Atmaca. Analysis of a frequency response of a computer network for its self-adaptation using frequency modulation of strategy. In *ISCIS*, 2019.
- [91] Erol Gelenbe. On approximate computer system models. *Journal of the ACM (JACM)*, 22(2) :261–269, 1975.